Faculty of Science and Engineering

School of Electrical Engineering, Computing, and Mathematical Sciences

Robust Techniques for Acoustic Feedback Control in Hearing Aids

Linh Thi Thuc Tran

This thesis is presented for the Degree of
Doctor of Philosophy
of
Curtin University

February 2018

DECLARATION

To the best of my knowledge and belief this thesis contains no material previously published by any other person except where due acknowledgment has been made. This thesis contains no material which has been accepted for the award of any other degree or diploma in any university.

Linh Thi Thuc Tran

16 February 2018

ACKNOWLEDGMENTS

First, I would like to express my sincere appreciation to my supervisor Prof. Dr. Sven Nordholm for his exceptional guidance and valuable discussions during my course of PhD degree. His encouragement as well as his generosity to share his knowledge and experience play an important role in the success of my studies. I would like to thank my co-supervisor Dr. Hai H. Dam and committee chair Dr. Yee-Hong Leung for their kind support during my term.

Special thanks go to Dr. Renato Nakagawa for his willingness to share codes and knowledge. Your kind help through lots of beneficial discussions has significantly assisted me during the early stage of my studies.

I would especially like to thank Prof. Dr.-Ing. Simon Doclo for providing me the opportunity to visit his laboratory for several weeks in the university of Oldenburg, Germany. I also gratefully acknowledge Henning Schepker for his effective collaboration. Thanks again for exchanging ideas and codes, your helpful feedback and your hospitality. I would also like to thank Prof. Felix Albu for sharing codes and useful suggestions.

My special gratitude also goes to Dr. Manora Caldera, Dr. John Siquilini, Prof. Yue Rong, who provided me the sessional teaching in the Curtin university. It was my great pleasure to work with you during the last years. In addition, I am thankful my colleagues at the department of Electrical and Computer Engineering for numerous of interesting discussions and pleasant working atmosphere. I will never forget the lunch times we had together, during which I could temporarily disconnect from my hard work and refresh my mind.

I extremely acknowledge Vietnamese Government, the School of Electrical Engineering and Computing at Curtin university for their generous financial and administrative support.

Finally, I would like to thank my parents who are always with me and support for all my dreams and decisions.

ABSTRACT

Nowadays, using a hearing aid (HA) is the most common treatment for hearing impaired people to improve their hearing capability due to its simplicity and efficiency. However, one of major problems in HAs is acoustic feedback which is caused by the acoustic coupling of the loudspeaker signal into the microphone of a HA. This acoustic feedback may lead the HA to be unstable and produce howling in some cases. Consequently, the signal quality of the system is degraded as well as maximum amplification is limited. To address the acoustic feedback problem, adaptive feedback cancellation (AFC) approaches are the most potential approaches. However, the standard AFC approach results in bias in estimation of the feedback path. The bias relates to the possibly high correlation between the loudspeaker and the incoming signal. The larger the bias, the worse the system performance is achieved. This correlation is an inherent problem of the closed-loop systems that the hearing aids and the sound reinforce systems (e.g., public address systems) are typical examples.

Many solutions to reduce this bias were proposed in the literature. Among them the prediction error method based AFC (PEM), which used pre-filters to pre-whiten the inputs of adaptive filter, was one of the most interesting methods for adaptive feedback cancellation in HAs, providing a significant performance improvement compared to the standard AFC method. However, the PEM applications are still limited to single-microphone single-loudspeaker (SMSL) HAs. Other recent research focus on using multi-microphone, variable step-size (VSS) control, subband, and fast-converging adaptive filter (FCAF) techniques for AFC in HAs. Recently, a trend of developing new AFC methods is based on a combination of different AFC techniques/methods to take advantage of benefits of each individual technique. The target of this dissertation is to develop new AFC methods for HAs following that trend such that the proposed methods enhance convergence and tracking rate while retaining low steady-state error of the system. Moreover, these proposed methods are

robust against different types of the incoming signals as well as against sudden changes in the acoustic feedback paths.

The first main contribution of this dissertation is to investigate the application of the PEM to a two-microphone single-loudspeaker HA with detailed theoretical analysis as well as practical experiments. Moreover, a new derivation for optimal filters in the two-microphone adaptive feedback control (AFC2) method will be provided.

The second contribution is to integrate FCAF techniques such as the APA, or the proportionate normalized least mean squares (PNLMS) algorithm, or the improved PNLMS (IPNLMS) algorithm into the PEM for the SMSL HAs.

The third contribution is to propose a novel variable step-size algorithm, called improved practical variable step-size (IPVSS) and then to apply it successfully for the PEM in the SMSL HAs.

CONTENTS

LIST OF FIGURES

LIST OF TABLES

Acronyms and Abbreviations

ADC	analog-to-digital
AEC	acoustic echo control
AEQ	automatic equalization
AFC	adaptive feedback cancellation
AFC2	two microphone method for feedback cancellation
AFC2-TD	AFC2 using transform domain processing
AGC	automatic gain control
APA	affine projection algorithm
ASG	added stable gain
$\overline{ASG}$	average added stable gain
BTE	behind-the-ear
CIC	completely-in-the-canal
DAC	digital-to-analog
dB	decibel
DFT	discrete Fourier transform
DCT	discrete cosine transform
DTD	double-talk detector
FS	frequency shifting
FIR	finite impulse response
FSNR	feedback to (incoming) signal plus noise ratio
FSR	feedback to (incoming) signal ratio
HA	hearing aid
FCAF	fast-converging adaptive filtering (algorithm)
IPNLMS	improved proportionate NLMS
IPVSS	improved practical variable step-size
IPVSS-APA	IPVSS for APA
IPVSS-NLMS	IPVSS for NLMS
IR	impulse response

ITC	in-the-canal
ITE	in-the-ear
KLT	Karhunen-Loeve transform
LMR-APA	Levenberg-Marquardt regularized APA
LMR-NLMS	Levenberg-Marquardt regularized NLMS
LMS	least mean squares
LTI	linear time-invariant
MIS	misalignment
MIS – H	misalignment for estimating $H(q)$
$\overline{MIS}$	average misalignment
MMSL	multi-microphone single-loudspeaker
MSG	maximum stable gain
NF	notch filter
NLMS	normalized least mean squares (algorithm)
NPVSS-NLMS	non-parametric VSS NLMS
PA	public address
PEAQ	perceptual evaluation of audio quality
PEM	prediction error method
PEM-AFC	PEM based adaptive feedback canceller
PEM-AFC2	combination of PEM and AFC2
PEM-APA	PEM using APA
PEM-NLMS	PEM using NLMS
PEM-IPNLMS	PEM using improved proportionate NLMS
PEM-IPNLMS	PEM using improved proportionate NLMS
PEM-IPVSS-NLMS	PEM using IPVSS for NLMS
PEM-IPVSS-APA	PEM using IPVSS for APA
PEM-PNLMS	PEM using proportionate NLMS
PEM-VSS-MDNLMS	PEM using VSS-MDNLMS
PESQ	perceptual evaluation of speech quality
PM	phase modulation
PN	probe noise
PNLMS	proportionate NLMS

PVSS	practical variable step-size
PVSS-NLMS	PVSS for NLMS
RLS	recursive least squares (algorithm)
RTF	relative transfer function
SMSL	single-microphone single-loudspeaker
SNR	signal-to-noise ratio
SSN	speech shaped noise
TD	transform domain processing
VSS	variable step-size
VSS-APA	variable step-size for APA
VSS-MDNLMS	variable step-size modified decorrelation NLMS
VSS-NLMS	variable step-size for NLMS
VSS-PNLMS	variable step-size for PNLMS algorithm
VSS-IPNLMS	variable step-size for IPNLMS algorithm
WHO	world health organization

Notations and Symbols

$C(q)$	transfer function of the closed-loop system
$\overline{C}(q)$	transfer function of the closed-loop AFC system
$E\{\cdot\}$	expectation operation
$e(k)$	error signal
$e_p(k)$	pre-whitened error signal
ϵ	forgetting factor
d_{fb}	delay in the feedback canceller path
d_k	delay in the forward path
δ, ζ	regularization factors
$F(q)$	transfer function of the feedback path
$\hat{F}(q)$	transfer function of the estimated feedback path
$\hat{F}_i(q)$	transfer function of the ith estimated feedback path
$\mathbf{f}$	impulse response of the feedback path
$\mathbf{f}_i$	impulse response of the ith acoustic feedback path
$\mathbf{f}_{2_\mathbf{h}}$	impulse response of the product $F_2(q)H(q)$
$\mathbf{f}_{2_{\hat{\mathbf{h}}}}$	impulse response of the product $F_2(q)\hat{H}(q)$
f_s	sampling frequency
f_0	amount of frequency shifting
$\hat{\mathbf{f}}$	impulse response of the estimated feedback path
$G^{-1}(q)$	the incoming signal model
$\hat{G}(q)$	the estimate of $G(q)$
$H(q)$	relative transfer function
$\mathbf{h}$	impulse response of the relative transfer function
$\hat{H}(q)$	the estimated RTF
$\hat{\mathbf{h}}$	impulse response of the estimated RTF
$\mathbf{I}$	identity matrix
$J(.)$	cost function
k	discrete-time index

$K(q)$	transfer function of the forward path
$\|K\|$	gain of the forward path
$\|K(e^{j\omega})F(e^{j\omega})\|$	loop gain
$\angle K(e^{j\omega})F(e^{j\omega})$	loop phase
$n(k)$	white background noise
$n_p(k)$	pre-filtered (white) noise
μ	step-size
μ_U	upper limit of the step-size
μ_L	lower limit of the step-size
$\mu(k)$	variable step-size
$\mu_i(k)$	variable step-size for ith projection order
$\|\cdot\|_{l_i}$	l_i-norm
L_f	length of the true feedback path
$L_{\hat{f}}$	length of the estimated feedback path
L_h	length of the RTF
$L_{\hat{h}}$	length of the estimated RTF
P	projection order of the APA
q^{-1}	discrete-time delay operator
$\boldsymbol{R}_{\mathbf{m}}$	auto-correlation matrix of a vector $\mathbf{m}$
$\boldsymbol{R}_{\mathbf{mn}}$	cross-correlation matrix between two vectors $\mathbf{m}$ and $\mathbf{n}$,
$r(k)$	probe noise
$\boldsymbol{r}_{\mathbf{m}\varsigma}$	cross-correlation vector between a vector $\mathbf{m}$ and a scalar ς
$u(k)$	incoming signal
$u_i(k)$	the ith incoming signal
$v(k)$	acoustic feedback signal
$\hat{v}(k)$	estimated feedback signal
ω	angular frequency
$w(k)$	white Gaussian noise sequence
$x(k)$	microphone signal
$x_i(k)$	the ith microphone signal
$x_p(k)$	pre-whitened microphone signal
$y(k)$	loudspeaker signal

$y_i(k)$	the ith loudspeaker signal
$y_{FS}(k)$	loudspeaker signal after frequency shifting
$y_p(k)$	pre-whitened loudspeaker signal
$\xi(k)$	residual error caused by undermodeling the RTF
$\hat{\sigma}^2_{e_p}(k)$	power of pre-whitened error signal
$\hat{\sigma}^2_{u_p}(k)$	power of pre-whitened incoming signal
$\hat{\sigma}^2_{x_p}(k)$	powers of pre-whitened microphone signal
$\hat{\sigma}^2_{\hat{v}_p}(k)$	powers of estimated feedback signal after pre-whitening
$\hat{\sigma}^2_{y_p}(k)$	power of the pre-whitened loudspeaker signal
η	positive weighting factor

CHAPTER 1
Introduction

1.1 Motivation

Nowadays, the number of hearing impaired people have been increasing rapidly. Many reasons contribute to human's hearing loss including exposure to noise, ageing, genetics, some diseases or certain medications. People who suffer from hearing loss face with difficulties in studying, working and living. To help those people improve their hearing capability, there are some treatments for hearing loss such as cochlear implants, using assistive listening devices or using hearing aids. Among those the most common and simplest treatment is to use hearing aids.

However, one of the major problems in hearing aids (HAs) as well as sound reinforcement systems is acoustic feedback caused by a coupling of the loudspeaker signal into microphone. Acoustic feedback lowers the achievable maximum amplification as well as signal quality. In the past five decades, lots of solutions for eliminating or reducing this negative effects of acoustic feedback, including feedforward suppression techniques (e.g., gain reduction, delay insertion, probe noise insertion, phase modulation and frequency shifting) and adaptive feedback cancellation (AFC) techniques have been studied. Among those the AFC techniques are the most effective approaches. Although the existing acoustic feedback control approaches can completely or partly cancel the acoustic feedback, under some conditions the system may still be unstable and howling effect may present [2]. Thus, a reliable method for acoustic feedback control is still sought after.

The motivation of this thesis is to investigate, develop and evaluate robust techniques for acoustic feedback control in HAs. Here robustness is defined

as the sensitivity of the techniques toward a variety of incoming signals and sudden changes in the feedback paths. Those techniques focus on adaptive feedback cancellation, which are applied for either single-microphone single-loudspeaker (SMSL) or multi-microphone single-loudspeaker (MMSL) HAs to improve their performance by lowering the bias in the estimation of the feedback path, enhancing the convergence/tracking rates while maintaining good signal quality.

For SMSL HAs, the thesis develops variant solutions to enhance adaptive feedback cancellation. Those AFC solutions include the implementation of fast-converging adaptive filtering (FCAF) algorithms in conjunction with the prediction error method (PEM), and the development of a novel variable step-size algorithm which can work effectively with different adaptive filtering algorithms such as the normalized least-mean-squares (NLMS) algorithm and the affine projection algorithm (APA).

For MMSL HAs, one potential AFC method called two microphone method for feedback cancellation (AFC2) was originally introduced in [3]. In this method an additional microphone was used to predict an incoming signal, then this predicted incoming signal was removed from adaptation process, resulting in a lower bias in the estimate of the feedback path. However, the "so-called" optimal solution in [3] consists of a derivation problem which is analyzed in detail in Section 2.4.2. To address that derivation problem, a novel derivation for the AFC2 approach is also proposed in this thesis. Moreover, a new AFC method based on a combination of the AFC2 method and the PEM, namely the PEM-AFC2, is also developed to further enhance the performance of those individual methods.

1.2 Thesis contribution

This work focuses on studying and implementing adaptive feedback cancellation techniques which are robust against different types of incoming signals such as male speech, female speech and music, and against sudden changes in the feedback paths. The proposed methods are evaluated with real speech and music as the incoming signals as well as with a sudden change of the feedback

path. The original contributions of this dissertation are as follows:

For the AFC solutions using MMSL:

- Provided a novel derivation for the AFC2 approach. In addition, the PEM is integrated into the AFC2 to further exploit the benefits of both individual methods, resulting in significant performance improvements.

For the AFC solutions using SMSL:

- Studied the implementation of different adaptive filtering algorithms in combination with the prediction error method for acoustic feedback control in hearing aids. In particular, the APA, the proportionate NLMS (PNLMS) and the improved PNLMS are applied to the PEM in order to considerably improve the convergence rate and tracking rate of the system while a low steady-state error is still maintaining.
- Proposed a new variable step-size algorithm, called improved practical variable step-size (IPVSS). The IPVSS has been successfully implemented for variety of adaptive filtering algorithms such as the NLMS, and the APA, in combination with the PEM in order to enhance the performance of the system. The frequency shifting (FS) is also considered as a technique which can decorrelate the loudspeaker signal and the incoming signal, resulting in significant performance improvement.

The contribution of this dissertation is summarized in Table 1.1.

1.3 Thesis outline

The thesis comprises six chapters. Chapter 1 provides the introduction which includes a brief introduction of the thesis, the motivation, thesis contribution and the outline. The chapter 1 is completed by a list of peer-reviewed publications.

Chapter 2 states the acoustic feedback problem and the necessity of acoustic feedback control techniques in hearing aids. Several solutions for acoustic feedback control including feedforward suppression as well as adaptive feedback cancellation using either MMSL or SMSL are reviewed and discussed. The

Table 1.1: Proposed AFC methods in this dissertation.

AFC methods	Two-microphone	PEM	Adaptive filtering algorithm	VSS control	FS
PEM-AFC2	✓	✓	NLMS		
PEM-APA		✓	APA		
PEM-PNLMS, PEM-IPNLMS		✓	PNLMS, IPNLMS		
PEM-IPVSS-NLMS		✓	NLMS	✓	
PEM-IPVSS-APA		✓	APA	✓	
PEM-IPVSS-NLMS-FS		✓	NLMS	✓	✓
PEM-IPVSS-APA-FS		✓	APA	✓	✓

chapter also provides evaluation measures which use to evaluate the performance and the quality of an AFC algorithm.

Chapter 3 proposes a new derivation which completely solve the mathematical problem of the "so-called" optimal solution for the AFC2 method introduced in [3]. Moreover, a combination of the PEM and the AFC2 method is proposed, namely PEM-AFC2, to further reduce the bias in estimation of the feedback path. Derivation for the proposed PEM-AFC2, which demonstrates that a better solution for bias deduction can be obtained compared to the AFC2 approach, is also provided. Furthermore, the theoretical derivation has been verified by experimental results.

Chapter 4 introduces the applications of fast-converging adaptive filtering algorithms such as the APA and the PNLMS/IPNLMS to the PEM for acoustic feedback control in hearing aids. While the APA uses not only the current but also the previous loudspeaker signals as input signals to the adaptive filter, the PNLMS/IPNLMS algorithms exploit the shape of the estimated feedback paths to compute the tap-dependent step-size. As a result, those adaptive filtering algorithms are powerful in improving convergence and tracking rates whilst maintaining a low steady-state error compared to the conventional LMS and NLMS algorithms, especially when the incoming signal is spectrally coloured.

Chapter 5 provides a novel variable step-size solution, the IPVSS, which is then integrated into the PEM using either the NLMS algorithm or the APA. By using the IPVSS, the adaptive filter tends to pick up the high values of the step-size when the system is unstable or close to instability and to get the low step-size values when the system is converged, resulting in improved convergence and tracking rates while maintaining a low steady-state error. Moreover, a small frequency shifting (FS) is added to provide further decorrelation between loudspeaker and incoming signals while keeping signal quality almost unchanged.

Chapter 6 concludes the thesis and introduces some future works.

1.4 List of peer-reviewed publications

The following papers have been published or accepted based on certain works in this dissertation:

1. **Linh T. T. Tran**, S. Nordholm, H. Schepker, H. H. Dam, and S. Doclo, "Two-Microphone Hearing Aids using Prediction Error Method for Adaptive Feedback Control", IEEE/ACM Transaction on Audio, Speech and Language Processing, May 2018.
2. S. Nordholm, H. Schepker, **Linh T. T. Tran**, and S. Doclo, "Stability-Controlled Hybrid Adaptive Feedback Cancellation Scheme for Hearing Aids", Journal of the Acoustical Society of America, Jan. 2018.
3. **Linh T. T. Tran**, H. Schepker, S. Doclo, H. H. Dam, and S. Nordholm, "Adaptive Feedback Control using Improved Variable Step-Size Affine Projection Algorithm for Hearing Aids," in Proc. Asia-Pacific Signal and Information Processing Association Annual Summit and Conference (APSIPA-ASC), Kuala Lumpur, Malaysia, Dec. 2017.
4. **Linh T. T. Tran**, H. Schepker, S. Doclo, H. H. Dam, and S. Nordholm, "Proportionate NLMS for adaptive feedback control in hearing aids," in Proc. IEEE International Conference on Acoustics, Speech, and Signal Processing (ICASSP), New Orleans, USA, Mar. 2017, pp. 211-215.
5. **Linh T. T. Tran**, H. Schepker, S. Doclo, H. H. Dam, and S. Nordholm, "Improved practical variable step-size algorithm for adaptive feedback control in hearing aids," in Proc. International Conference on Signal Processing and Communication System (ICSPCS), Surfers Paradise, Gold Coast, Australia, Dec. 2016.
6. **Linh T. T. Tran**, H. H. Dam, and S. Nordholm, "Affine projection algorithm for acoustic feedback cancellation using prediction error method in hearing aids," Proc. IEEE International Workshop on Acoustic Signal Enhancement (IWAENC), Xi'an, China, Sept. 2016.
7. **Linh T. T. Tran**, H. H. Dam, H. Schepker, S. Doclo, and S. E. Nordholm, "Evaluation of two-microphone acoustic feedback cancellation using uniform and non-uniform sub-bands in hearing aids," in Proc. Asia-Pacific

Signal and Information Processing Association Annual Summit and Conference (APSIPA-ASC), Hong Kong, Dec. 2015, pp. 308-313.

8. **Linh T. T. Tran**, S. Nordholm, H. Dam, W. Yan, and C. Nakagawa, "Acoustic feedback cancellation in hearing aids using two microphones employing variable step size affine projection algorithms," in Proc. 20th IEEE International Conference on Digital Signal Processing (DSP), Singapore, July 2015, pp. 1191–1195.
9. F. Albu, **Linh T. T. Tran**, S. Nordholm, "A Combined Variable Step Size Strategy for Two Microphones Acoustic Feedback Cancellation using Proportionate Algorithms", in Proc. Asia-Pacific Signal and Information Processing Association Annual Summit and Conference (APSIPA-ASC), Kuala Lumpur, Malaysia, Dec. 2017.
10. H. Schepker, **Linh T. T. Tran**, S. Nordholm, and S. Doclo, "Combining Null-Steering and Adaptive Filtering for Acoustic Feedback Cancellation in a Multi-Microphone Earpiece" in Proc. European Signal Processing Conference (EUSIPCO), Kos Island, Greece, Aug. 2017.
11. F. Albu, **Linh T. T. Tran**, S. Nordholm, "Two-Microphone Acoustic Feedback Cancellation using NLMS based Algorithms", in Proc. International Conference on Electronics, Computers and Artificial Intelligence, Targoviste, Romania, June 2017.
12. H. Schepker, **Linh T. T. Tran**, S. Nordholm, and S. Doclo, "Null-steering beamformer for acoustic feedback cancellation in a multi-microphone earpiece optimizing the maximum stable gain," in Proc. IEEE International Conference on Acoustics, Speech, and Signal Processing (ICASSP), New Orleans, USA, Mar. 2017, pp. 341-345.
13. H. Schepker, **Linh T. T. Tran**, S. Nordholm, and S. Doclo, "A Robust Null-Steering Beamformer for Acoustic Feedback Cancellation for a Multi-Microphone Earpiece", in Proc. 12th ITG Conference on Speech Communication, Paderborn, Germany, Oct. 2016, pp. 165-169.
14. H. Schepker, **Linh T. T. Tran**, S. Nordholm, and S. Doclo, "Acoustic feedback cancellation for a multi-microphone earpiece based on a nullsteering beamformer," in Proc. IEEE International Workshop on Acoustic Signal

Enhancement (IWAENC), Xi'an, China, Sept. 2016.

15. H. Schepker, **Linh T. T. Tran**, S. Nordholm, and S. Doclo, "Improving adaptive feedback cancellation in hearing aids using an affine combination of filters," in Proc. IEEE International Conference on Acoustics, Speech, and Signal Processing (ICASSP), Shanghai, China, Mar. 2016, pp. 231-235.

CHAPTER 2
Background

Chapter's key points: background on

- Hearing loss and hearing aids
- Acoustic feedback problem
- Acoustic feedback control
- Adaptive feedback cancellation approaches
- Evaluation measures

This chapter first provides an overview of the hearing loss situation in the world population and the necessity of hearing aids for hearing impaired patients, cf. Section 2.1. Second it mentions one of the major problems of hearing aids, the acoustic feedback, in Section 2.2. Then Section 2.3 discusses the existing solutions for acoustic feedback problem in literature, which include feedforward suppression techniques and adaptive feedback cancellation techniques. Since this thesis only focuses on the latter techniques, some widely known adaptive feedback cancellation approaches using single-microphone single-loudspeaker (SMSL) as well as multiple-microphone single-loudspeaker (MMSL) are briefly reviewed in Section 2.4. The differences between the acoustic echo cancellation and the acoustic feedback cancellation are also highlighted in this section. Finally, the common measures used to evaluate the performance of the AFC approaches are given in Section 2.5.

2.1 Hearing loss and hearing aids

2.1.1 Hearing loss

Hearing loss or hearing impairment refers to a partial or total inability to hear [4]. The severity of hearing loss can be classified into 5 degrees, namely mild hearing loss, moderate hearing loss, moderately severe hearing loss, severe hearing loss and profound hearing loss. Table 2.1 shows the severity of hearing loss in decibels (dB) [1]. There are variety of factors causing hearing loss such as ageing, exposure to noise, genetics, some diseases or certain medications, etc. People, who suffer from hearing loss, find difficulty in communicating with others. For children, hearing loss causes adverse impacts on ability to learn spoken languages. For adults, the exclusion from communication results in frustration, loneliness, especially for older people. According to the World Health Organization's (WHO) data [5], approximately 5% of the world's population (corresponding to 360 million people) have disabling hearing loss, and 32 millions of them are children. The data also show that 1.1 billion people are at risk of hearing loss because of exposure to loud noise. Moreover, population ageing is also a major reason of hearing loss since there is a rapid increase in numbers of elderly people whose ability to hear reduces gradually with ageing. It is said that from year 2000 to 2050 the number of people who are over 60 years old will double, corresponding to an increase from 11% to 22% [6]. Approximately one-third of older people between the ages of 61 and 70 and more than 80 percent of those who are older than 85 years old suffer from hearing loss [7]. The treatments for hearing loss include cochlear implants, and use of hearing aids or assistive listening devices. Among those the most common and simplest treatment is to wear hearing aids.

2.1.2 Hearing aids

A hearing aid is an electronic device which helps hearing impaired people to restore their hearing capability. Normally a hearing aid is constructed by a microphone, a receiver (loudspeaker), an amplifier and a battery. Firstly, the microphone picks up sound waves from surrounding environment, then those sound waves are converted into electrical signals. Secondly, those electrical

Table 2.1: Severity of hearing loss (dB) [1].

Severity	Hearing Threshold (dB)
Mild	26 - 40
Moderate	41 - 55
Moderately severe	56 - 70
Severe	71 - 90
Profound	90

signals are amplified by using an amplifier before they are transferred to the loudspeaker. Finally, the loudspeaker transforms the electrical signals back into the sound signals which are then delivered to the ear canal. A battery provides power supply for all elements of a hearing aid.

Nowadays, there are two main types of hearing aids based on their relative positions to the ear, namely behind-the-ear (BTE) hearing aids, and in-the-ear (ITE) hearing aids. The ITE hearing aids are divided into two classes, completely-in-the-canal (CIC) and in-the-canal (ITC) hearing aids. Along with the development of technologies, the structure of modern hearing aids becomes more complex. A hearing aid may be integrated with more than one microphone and one loudspeaker and a multitude of audio signal processing techniques. It has more functionalities and provides better signal quality whilst its size becomes smaller and smaller. The latest products of digital hearing aids have new features which allow them to communicate with other devices, for instance, smartphones, hearing loops, etc., via Bluetooth [8].

2.2 Acoustic feedback problem

Acoustic feedback refers to a phenomenon in which a loudspeaker signal is partly coupled into a microphone. Thus the microphone signal consists not only the incoming signal but also the acoustic feedback signal. This microphone signal is then looped back into the loudspeaker through a signal processing path (so-called the forward path). By that way, a closed-loop system is generated, cf. Figure 2.1.

Acoustic feedback is the cause for the degradation of the received sound quality

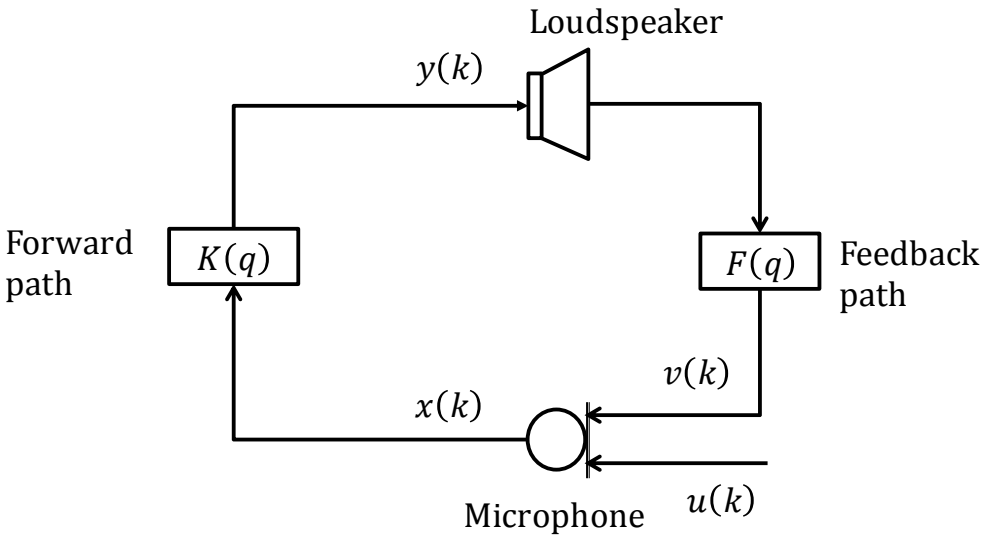

Figure 2.1: Acoustic feedback system.

as well as for the limitation of the achievable maximum stable gain. It may drive the system to be unstable. Under certain situations, the "howling" may occur.

The sound reinforcement systems (for instance, public address (PA) systems) and the hearing aids are two typical examples of the realistic acoustic feedback systems which suffer from acoustic feedback problem.

For simplicity, assume that all AFC systems which are mentioned in this dissertation are discrete-time, linear time-invariant and have stationary incoming signals. Throughout this dissertation, vectors and matrices are emphasized using lower and upper letters in bold, respectively. $E\{.\}$ denotes the expectation operation and the superscript T denotes transposition. The autocorrelation matrix of a vector $\mathbf{m}$, the cross-correlation matrix between two vectors $\mathbf{m}$ and $\mathbf{n}$, and the cross-correlation vector between a vector $\mathbf{m}$ and a scalar ς are represented by $\boldsymbol{R}_{\mathbf{m}}$, $\boldsymbol{R}_{\mathbf{mn}}$ and $\boldsymbol{r}_{\mathbf{m}\varsigma}$, respectively, i.e., $\boldsymbol{R}_{\mathbf{m}} = E\{\mathbf{m}\mathbf{m}^T\}$, $\boldsymbol{R}_{\mathbf{mn}} = E\{\mathbf{m}\mathbf{n}^T\}$, and $\boldsymbol{r}_{\mathbf{m}\varsigma} = E\{\mathbf{m}\varsigma\}$.

Figure 2.1 illustrates the acoustic feedback problem. The microphone signal and loudspeaker signal are denoted as $x(k)$ and $y(k)$, respectively. The feedback path $F(q)$ consists of the features of the analog-to-digital (ADC) and digital-to-analog (DAC) converters, the frequency characteristic of the micro-

phone and the loudspeaker, and the acoustic feedback path. It can be represented as a polynomial transfer function in q, i.e.,

$$F(q) = \mathbf{f}^T \mathbf{q}, \tag{2.1}$$

where $\mathbf{f} = \left[f_0, f_1, \ldots, f_{L_f-1}\right]^T$ is a vector of length L_f denoting the true feedback path, and $\mathbf{q} = \begin{bmatrix} 1 & q^{-1} & \ldots & q^{-L_f+1} \end{bmatrix}^T$. The notation q^{-1} is the discrete-time delay operator. The acoustic feedback signal is defined as

$$v(k) = F(q)\, y(k) = \mathbf{f}^T \mathbf{y}(k), \tag{2.2}$$

where k is the discrete-time index, and $y(k)$ is the loudspeaker signal, $\mathbf{y}(k) = [y(k), y(k-1), \ldots, y(k-L_f+1)]^T$ is a vector of length L_f . The microphone signal $x(k)$ is a combination of the incoming signal (or desired signal) $u(k)$ and the acoustic feedback signal $v(k)$, i.e.,

$$x(k) = u(k) + v(k) = u(k) + F(q)\, y(k). \tag{2.3}$$

In the ideal case, the loudspeaker signal is produced by processing the microphone signal using the forward path $K(q)$ as follows

$$y(k) = K(q)\, x(k). \tag{2.4}$$

Assuming that the forward path $K(q)$ includes an amplifier with gain $|K|$ and a delay d_k such that $d_k \geqslant 1$ sample, i.e.,

$$K(q) = q^{-d_k} |K|. \tag{2.5}$$

The acoustic feedback system is known as a closed-loop system due to the presence of the forward path. By substituting Eq. (2.3) into Eq. (2.4), the transfer function $C(q)$ of the closed-loop system from the incoming signal $u(k)$ to the loudspeaker signal $y(k)$ is obtained as

$$C(q) = \frac{K(q)}{1 - K(q)\, F(q)}. \tag{2.6}$$

The stability condition of the above linear closed-loop system is determined based on the Nyquist stability criterion which is stated that the closed-loop system is unstable if the following conditions for the loop gain $|K\left(e^{j\omega}\right)F\left(e^{j\omega}\right)|$ and the loop phase $\angle K\left(e^{j\omega}\right)F\left(e^{j\omega}\right)$ are fulfilled [2, 9],

$$\begin{cases} |K\left(e^{j\omega}\right)F\left(e^{j\omega}\right)| \geq 1 \\ \angle K\left(e^{j\omega}\right)F\left(e^{j\omega}\right) = 2\pi n, \quad n \in \mathbb{Z} \end{cases}, \tag{2.7}$$

where $\omega \in [0, 2\pi]$ is the angular frequency, $K\left(e^{j\omega}\right)$ and $F\left(e^{j\omega}\right)$ are the frequency responses of the forward path and the acoustic feedback path, respectively.

The Nyquist stability criterion in Eq. (2.7) is essential for acoustic feedback control, since all acoustic feedback control methods effectively try to avoid either one or both of these conditions to be met [2].

2.3 Acoustic feedback control

Acoustic feedback is one of the major problems in hearing aids. During the past 50 years, many solutions for acoustic feedback control were given in the literature. In the beginning the research mainly focused on acoustic feedback control for the sound reinforcement systems, e.g., PA systems [2, 10, 11, 12, 13], while that kind of research for HA applications was considered in the last two decades [14, 15, 16, 17, 18, 19]. Those solutions either completely suppress the acoustic feedback or at least partially eliminate it manually or automatically. However, the system may still be unstable and howling may still occur in some circumstances [2]. Therefore, the demand for a reliable automatic acoustic feedback control approach is still growing.

Unlike a PA system, a HA has a much shorter impulse response (IR) of the acoustic feedback path. In fact, the length of the acoustic feedback path in PA systems is hundreds to thousands taps, whereas it is around 50-100 taps in HAs. The reason is that the distance between a loudspeaker and a microphone in a HA is much shorter than that in a PA system due to the small size of a hearing aid. In the PA systems, a microphone can be moved farther away from a loudspeaker to reduce the negative effects of acoustic feedback but this is not

possible to do in hearing aids. Nowadays, the trend of developing HA products aims at designing and producing reliable open-fit HAs with smaller sizes whilst enhancing sound quality and achievable maximum stable gain. Thus the acoustic feedback control for HA applications becomes more challenging than that for PA applications.

Generally, existing solutions for acoustic feedback control are categorized into feedforward suppression and adaptive feedback cancellation (AFC) approaches. This dissertation concentrates only on the automatic AFC methods for HAs.

2.3.1 Feedforward suppression

The feedforward suppression techniques are based on the idea that modifies the forward path by adding to it decorrelating operations such that the system is stable with the presence of the acoustic feedback path. Figure 2.2 presents the model of the feedforward suppression techniques. The simplest decorrelating operation is a delay which is used to decorrelate the loudspeaker and the incoming signal [20, 21]. Other common decorrelating operations include gain reduction, probe noise (PN), phase modulation (PM) and frequency shifting (FS).

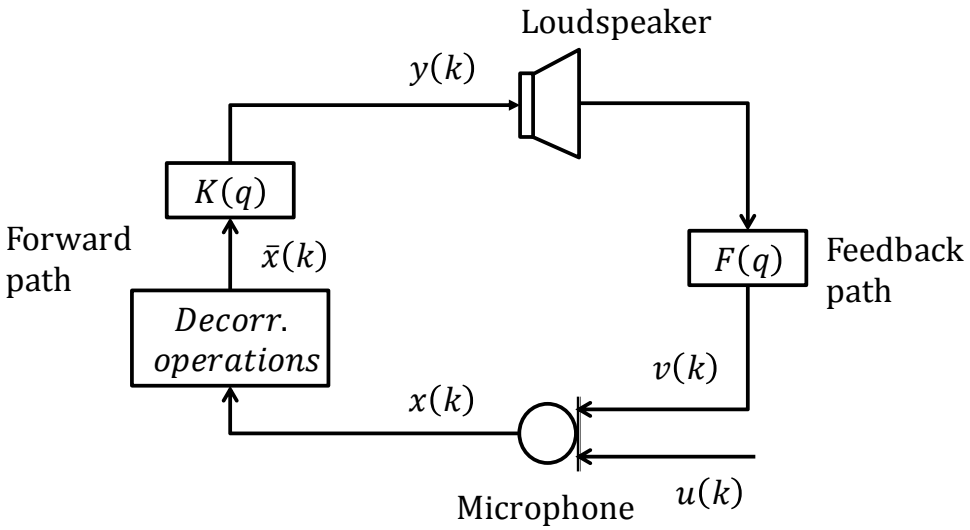

Figure 2.2: Feedforward suppression model.

In the gain reduction methods, the gain of the forward path is reduced such that the system drives away from the loop gain condition in the Nyquist stability criterion (cf. Eq. (2.7)). The gain reduction methods are classified into

automatic gain control (AGC) methods, automatic equalization (AEQ) methods and notch-filter-based (NF) methods [2]. Among them the most interesting methods are the NF methods. In the NF methods [22, 23, 24, 25, 26, 27, 28, 29], first the howling is detected, then the gain reduction is employed in the narrow frequency band around the critical frequencies, whenever the howling occurs. However, this method is reactive due to the fact that howling often occurs before it is actually identified [15, 22, 30, 31].

In the PN methods, a probe signal which is commonly white Gaussian noise is added to the loudspeaker signal [17, 19, 32, 33, 34, 35]. As a result, the correlation between the loudspeaker signal and the incoming signal is reduced and an improvement in the performance of the system is achieved. However, the power of the inserted probe noise needs to be controlled such that it is inaudible for the hearing aid user.

In the PM methods [36, 37, 38], the phase of the microphone signal is controlled such that the loop phase condition in the Nyquist criterion (Eq. (2.7)) is not satisfied. By this way, the stability of the closed-loop system can be enhanced, regardless of the loop gain condition.

In the FS methods, an amount of frequency shifting which plays a role as a nonlinear operation is used in the forward path [11, 36, 39, 40, 41]. Consequently, lower correlation between the loudspeaker and the incoming signal is obtained, resulting in a higher maximum stable gain (MSG). However, a larger amount of FS may generate roughness in the signals, thus a small amount of FS (f_0) is recommended, i.e., $0 < f_0 \leq 10\,\mathrm{Hz}$ in order to obtain a reasonable correlation reduction and to avoid significant sound quality distortions [42].

The main disadvantage of the feedforward suppression approaches is that the improvement in the achievable MSG is limited [30, 36]. Moreover, the feedforward suppression approaches compromise the basic frequency response of the system, thus may cause negative effect on the sound quality [31].

2.3.2 Adaptive feedback cancellation

In reality, the acoustical environment to which the hearing aids is exposed can

vary significantly due to a variety of reasons such as chewing, yawning, coughing, sneezing, putting a palm on the face or the ear, using the telephone or mobile phone, moving the head, etc., resulting in significant changes in the acoustic feedback path. That is why an adaptive feedback canceler is needed. Recently, adaptive feedback cancellation (AFC) techniques have become popular solutions.

A standard continuous AFC model for a SMSL hearing aid is depicted in Figure 2.3. In this method, an adaptive filter $\hat{F}(q)$ is used to estimate the true acoustic feedback path $F(q)$. The estimated feedback signal $\hat{v}(k)$ is computed as

$$\hat{v}(k) = \hat{F}(q)\, y(k) = \hat{\mathbf{f}}^T \mathbf{y}(k), \tag{2.8}$$

where $\hat{\mathbf{f}} = \left[\hat{f}_0, \hat{f}_1, \ldots, \hat{f}_{L_{\hat{f}}-1}\right]^T$ is a vector of length $L_{\hat{f}}$ denoting the estimated IR of the true acoustic feedback path, and $\mathbf{y}(k) = \left[y(k), y(k-1), \ldots, y\left(k - L_{\hat{f}} + 1\right)\right]^T$ is a vector of length $L_{\hat{f}}$ denoting the loudspeaker signal. The error signal $e(k)$ is produced by subtracting the estimated feedback signal $\hat{v}(k)$ from the microphone signal $x(k)$, i.e.,

$$e(k) = x(k) - \hat{v}(k) = x(k) - \hat{\mathbf{f}}^T \mathbf{y}(k), \tag{2.9}$$

where $x(k)$ is defined in a manner analogous to Eq. (2.3).

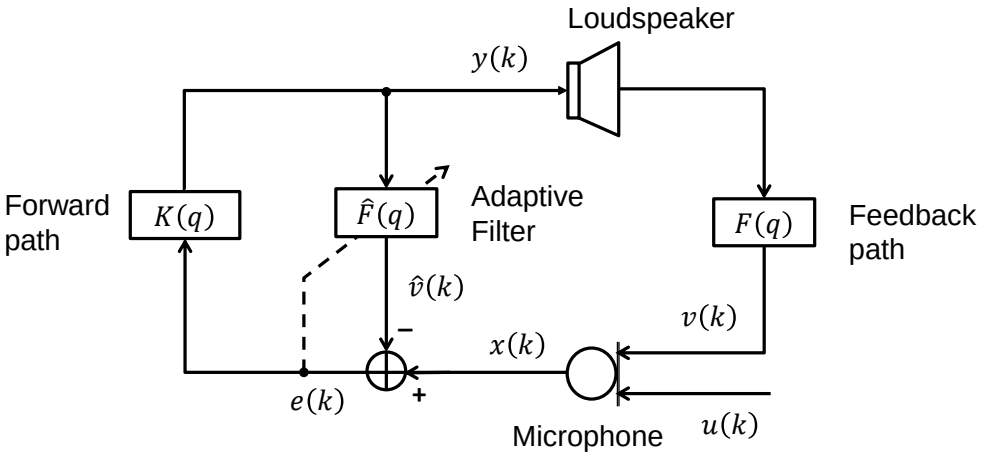

Figure 2.3: Standard adaptive feedback cancellation.

The loudspeaker signal $y(k)$ is generated by processing this error signal using

the forward path $K(q)$ as follows

$$y(k) = K(q)\, e(k). \tag{2.10}$$

The transfer function $\overline{C}(q)$ of the closed-loop AFC system from the incoming signal $u(k)$ to the loudspeaker signal $y(k)$ can be expressed as

$$\overline{C}(q) = \frac{K(q)}{1 - K(q)\left[F(q) - \hat{F}(q)\right]}. \tag{2.11}$$

If there is a perfect estimate of the acoustic feedback path, i.e., $\hat{F}(q) = F(q)$, the ideal case where the loudspeaker signal is a delayed and amplified version of the incoming signal will be obtained.

2.4 Adaptive feedback cancellation approaches

The AFC approaches can be classified into single-microphone single-loudspeaker (SMSL) AFC approaches as well as multi-microphone single-loudspeaker (MMSL) AFC approaches.

2.4.1 SMSL AFC approaches

Standard AFC

This part describes the adaptation process in the standard AFC method which is widely used for HAs [15, 43, 44] (cf. Figure 2.3). In order to estimate the acoustic feedback, firstly the cost function is defined by the mean square error, i.e.,

$$J\left(\hat{\mathbf{f}}\right) = E\left\{e^2(k)\right\} = E\left\{\left[x(k) - \hat{\mathbf{f}}^T \mathbf{y}(k)\right]^2\right\}. \tag{2.12}$$

Secondly, minimizing the cost function with respect to (w.r.t) $\hat{\mathbf{f}}$, i.e.,

$$\min_{\hat{\mathbf{f}}} E\left\{\left[x(k) - \hat{\mathbf{f}}^T \mathbf{y}(k)\right]^2\right\}, \tag{2.13}$$

results in the Wiener solution

$$\hat{\mathbf{f}} = E\left\{\mathbf{y}(k)\, \mathbf{y}^T(k)\right\}^{-1} E\left\{\mathbf{y}(k)\, x(k)\right\}. \tag{2.14}$$

Substituting Eq. (2.3) into Eq. (2.14) results in [20]

$$\hat{\mathbf{f}} = \mathbf{f} + \underbrace{\boldsymbol{R}_{\mathbf{y}}^{-1}\boldsymbol{r}_{\mathbf{y}u}}_{bias}. \tag{2.15}$$

The estimation of acoustic feedback path in Eq. (2.15) yields a bias. This bias is a result of the correlation between the loudspeaker and incoming signal if the incoming signal is spectrally coloured (e.g., speech, tones, or music). Consequently, the output signal becomes distorted [20, 31].

A variety of adaptive filtering algorithms can be used to recursively approximate the acoustic feedback path, such as least-mean-squares (LMS) algorithm, normalized least-mean-squares (NLMS) algorithm, recursive least-squares (RLS) algorithm, affine projection algorithm (APA) and proportionate NLMS (PNLMS) algorithm [45, 46]. One of the most widely known adaptive algorithms is the LMS algorithm, which can be expressed as follows

$$\hat{\mathbf{f}}\left(k\right) = \hat{\mathbf{f}}\left(k-1\right) + \mu\mathbf{y}\left(k\right)e\left(k\right), \tag{2.16}$$

where μ is a step-size which controls the stability of the algorithm. The main advantage of the LMS algorithm is its simplicity, but it suffers from a gradient noise amplification problem when $\mathbf{y}\left(k\right)$ is large since the second term of Eq. (2.16) is directly proportional to $\mathbf{y}\left(k\right)$. To cope with that gradient problem, the normalized least mean squares (NLMS) algorithm that the second term of Eq. (2.16) is normalized w.r.t the squared Euclidean norm of the vector $\mathbf{y}\left(k\right)$, i.e., [45]

$$\hat{\mathbf{f}}\left(k\right) = \hat{\mathbf{f}}\left(k-1\right) + \frac{\mu}{\left\|\mathbf{y}\left(k\right)\right\|_2^2 + \delta_{NLMS}}\mathbf{y}\left(k\right)e\left(k\right), \tag{2.17}$$

where δ_{NLMS} is a small positive value added to avoid division by zero. As a result, the NLMS algorithm converges quicker than the LMS algorithm and becomes the most common adaptive filtering algorithm in practice. Although the convergence behavior of the NLMS algorithm is faster than the LMS algorithm, its convergence is still not fast enough when the input signal of the adaptive filter is spectrally coloured. To further improve the convergence of the NLMS

algorithm, some alternative solutions are introduced in the literature, including the RLS algorithm, the APA, and the PNLMS algorithm. However, those adaptive filter algorithms require an increase in the computational complexity.

In the RLS algorithm, the acoustic feedback path can be recursively updated as [45, 46]

$$\hat{\mathbf{f}}(k) = \hat{\mathbf{f}}(k-1) + \mathbf{\Theta}(k)\,\mathbf{y}(k)\,e(k), \tag{2.18}$$

$$\mathbf{\Theta}(k) = \frac{\mathbf{P}(k-1)}{\mathbf{y}^T(k)\,\mathbf{P}(k-1)\,\mathbf{y}(k) + \epsilon}, \tag{2.19}$$

$$\mathbf{P}(k) = \epsilon^{-1}\left[\mathbf{P}(k-1) - \mathbf{\Theta}(k)\,\mathbf{y}(k)\,\mathbf{y}^T(k)\,\mathbf{P}(k-1)\right], \tag{2.20}$$

where $0 < \epsilon < 1$ is the forgetting factor, and $\mathbf{P}(0) = \delta_{RLS}\mathbf{I}$ with the identity matrix $\mathbf{I}$ and the regularization factor δ_{RLS}.

In the APA, P most recent input vectors is exploited to estimate the IR of an adaptive filter, where P denotes the projection order. The acoustic feedback path is updated using the APA as follows [46]

$$\hat{\mathbf{f}}(k) = \hat{\mathbf{f}}(k-1) + \mu\mathbf{Y}(k)\left[\mathbf{Y}^T(k)\,\mathbf{Y}(k) + \delta_{APA}\mathbf{I}_P\right]^{-1}\mathbf{e}(k), \tag{2.21}$$

where $\mathbf{I}_P$ is the $P \times P$ identity matrix; δ_{APA} is a regularization factor; $\mathbf{Y}(k)$ and $\mathbf{e}(k)$ are the input matrix of adaptive filter $\hat{F}(q)$ and the error vector, respectively.

$$\mathbf{Y}(k) = \left[\mathbf{y}(k), \mathbf{y}(k-1), \ldots, \mathbf{y}(k-P+1)\right], \tag{2.22}$$

$$\mathbf{e}(k) = \mathbf{x}(k) - \mathbf{Y}^T(k)\,\hat{\mathbf{f}}(k),$$

where $\mathbf{x}(k) = [x(k), x(k-1), \ldots, x(k-P+1)]^T$ is the microphone vector of length P and $\mathbf{e}(k) = [e(k), e(k-1), \ldots, e(k-P+1)]^T$ is the error vector of length P. If $P = 1$, the APA becomes the NLMS algorithm.

The estimated computational complexity per iteration for above mentioned adaptive filtering algorithms are compared in terms of the number of real additions and real multiplications for real-valued data (cf. Table 2.2) and for complex-valued data (cf. Table 2.3) [46].

Table 2.2: A comparison of the estimated computational complexity per iteration for mentioned adaptive filtering algorithms for real-valued data.

Algorithms	Multiplications	Additions
LMS	$2L_{\hat{f}} + 1$	$2L_{\hat{f}}$
NLMS	$3L_{\hat{f}} + 1$	$3L_{\hat{f}}$
RLS	$L_{\hat{f}}^2 + 5L_{\hat{f}} + 1$	$L_{\hat{f}}^2 + 3L_{\hat{f}}$
APA	$(P^2 + 2P)\, L_{\hat{f}} + P^3 + P$	$(P^2 + 2P)\, L_{\hat{f}} + P^3 + P^2$

Table 2.3: A comparison of the estimated computational complexity per iteration for mentioned adaptive filtering algorithms for complex-valued data.

Algorithms	Multiplications	Additions
LMS	$8L_{\hat{f}} + 2$	$8L_{\hat{f}}$
NLMS	$10L_{\hat{f}} + 2$	$10L_{\hat{f}}$
RLS	$4L_{\hat{f}}^2 + 16L_{\hat{f}} + 1$	$4L_{\hat{f}}^2 + 12L_{\hat{f}} - 1$
APA	$4\left[(P^2 + 2P)\, L_{\hat{f}} + P^3 + P\right]$	$4\,(P^2 + 2P)\, L_{\hat{f}} + 4P^3 + 2P^2$

AFC using pre-filters

The AFC using pre-filters has been a promising method for reducing bias in the estimate of acoustic feedback path in hearing aids. In this method, a pre-filter, which is an estimated inverse model of the incoming signal, is used to pre-whiten the inputs of the adaptive filter $\hat{F}(q)$. The AFC methods using fixed pre-filters have been introduced in [47, 48] with an assumption that the incoming signal model $G^{-1}(q)$ was known and inversely stable. However, the incoming signal model practically is unknown and highly time-varying. Hence, it is necessary to adaptively estimate $G^{-1}(q)$. In [16], the so-called prediction error method based adaptive feedback cancellation (PEM) which employed the adaptive pre-filter has been proposed. Simulations in [16] showed that the PEM yielded a significant performance improvement compared to the standard AFC methods for both real speech and music as the incoming signals. It also provided better performance than the AFC method using fixed pre-filters proposed in [48]. Variants of the PEM have been studied in [31, 49, 50, 51, 52, 53].

Figure 2.4 illustrates the PEM model. The PEM is developed based on an

assumption that the incoming signal is modeled by passing a white Gaussian noise sequence $w(k)$ through a monic and inversely stable all-pole filter $G^{-1}(q)$, i.e.,

$$u(k) = G^{-1}(q)\, w(k). \tag{2.23}$$

The microphone and loudspeaker signals are pre-whitened by using the filter $\hat{G}(q)$ which is an estimate of $G(q)$ as follows

$$x_p(k) = \hat{G}(q)\, x(k), \tag{2.24}$$

$$y_p(k) = \hat{G}(q)\, y(k), \tag{2.25}$$

where $x_p(k)$ and $y_p(k)$ are the pre-whitened microphone signal and pre-whitened loudspeaker signal, respectively. Subtracting the estimation of pre-whitened feedback signal from the pre-whitened microphone signal yields the pre-whitened error signal $e_p(k)$ as

$$e_p(k) = x_p(k) - \hat{\mathbf{f}}^T \mathbf{y}_p(k), \tag{2.26}$$

where $\mathbf{y}_p(k) = \left[y_p(k), y_p(k-1), \ldots, y_p\left(k - L_{\hat{f}} + 1\right)\right]^T$ is a $L_{\hat{f}}$-dimensional vector representing the loudspeaker signal.

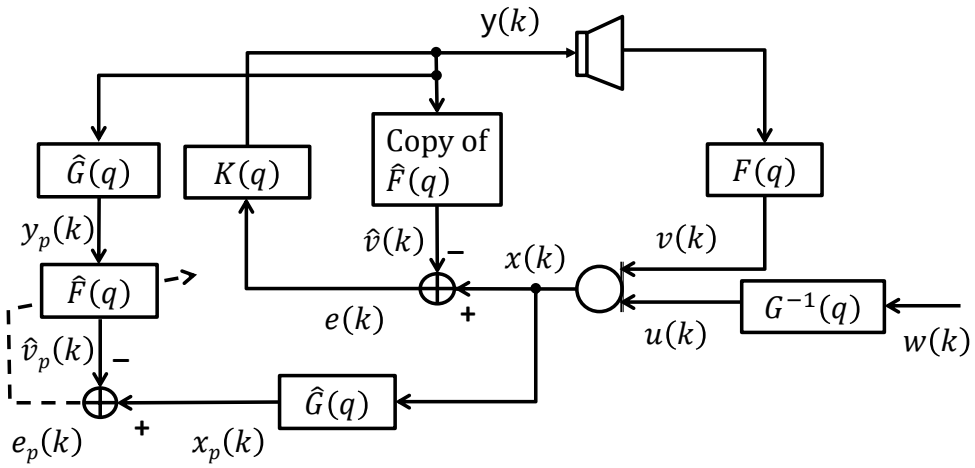

Figure 2.4: PEM model.

Minimizing the mean square pre-whitened error signal, $E\left\{e_p^2(k)\right\}$, results in the optimal weight vector of the estimated feedback path in the PEM as follows:

$$\hat{\mathbf{f}} = E\left\{\mathbf{y}_p(k)\, \mathbf{y}_p^T(k)\right\}^{-1} E\left\{\mathbf{y}_p(k)\, x_p(k)\right\}, \tag{2.27}$$

$$\hat{\mathbf{f}} = \mathbf{f} + \underbrace{\boldsymbol{R}_{\mathbf{y}_p}^{-1} \boldsymbol{r}_{\mathbf{y}_p u_p}}_{bias}, \tag{2.28}$$

where $u_p(k)$ is denoted as

$$u_p(k) = \hat{G}(q)\, u(k). \tag{2.29}$$

Substituting Eq. (2.23) and Eq. (2.29) into Eq. (2.28) yields a bias-free solution for the estimate of acoustic feedback path if the assumption in Eq. (2.23) is fulfilled, $\hat{G}(q) = G(q)$, and there exists at least one sample delay in the forward path [49].

In the PEM, the estimated coefficients of acoustic feedback path are recursively updated using the NLMS algorithm as follows

$$\hat{\mathbf{f}}(k) = \hat{\mathbf{f}}(k-1) + \frac{\mu}{\|\mathbf{y}_p(k)\|_2^2 + \delta_{NLMS}} \mathbf{y}_p(k)\, e_p(k). \tag{2.30}$$

Note that the accuracy of the feedback path estimate $\hat{F}(q)$ strongly depends on the accuracy of the incoming signal model estimate $\hat{G}(q)$ [47].

Subband techniques

Subband techniques for adaptive filtering were widely used to identify long IRs with hundreds to thousands of taps like the echo paths in the AEC contexts. Generally these techniques use an analysis filter bank to separate the input signal into subband signals. A short-length adaptive filter is implemented per subband in time-domain. The subband signals can be decimated to considerably lower the spectral dynamic range within a subband, resulting in an improvement in convergence rate. Then these subband signals can be interpolated and processed by using a suitable synthesis filter bank to produce an estimate of the original signal. The subband techniques do not only enhance convergence rate of adaptive filters but also reduce the computational complexity since multiple short-length adaptive filters are implemented instead of a long full-length adaptive filter. The conventional subband AEC approaches can be found in [54, 55, 56]. The disadvantages of those methods include a delay introduced in the signal path (to far-end) and a possible degradation of the

signal quality since the decimation in the subband implementation may cause aliasing effects [57, 58]. To remove that delay a new structure for subband AEC methods, namely delayless subband adaptive filter architecture in which the adaptive weights are computed in subbands, but collectively transformed into an equivalent set of fullband filter coefficients has been proposed for both active noise control and AEC applications [59, 60, 61, 62, 63, 64, 65]. This new architecture provides no delay in the signal path while retaining all benefits of the conventional subband adaptive filter such as fast convergence and low computational burden. Moreover, it can significantly reduce the aliasing effects.

Unlike the AEC systems, HAs suffer from the possibly strong correlation between the incoming signal and loudspeaker. Therefore, modified solutions of subband adaptive filter for the AFC in HAs are necessary. Commonly those solutions require some additional techniques such as either the PEM or multiple microphones to pre-whiten the inputs of adaptive filters, resulting in a significant reduction of that inherent correlation. In [66] an AEC/AFC method which integrates transform domain processing (TD) with the PEM is proposed. The idea is to apply a unitary orthogonal transform, e.g., the discrete Fourier transform (DFT) or discrete cosine transform (DCT), to the pre-whitened input signal of an adaptive filter. The DFT or DCT may be considered as a bank of parallel filters which is tuned to different portions of the bandwidth of the input signal. However, the DFT is not the optimum transform for speech input signals due to its complex coefficients. The DCT (with real coefficients) which is closer to the optimal Karhunen-Loeve transform (KLT) is preferred for speech input signals [67]. A combination of TD with two-microphone AFC (AFC2) is introduced in [68], called the AFC2-TD. In this method, the second microphone is used to eliminate the contribution of the incoming signal to the identification of the feedback path. As a result, less correlation is achieved, leading to less bias in the feedback path identification. In the AFC2-TD, the DFT or DCT is implemented not only for the input signal of the adaptive filter as in [66], but also for the error signal. An adaptive filter is used in each subband to adapt a specific portion of the bandwidth. Then the fullband adaptive filter is syn-

thesized by adding the estimated coefficients of those subband adaptive filters together [68]. The subband signals after transform domain process are almost uncorrelated to each other [45, 67]. The convergence rate of adaptive filtering algorithms in the transform domain can be enhanced since an appropriate power normalization can convert the input autocorrelation matrix to a normalized matrix whose eigenvalue spread will be much smaller than that of the original input signal. Although improving the convergence was the original contribution of TD adaptive filtering, it turns out that the implicit decorrelation of the transformed input vector can be exploited in the PEM-based AFC and AEC [66, 67].

A drawback of the DFT/DCT filter bank is its large degree of spectral overlap, leading to severe aliasing distortion. Thus alternative designs of filter banks with smaller spectral overlap and without a large increase in the computational complexity are desirable. The aliasing can be reduced by decimating the subband signals by a factor less than the number of subbands [69]. In [70] an AFC method which uses subband technique in conjunction with the PEM, FS and variable step-size (VSS) control has been proposed for HAs to cope with strongly correlated input signals such as music. In that work, the PEM and adaptation process are implemented in each subband, whereas the FS is applied to the fullband loudspeaker signal. The VSS algorithms are used in subband adaptive filters in order to further control the convergence rate of the system. In [71] a combination of the delayless subband technique [59] with the PEM [16] is suggested for the AFC in HAs. This approach uses the PEM to pre-whiten the fullband loudspeaker and microphone signals which are used to compute the pre-whitened error signal. Then the delayless subband technique is implemented such that the pre-whitened loudspeaker signal and pre-whitened error signal are input signals of analysis filter banks. The prototype filter used to generate analysis filter banks is the one typically used in the uniform DFT modulated filter bank method [72]. In [73] a delayless multiband-structured subband implementation of the feedback canceler, which is inspired from the idea of [58, 65], is integrated with the PEM to further reduce the aliasing and band-edge effects.

VSS techniques

The conventional NLMS algorithm employs a fixed step-size, which leads to a trade-off between the convergence/tracking rate and the steady-state error due to a high step-size corresponding to a fast convergence and a quick tracking rate but a high steady-state error while a low step-size corresponding to a slow convergence and a slow tracking rate but low steady-state error. Therefore, the VSS techniques provide potential solutions to improve that trade-off, resulting in a fast convergence, a quick tracking rate as well as a low steady-state error. Generally the VSS techniques use a discrete-time variable step-size $\mu(k)$ instead of a fixed step-size μ to estimate the acoustic feedback path. This variable step-size $\mu(k)$ is controlled in a way such that it tends to take large values when the system is unstable or close to instability (for example, in the beginning of the simulation or when the feedback path suddenly changes), and to take small values when the system converges. As a result, the system will converge fast while still maintaining a low steady-state error. The quick tracking rate is also obtained.

The VSS for NLMS (VSS-NLMS) algorithms are popular in the AEC contexts where the incoming signal and the loudspeaker are independent [74, 75, 76, 77, 78, 79, 80, 81, 82]. In most of the existing VSS-NLMS algorithms, the variable step-size is computed based on some parameters which are unknown or not easy to be tuned in practice. In [77] a fair comparison among several of those VSS-NLMS algorithms are considered. The non-parametric VSS NLMS (NPVSS-NLMS) which is introduced in [79] is one of the most compelling VSS algorithms. This algorithm computes the variable step-size $\mu(k)$ based on the power of system noise. In the AEC applications, this system noise is the near-end signal. For the single-talk scenario where the near-end signal contains only the background noise, this power can be estimated during silences. However, this power can not be found easily for the double-talk scenario where the near-end signal contains both the background noise and the near-end speech [83]. To overcome that problem, variants of the NPVSS-NLMS algorithms have been proposed in [80, 81]. In those algorithms the unknown power of the near-end

signal is approximated by using the combinations of other known parameters such as the estimated power of the loudspeaker signal, the estimated power of error signal, the estimated power of microphone signal, and the estimated correlation between the error signal and the loudspeaker. Besides the NLMS algorithm, the VSS techniques can be integrated with some other adaptive filtering algorithms such as the APA (called VSS-APA) [77, 84, 85, 86, 87], and the PNLMS/IPNLMS (VSS-PNLMS/-IPNLMS) algorithms [88].

Although the VSS techniques are popular for the AEC context, their applications for the AFC contexts are still limited due to the possible high correlation between the incoming signal and the loudspeaker. We found that not all VSS algorithms which are successfully applied to the AEC applications can work well in the AFC applications due to the remaining correlation [89]. Thus alternative solutions are required. The VSS techniques for the AFC in hearing aids can be found in [70, 90, 91]. In those techniques, first the above correlation needs to be reduced by means of injecting probe noise into the loudspeaker [90] or using (white) background noise and prefilters [91] or using a combination of prefilters, subband techniques and frequency shifting [40]. Then the VSS techniques are applied to estimate the acoustic feedback path. Other adaptive filtering algorithms such as the APA and the PNLMS algorithms can be integrated into the VSS techniques [92, 93, 94, 95, 96] for the AFC in HAs. However, the use of those algorithms may significantly increase computational complexity, especially when a high projection order is chosen. In [97], the AFC method which employs prefilters in conjunction with an affine combination of two NLMS adaptive filters has been proposed for HAs. This method is based on the idea that using prefilters to reduce the inherent correlation between the loudspeaker and the incoming signal, then combining the output of two adaptive filters with different step-sizes (one step-size is much larger than another) [98, 99, 100] to improve the system's performance.

2.4.2 MMSL AFC approaches

The performance of HAs can be improved by using multiple microphones for adaptive feedback cancellation. In general, the MMSL AFC approaches can

be classified into two groups. The first group focuses on using a linear beamformer to spatially filter the microphone or incoming signals (called the beamforming AFC group) [101, 102, 103] and the second group without use of any beamformer, but an FIR filter to adaptively estimate the incoming signal which is then removed from the filter adaptation process (called AFC2 group) [3, 104].

Beamforming AFC

A beamformer can be used in MMSL AFC methods for a combination of acoustic feedback cancellation and noise reduction [105, 106]. In these schemes, a beamformer is exploited at the outputs of microphones such that a strong beam can be steered towards the target direction and zeroes can be steered to other directions. The beamformer can be either fixed or adaptive. In a fixed beamformer, the filter coefficients are data-independent, i.e., they do not depend on the change of the acoustic environment. In contrast, the filter coefficients of an adaptive beamformer are data-dependent, i.e., they are adapted to respond to time-varying acoustic environment [102]. In [101, 107] the acoustic feedback has been canceled by using multi-channel adaptive system, then a traditional linear beamformer [108] is applied to the error signals in order to perform spatial filtering of the incoming signals, see Figure 2.5. In [109] a fixed beamformer is integrated into a novel developed earpiece [110] which consists of three microphones and one loudspeaker. The loudspeaker is placed in the vent, whereas one microphone is placed in the concha, one in the ear canal and the another one in the vent close to the loudspeaker. This beamformer is designed such that it steers a spatial null in the direction of the hearing aid loudspeaker, thus the acoustic feedback signal from loudspeaker can be ideally suppressed.

In principle, the beamformer can be applied either on the microphone signals (i.e., before the AFC process) or on the error signals (i.e., after the AFC process). In the former case, a single-channel AFC is implemented on the beamformer processed output signal. This setup provides less computational complexity, but the beamformer may cause negative impact on the feedback cancellation process, leading to signal distortion. In the latter case, a multi-channel AFC

is required. This increases the computational complexity, but there is no effect of the beamformer on the feedback cancellation process [111]. Figure 2.5 illustrates the MMSL AFC with beamformer located after AFC process [101, 107].

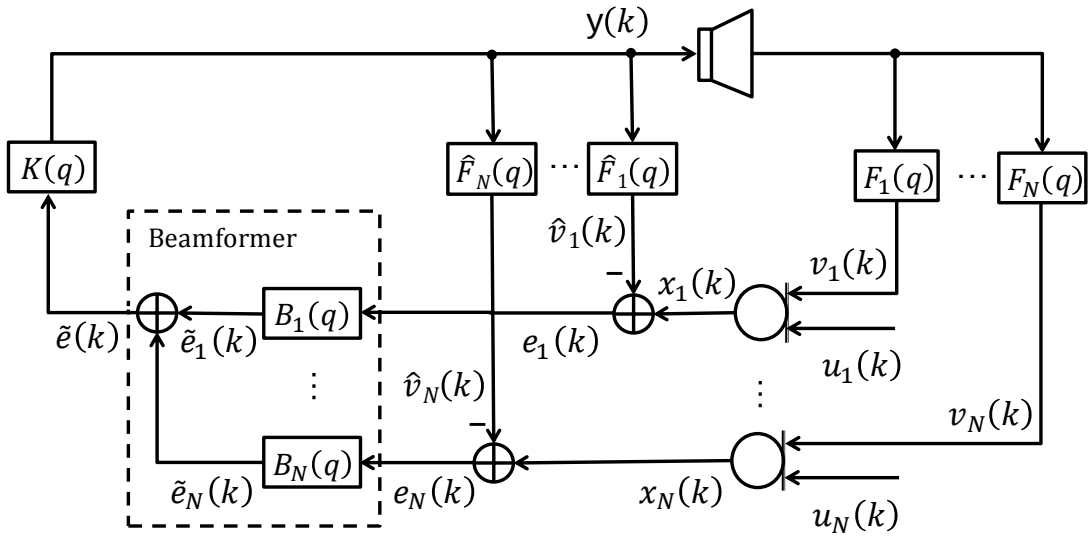

Figure 2.5: MMSL AFC with beamformer located after AFC process.

AFC2 method review

Recently, the AFC system using two microphones and one loudspeaker introduced in [3, 104] has become a potential method. It is known that in the standard AFC method the incoming signal behaves as a disturbance for the identification of the feedback path. Therefore, the main idea of the AFC2 method is to remove the contribution of the incoming signal in the identification process of the adaptive filter. To do that the second microphone is added and an estimate of the relative transfer function between two microphones, $\hat{H}(q)$, is used to compute the estimate of the incoming signal. Then the estimated incoming signal $\hat{u}_1(k)$ is subtracted from the error signal $e_1(k)$, resulting in a new error signal $e(k)$. This new error signal is used to control the adaptation process in adaptive filters $\hat{F}_1(q)$ and $\hat{H}(q)$.

Figure 2.6 illustrates the AFC2 model, in which the main microphone is located in the ear canal (Mic1) and the second microphone (Mic2) is placed behind the ear. The loudspeaker is placed near the main microphone (Mic1). The distance between the two microphones needs to be far enough to ensure that the second feedback signal is more attenuated than the first feedback signal [3, 104]. Each

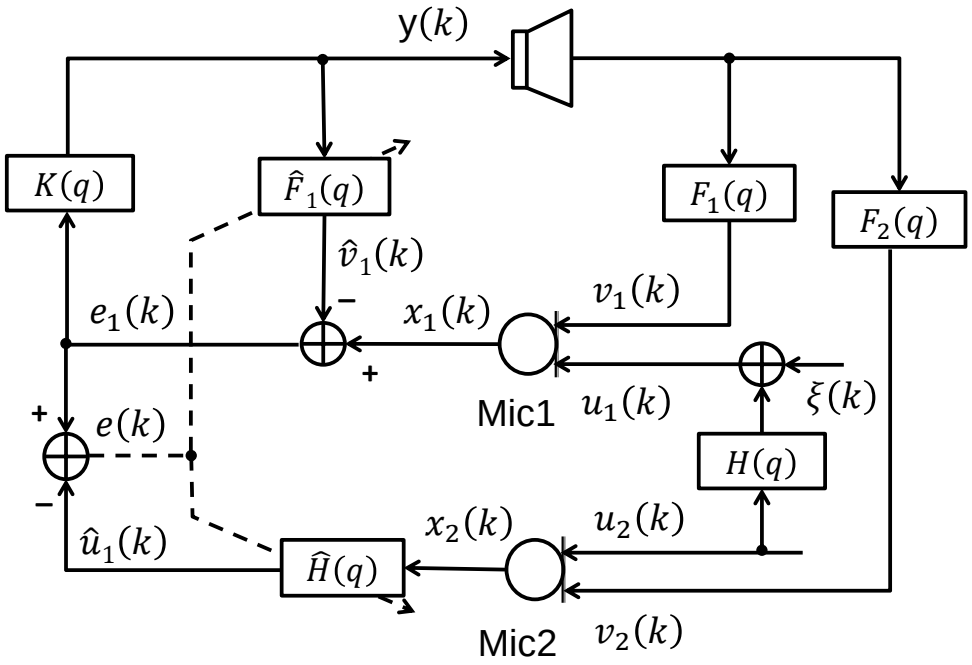

Figure 2.6: AFC2 model.

microphone receives the incoming signal from the surrounding environment as well as a feedback signal, i.e.,

$$x_1(k) = u_1(k) + \mathbf{f}_1^T \mathbf{y}(k), \tag{2.31}$$

$$x_2(k) = u_2(k) + \mathbf{f}_2^T \mathbf{y}(k), \tag{2.32}$$

where $\mathbf{f}_i = \left[f_{i,0}, f_{i,1}, \ldots, f_{i,L_f-1}\right]^T$ with $i = 1, 2$ is a FIR filter of length L_f modeling the ith acoustic feedback path; $\mathbf{y}(k)$ is the loudspeaker signal vector of length L_f and $u_i(k)$ is the incoming signal received at the ith microphone. The filter $\mathbf{f}_i$ is represented as $F_i(q) = \mathbf{f}_i^T \mathbf{q}$. Assuming that the incoming signals at both microphones are related as

$$u_1(k) = \mathbf{h}^T \mathbf{u}_2(k) + \xi(k), \tag{2.33}$$

where $\mathbf{h} = [h_0, h_1, \ldots, h_{L_h-1}]^T$ is the impulse response of the relative transfer function (RTF) $H(q)$ of length L_h, $\mathbf{u}_2(k)$ is a vector of the second incoming signal with an appropriate length and $\xi(k)$ is the residual error caused by undermodeling the RTF.

As mentioned above, the second microphone provides additional information. This information is utilized to estimate the first incoming signal $u_1(k)$ which is then subtracted from the error signal $e_1(k)$, forming a new error signal $e(k)$, i.e.,

$$e(k) = e_1(k) - \hat{u}_1(k), \tag{2.34}$$

where

$$\begin{aligned} e_1(k) &= x_1(k) - \hat{v}_1(k) \\ &= u_1(k) + \left(\mathbf{f}_1^T - \hat{\mathbf{f}}_1^T\right)\mathbf{y}(k), \end{aligned} \tag{2.35}$$

and

$$\hat{u}_1(k) = \hat{\mathbf{h}}^T \mathbf{x}_2(k), \tag{2.36}$$

where $\hat{\mathbf{f}}_1$ is the estimate of $\mathbf{f}_1$, $\hat{v}_1(k) = \hat{\mathbf{f}}_1^T \mathbf{y}(k)$ is the output of the feedback canceler, $\mathbf{x}_2(k) = [x_2(k), x_2(k-1), \ldots, x_2(k-L_{\hat{h}}+1)]^T$ is a $L_{\hat{h}}$-dimensional vector denoting the second microphone signal and $\hat{\mathbf{h}} = \left[\hat{h}_0, \hat{h}_1, \ldots, \hat{h}_{L_{\hat{h}}-1}\right]^T$ is a vector of length $L_{\hat{h}}$ representing the IR of the FIR filter $\hat{H}(q)$ used to identify $H(q)$.

The loudspeaker signal is equal to

$$y(k) = K(q)\, e_1(k). \tag{2.37}$$

The error signal $e(k)$ is used to control the adaptation processes of both $\hat{F}_1(q)$ and $\hat{H}(q)$, resulting in a lower bias [3].

Theoretical analysis

In this part, the theoretical analysis for the AFC2 method, which was derived in [3], is briefly reviewed.

Substituting Eq. (2.36), Eq. (2.33), and Eq. (2.32) into Eq. (2.34) leads to

$$\begin{aligned} e(k) &= \left(\mathbf{f}_1^T - \hat{\mathbf{f}}_1^T\right)\mathbf{y}(k) + \left(\mathbf{h}^T - \hat{\mathbf{h}}^T\right)\mathbf{u}_2(k) \\ &\quad - \mathbf{f}_{2_{\hat{\mathbf{h}}}}^T \mathbf{y}(k) + \xi(k) \\ &= \bar{\mathbf{f}}_1^T \mathbf{y}(k) + \bar{\mathbf{h}}^T \mathbf{u}_2(k) - \mathbf{f}_{2_{\hat{\mathbf{h}}}}^T \mathbf{y}(k) + \xi(k), \end{aligned} \tag{2.38}$$

where $\bar{\mathbf{f}}_1 = \mathbf{f}_1 - \hat{\mathbf{f}}_1$, $\bar{\mathbf{h}} = \mathbf{h} - \hat{\mathbf{h}}$ and $\mathbf{f}_{2_{\hat{\mathbf{h}}}} = \left[f_{2_{\hat{\mathbf{h}},0}}, \ldots, f_{2_{\hat{\mathbf{h}},L_{f-1}}} \right]^T$ is the coefficient vector of product $\hat{H}(q) F_2(q)$.

Let $\mathbf{x}(k) = [\mathbf{y}^T(k) \;\; \mathbf{u}_2^T(k)]^T$, $\mathbf{z}(k) = [\mathbf{y}^T(k) \;\; \mathbf{0}^T]^T$, and the vectors $\bar{\mathbf{a}}$ and $\bar{\mathbf{b}}$ be defined as

$$\bar{\mathbf{a}} = \left[\bar{\mathbf{f}}_1^T \;\; \bar{\mathbf{h}}^T \right]^T, \tag{2.39}$$

$$\bar{\mathbf{b}} = \left[\mathbf{f}_{2_{\hat{\mathbf{h}}}}^T \;\; \mathbf{0}^T \right]^T, \tag{2.40}$$

where the null vectors have the dimension of $L_{\hat{h}}$.

Then the error signal $e(k)$ can be reformulated as

$$e(k) = \bar{\mathbf{a}}^T \mathbf{x}(k) - \bar{\mathbf{b}}^T \mathbf{z}(k) + \xi(k). \tag{2.41}$$

Minimizing the cost function $J(\bar{\mathbf{a}}) = E\{e^2(k)\}$ with respect to $\bar{\mathbf{a}}$ results in the following so-called optimal solution

$$\bar{\mathbf{a}}_o = \begin{bmatrix} \bar{\mathbf{f}}_{1_o} \\ \bar{\mathbf{h}}_o \end{bmatrix} = \boldsymbol{R}_{\mathbf{x}}^{-1} \boldsymbol{R}_{\mathbf{xz}} \bar{\mathbf{b}} - \boldsymbol{R}_{\mathbf{x}}^{-1} \boldsymbol{r}_{\mathbf{x}\xi}. \tag{2.42}$$

As we can see from Eq. (2.39) and Eq. (2.40), the term $\hat{\mathbf{h}}$ appears in both definitions of $\bar{\mathbf{a}}$ and $\bar{\mathbf{b}}$, so that the "so-called" optimal solution for $\min_{\bar{\mathbf{a}}} \{E\{e^2(k)\}\}$ received in Eq. (2.42) is actually not an optimal solution for $\bar{\mathbf{a}}$. In this thesis a correct derivation is presented.

Acoustic echo cancellation (AEC) vs. acoustic feedback cancellation

The acoustic echo problem often occurs in the hands-free telephone sets and teleconferencing systems, where the loudspeaker receives speech signal from far-end. Then a part of acoustic signal radiated from the loudspeaker is fed back to the remote user via the microphone, which is considered as the so-called echo [112]. Similar to the feedback path, the echo path may be time varying according to the change of the acoustic environment in the room, e.g., opening or closing doors/windows, people moving around the room. Figure 2.7 demonstrates a conventional AEC model with SMSL. Like in the AFC

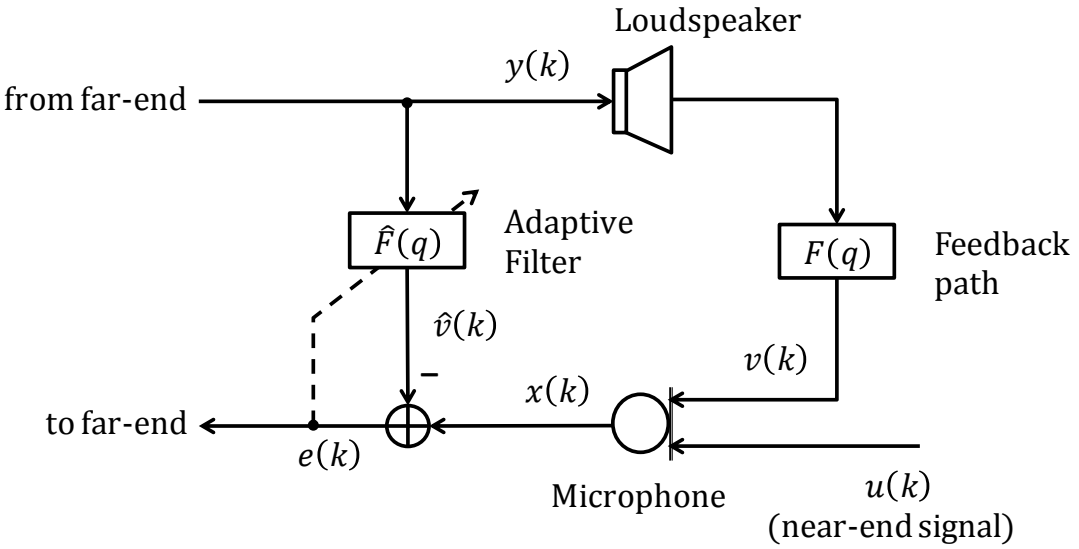

Figure 2.7: Conventional AEC model.

methods, an adaptive filter is also used in the AEC methods to estimate the echo path $F(q)$. The estimated echo path then is used to compute the estimated echo signal $\hat{v}(k)$ which is subtracted from the microphone signal $x(k)$ to form the error signal $e(k)$. Since the acoustic echo problem looks alike the acoustic feedback problem, some solutions dealt with both AEC and AFC have been proposed in the literature [66, 101, 107]. In contrast to the AFC systems in which the microphone signal consists of the feedback signal and the incoming signal (near-end signal), the microphone signal in the AEC systems may include either the echo signal (in the scenario of single-talk) or both the echo signal and the near-end signal (in the scenario of double-talk). Double-talk occurs when both far-end speech and near-end speech are available at the same time. Thus the echo problem in the double-talk scenario seem to be similar to the feedback problem. However, the major difference between the AEC and AFC systems is the absence of the forward path which is apparent in the AFC systems. In the AEC systems the loudspeaker signal comes from the far-end, while the error signal is sent to the far-end. The near-end and the far-end here mean the receiving and the transmitting ends of a communication channel, respectively. Therefore, the AEC systems are considered as open-loop systems, whereas the AFC systems are closed-loop systems.

The main problems in AEC systems are the double-talk and the non-uniqueness

problems. To solve the double-talk problem a double-talk detector (DTD) is implemented in order to detect the presence of the near-end signal. When the near-end signal is detected, the adaptive process is temporarily slowed down or frozen. Many solutions for the DTD can be found in [113, 114, 115, 116]. The non-uniqueness problem [117] is caused by the strong correlation among loudspeaker signals in stereo or multi-channel audio systems. Solutions for the non-uniqueness problem can be found in [117] .

Due to the differences between the AEC and AFC problems, some solutions for the AEC problem may not work effectively for the AFC problem and vice versa. Thus alternative solutions for the AFC problem are desirable.

2.5 Evaluating performance of AFC methods

As aforementioned, the acoustic feedback systems suffer from the acoustic feedback problem that deteriorates the signal quality as well as degrades the maximum achievable amplification. Recently, the most common and efficient acoustic feedback control methods are adaptive feedback cancellation (AFC) methods, where an adaptive filter is used in the feedback canceler's path to estimate the true feedback path. To evaluate and compare the performance of different AFC methods both objective and subjective tests can be used. The objective tests carry out measures based on the computer simulations, whereas the subjective tests use measures based on listeners. In the scope of this thesis, only the objective measures are considered. In particular, three most common objective measures including misalignment, maximum stable gain and added stable gain are used to evaluate the performance of AFC methods for hearing aids.

The misalignment (MIS) measures the distance between the true and the estimated feedback path [49, 118], i.e.,

$$\mathrm{MIS} = 10\log_{10}\left(\frac{\int_0^{\pi}\left|F\left(e^{j\omega}\right) - e^{-j\omega d_{fb}}\hat{F}\left(e^{j\omega}\right)\right|^2 \mathrm{d}\omega}{\int_0^{\pi}\left|F\left(e^{j\omega}\right)\right|^2 \mathrm{d}\omega}\right), \tag{2.43}$$

where d_{fb} is a delay in the feedback canceler's path; $F\left(e^{j\omega}\right)$ and $\hat{F}\left(e^{j\omega}\right)$ are frequency responses of the true and estimated feedback path at the normalized

angular frequency ω, respectively.

The maximum stable gain (MSG) is defined as the largest gain assuming a flat frequency response $K(q)$ for hearing aid [49, 118], i.e.,

$$\mathrm{MSG} = 10\log_{10}\left(\min_{\omega}\frac{1}{\left|F\left(e^{j\omega}\right) - e^{-j\omega d_{fb}}\hat{F}\left(e^{j\omega}\right)\right|^2}\right). \tag{2.44}$$

The added stable gain (ASG) is defined as the additional gain which is possible by using the feedback canceler [49], i.e.,

$$\mathrm{ASG} = \mathrm{MSG} - 10\log_{10}\left(\min_{\omega}\frac{1}{\left|F\left(e^{j\omega}\right)\right|^2}\right). \tag{2.45}$$

Moreover, the perceptual evaluation of speech quality (PESQ) [119, 120] is also used to measure speech quality. In the PESQ measure, two speech inputs are required, one of them is the reference (original) speech signal and the other is the test (degraded) signal. The value of the speech quality at the output of the PESQ measure is in the range $[-0.5, 4.5]$, where the values around 4.5 means excellent signal quality and the values around -0.5 means very poor signal quality.

To measure audio quality the perceptual evaluation of audio quality (PEAQ) [121] is used. Similar to the PESQ measure, the PEAQ measure also requires an original audio signal as a reference and the other audio signal as a test (degraded) signal. The grades of the audio quality at the output of the PEAQ measure are in the range $[-4, 0]$, where the values around 0 means very good signal quality and the values around -4 means very poor signal quality. Table 2.4 shows the grades of the PEAQ measure corresponding to signal quality [122].

2.6 Conclusions

Using HAs is the most common and simplest treatment for hearing impaired people. However, HAs cope with acoustic feedback problem which reduces the maximum amplification as well as the signal quality of HAs. Among acoustic feedback control approaches the adaptive feedback cancellation approaches are

Table 2.4: PEAQ measures.

Grades	Description of impairments
0	Imperceptible
-1	Perceptible but not annoying
-2	Slightly annoying
-3	Annoying
-4	Very annoying

most efficient. Unfortunately, the standard AFC approach results in a bias in estimation of the feedback path due to the possibly high correlation between the loudspeaker and the incoming signal of a HA. To tackle this bias, either the SMSL AFC solutions such as the AFC using pre-filter, the AFC using subband techniques and the AFC with VSS algorithms or the MMSL solutions such as the beamformer or the AFC2 methods have been introduced in the literature. Some of existing AFC methods can significantly reduce this bias, but there is still a room to further lower it, leading to a further performance enhancement.

The following chapters aim at filling that room by proposing novel AFC methods which are strong at either reducing the bias in the estimate of feedback path or improving the convergence/tracking rates while preserving good signal quality when the incoming signal is spectrally coloured. Moreover, these proposed methods are robust toward different types of incoming signals and sudden changes in the feedback paths. In the next chapter, a new AFC method which is developed based on the AFC2 method will be proposed.

CHAPTER 3

Two-Microphone Adaptive Feedback Cancellation Techniques

Chapter's key points:

- New insights into AFC2
- PEM-AFC2
- Experimental results

3.1 Introduction

The standard SMSL AFC method faces a large bias in the estimate of feedback path. This bias is a result of the high correlation between the loudspeaker and the incoming signal [20]. A vast range of solutions for SMSL AFC have been proposed in the literature to reduce that bias [15, 16, 48, 66, 68, 70, 71, 77, 90, 93, 123]. Among them the AFC methods using pre-filter, or employing subband techniques or applying variable step-size control algorithms are the most common methods. Among the AFC methods using pre-filter, the PEM [16] is a dominant method. In the PEM, a pre-filter which is the estimate of the inverse model of the incoming signal is used to pre-whiten the input signals of the adaptive filter, resulting in significant performance improvement. However, the quality of the identification of the feedback path strongly depends on the accuracy of the estimate of the inverse incoming signal model [31]. Moreover, the PEM does not cope well with the periodic incoming signals [124]. Subband techniques [54, 58, 125] use an analysis filter bank to separate the inputs of the adaptive filter into narrower frequency bins. The adaptive process has been carried in each subband. The subband techniques can reduce the com-

putational complexity as well as enhance the convergence of adaptive filters. However, the conventional subband method often yields a delay and aliasing effects, leading to a possible degradation of the signal quality. To tackle that problem some delayless subband AFC methods have been investigated in [59, 71, 72, 65]. Other effective subband solutions which integrate transform domain into the PEM or into the AFC2 method have been introduced in [66, 68]. In those transform domain AFC methods, the analysis filter bank is created by using a unitary orthogonal transform (DFT or DCT) and the fullband adaptive filter is synthesized by adding the estimated coefficients of subband adaptive filters together [68]. The disadvantage of the DFT/DCT filter bank is its large degree of spectral overlap, resulting in severe aliasing distortion [69]. A combination of subband technique, pre-filter, FS and VSS was proposed in [40, 70] for AFC in HAs with music as the incoming signal. The AFC methods using VSS algorithms for HAs are discussed in detail in Chapter 5.

It can be seen from the recent research that the AFC is integrated with other techniques/algorithms for acoustic feedback control, resulting in far more robust AFC methods compared to the standard AFC method [2]. Following this trend this chapter proposes a new AFC solution based on the AFC2 method for HAs, called the PEM-AFC2, which integrates the PEM into the AFC2 method. In the proposed method, PEM-AFC2, the two-microphone adaptive feedback control (AFC2) method with two microphones and one loudspeaker is used. The incoming signals at the two microphones are related by a relative transfer function (RTF) which is used to predict the incoming signal at the main microphone. In addition, a pre-filter is employed to pre-whiten the loudspeaker and the microphone signals before the adaptive filter estimates. Derivations demonstrate that the proposed method yields a lower bias than either the PEM or the AFC2 method. A new derivation for optimal filters in the AFC2 method is also provided. The performance of the proposed method is evaluated for speech shaped noise (SSN) as incoming signal and with undermodeling the RTF as well as with perfect modeling the RTF. Moreover, different types of incoming signals and a sudden change of feedback paths are also considered. The experimental results show that the proposed approach yields a significant

performance improvement compared to existing popular AFC methods such as the PEM and the AFC2. Thus far, to the author's knowledge, studies into this AFC combination have not been reported. The results of this chapter have been presented in the author's journal article [126] (accepted).

3.2 New insights into AFC using two microphones for HA

As discussed in Section 2.4.2, the "so-called" optimal solution in Eq. (2.42) is in fact not an optimal solution due to the dependency on $\hat{\mathbf{h}}$. Therefore, an alternative derivation to completely solve that problem needs to be investigated. In the following a new derivation for the AFC2 is proposed. Considering that $\xi(k)$ is the residual error caused by undermodeling the RTF ($\xi(k) \neq 0$) , i.e.,

$$\xi(k) = \mathbf{h}_{res}^T \mathbf{u}_2(k), \tag{3.1}$$

where $\mathbf{h}_{res} = [\underbrace{0,\ldots,0}_{L_h}, h_{L_h},\ldots,h_{L_{h_{full}}-1}]^T$ is the impulse response of $H_{res}(q)$. The full RTF has impulse response $\mathbf{h}_{full} = \mathbf{h}+\mathbf{h}_{res}$, where $\mathbf{h} = [h_0,\ldots,h_{L_h-1}, \underbrace{0,\ldots,0}_{L_{h_{full}}-L_h}]^T$, $L_{h_{full}}$ is the length of $\mathbf{h}_{full}$.

The vector $\hat{\mathbf{h}}$ is now defined as $\hat{\mathbf{h}} = [\hat{h}_0,\ldots,\hat{h}_{L_{\hat{h}}-1}, \underbrace{0,\ldots,0}_{L_{h_{full}}-L_{\hat{h}}}]^T$ with $L_{\hat{h}} = L_h$.

In the new derivation, the error signal $e(k)$ can be obtained by substituting Eq. (2.33), Eq. (2.35), and Eq. (2.36) into Eq. (2.34), i.e.,

$$\begin{aligned} e(k) = {} & \mathbf{h}^T \mathbf{u}_2(k) + \xi(k) + \left(\mathbf{f}_1^T - \hat{\mathbf{f}}_1^T\right)\mathbf{y}(k) \\ & - \hat{\mathbf{h}}^T \mathbf{x}_2(k), \end{aligned} \tag{3.2}$$

where $\mathbf{u}_2(k)$ and $\mathbf{x}_2(k)$ are defined in a manner analogous to those described in Section 2.4.2, but with the length $L_{h_{full}}$.

Let $\mathbf{z}_1(k) = [\mathbf{y}^T(k) \;\; \mathbf{x}_2^T(k)]^T$, $\mathbf{z}_2(k) = [\mathbf{y}^T(k) \;\; \mathbf{u}_2^T(k)]^T$, $\mathbf{a} = \left[\hat{\mathbf{f}}_1^T \;\; \hat{\mathbf{h}}^T\right]^T$, and $\mathbf{b} =$

$[\mathbf{f}_1^T \ \mathbf{h}^T]^T$. The cost function is now defined as

$$\begin{aligned} J(\mathbf{a}) &= E\left\{e^2(k)\right\} \\ &= E\left\{\left[\mathbf{a}^T\mathbf{z}_1(k) - \left(\mathbf{b}^T\mathbf{z}_2(k) + \xi(k)\right)\right]^2\right\}. \end{aligned} \tag{3.3}$$

Minimizing the cost function in Eq. (3.3) results in the optimal solution

$$\mathbf{a}_o = \begin{bmatrix} \hat{\mathbf{f}}_{1_o} \\ \mathbf{h}_o \end{bmatrix} = \boldsymbol{R}_{\mathbf{z}_1}^{-1}\boldsymbol{R}_{\mathbf{z}_1\mathbf{z}_2}\mathbf{b} + \boldsymbol{R}_{\mathbf{z}_1}^{-1}\boldsymbol{r}_{\mathbf{z}_1\xi}. \tag{3.4}$$

The derivations for computing the terms $\boldsymbol{R}_{\mathbf{z}_1}^{-1}\boldsymbol{R}_{\mathbf{z}_1\mathbf{z}_2}\mathbf{b}$ and $\boldsymbol{R}_{\mathbf{z}_1}^{-1}\boldsymbol{r}_{\mathbf{z}_1\xi}$ are outlined in Appendix A. Hence,

$$\boldsymbol{R}_{\mathbf{z}_1}^{-1}\boldsymbol{R}_{\mathbf{z}_1\mathbf{z}_2}\mathbf{b} = \begin{bmatrix} \mathbf{f}_1 - \mathbf{f}_{2_\mathbf{h}} \\ \mathbf{h} \end{bmatrix}, \tag{3.5}$$

$$\boldsymbol{R}_{\mathbf{z}_1}^{-1}\boldsymbol{r}_{\mathbf{z}_1\xi} = \begin{bmatrix} \boldsymbol{B}_1 \\ \boldsymbol{B}_\mathbf{h} \end{bmatrix}, \tag{3.6}$$

where $\mathbf{f}_{2_\mathbf{h}}$ is a coefficient vector of the product $H(q)F_2(q)$ and

$$\boldsymbol{B}_\mathbf{h} = \boldsymbol{N}^T\boldsymbol{r}_{\mathbf{y}\xi} + \boldsymbol{Q}\boldsymbol{r}_{\mathbf{x}_2\xi}, \tag{3.7}$$

$$\boldsymbol{B}_1 = \boldsymbol{R}_\mathbf{y}^{-1}\boldsymbol{r}_{\mathbf{y}\xi} + \left(\boldsymbol{N}\boldsymbol{r}_{\mathbf{x}_2\xi} - \boldsymbol{N}\boldsymbol{R}_{\mathbf{x}_2\mathbf{y}}\boldsymbol{R}_\mathbf{y}^{-1}\boldsymbol{r}_{\mathbf{y}\xi}\right), \tag{3.8}$$

with $\boldsymbol{N} = -\boldsymbol{R}_\mathbf{y}^{-1}\boldsymbol{R}_{\mathbf{y}\mathbf{x}_2}\left(\boldsymbol{R}_{\mathbf{x}_2} - \boldsymbol{R}_{\mathbf{x}_2\mathbf{y}}\boldsymbol{R}_\mathbf{y}^{-1}\boldsymbol{R}_{\mathbf{y}\mathbf{x}_2}\right)^{-1}$, $\boldsymbol{Q} = \left(\boldsymbol{R}_{\mathbf{x}_2} - \boldsymbol{R}_{\mathbf{x}_2\mathbf{y}}\boldsymbol{R}_\mathbf{y}^{-1}\boldsymbol{R}_{\mathbf{y}\mathbf{x}_2}\right)^{-1}$.

Therefore, the optimal solution in Eq. (3.4) can be rewritten as

$$\hat{\mathbf{f}}_{1_o} = \mathbf{f}_1 - \mathbf{f}_{2_\mathbf{h}} + \boldsymbol{B}_1, \tag{3.9}$$

$$\mathbf{h}_o = \mathbf{h} + \boldsymbol{B}_\mathbf{h}. \tag{3.10}$$

For perfect modeling case, $\xi(k) = 0$, hence $\boldsymbol{r}_{\mathbf{y}\xi} = \boldsymbol{r}_{\mathbf{x}_2\xi} = \mathbf{0}$. The Eq. (3.7) - Eq. (3.10) can be reformulated as

$$\boldsymbol{B}_\mathbf{h} = \mathbf{0}, \tag{3.11}$$

$$\boldsymbol{B}_1 = \mathbf{0}, \tag{3.12}$$

$$\hat{\mathbf{f}}_{1_o} = \mathbf{f}_1 - \mathbf{f}_{2_\mathbf{h}}, \tag{3.13}$$

$$\mathbf{h}_o = \mathbf{h}. \tag{3.14}$$

In this case, there is no bias in the estimate of $H(q)$ and the accuracy of identification of $F_1(q)$ now only depends on the value of $\mathbf{f}_{2_\mathbf{h}}$. Thus, if the second feedback path $\mathbf{f}_2$ is weak compared to the first feedback path due to their assigned positions, i.e., $\mathbf{f}_2 \approx \mathbf{0}$, an unbiased estimate may be obtained. In practice, it is not possible to have $\mathbf{f}_2 \approx \mathbf{0}$ since the distance between the loudspeaker and the second microphone could not be too far due to the small size of a hearing aid. Moreover, $\xi(k)$ is not zero since it is difficult to model a physical system with no error.

In the AFC2 method, the optimal weight vectors $\hat{\mathbf{f}}_{1_o}$ and $\mathbf{h}_o$ in Eq. (3.4) can be recursively estimated as follows

$$\hat{\mathbf{f}}_1(k) = \hat{\mathbf{f}}_1(k-1) + \frac{\mu}{\|\mathbf{y}(k)\|_2^2 + \delta}\mathbf{y}(k)\, e(k), \tag{3.15}$$

$$\hat{\mathbf{h}}(k) = \hat{\mathbf{h}}(k-1) + \frac{\mu}{\|\mathbf{x}_2(k)\|_2^2 + \delta}\mathbf{x}_2(k)\, e(k), \tag{3.16}$$

where $e(k)$ is defined as in Eq. (3.2) and δ is a positive regularization factor.

3.3 Prediction error method based AFC for two-microphone HAs

The proposed PEM-AFC2 is based on the combination of two widely known methods, the PEM-AFC (a synonym of the PEM) and the AFC2. As a result, the proposed method inherits the benefits of both methods including lower bias terms, faster tracking rate as well as robust against different types of incoming signals and against sudden changes in the acoustic feedback paths. This section provides the theoretical analysis of the PEM-AFC2 in detail. This analysis is inspired from derivation of the PEM in [16] and the new derivation of the AFC2 in Section 3.2. The proposed derivations show that by pre-whitening the inputs of adaptive filters in the AFC2 method, the bias terms in the identifications of

the feedback channel $\hat{F}_1(q)$ and the FIR filter $\hat{H}(q)$ can be significantly reduced.

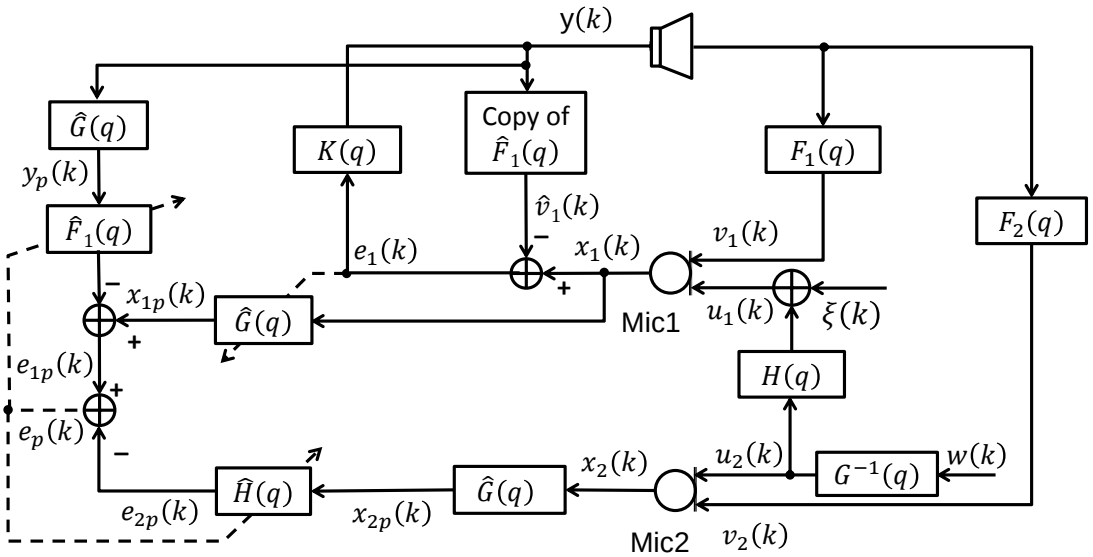

Figure 3.1: PEM-AFC2 model.

Figure 3.1 illustrates the proposed PEM-AFC2 model. Assuming that the second incoming signal $u_2(k)$ can be modeled as follows

$$u_2(k) = G^{-1}(q)\, w(k), \tag{3.17}$$

where $w(k)$ is a zero-mean, white Gaussian noise sequence and $G^{-1}(q)$ is a monic and inversely stable all-pole filter.

The loudspeaker and microphone signals are pre-whitened by $\hat{G}(q)$ which is an estimate of $G(q)$, before they are fed into adaptive filters. The pre-whitened error signal can be calculated as

$$e_p(k) = e_{1p}(k) - e_{2p}(k), \tag{3.18}$$

where $e_{1p}(k) = x_{1p}(k) - \hat{F}_1(q)\, y_p(k)$ and $e_{2p}(k) = \hat{H}(q)\, x_{2p}(k)$. The pre-whitened microphone and loudspeaker signals are defined as

$$x_{1p}(k) = \hat{G}(q)\, x_1(k), \tag{3.19}$$

$$x_{2p}(k) = \hat{G}(q)\, x_2(k), \tag{3.20}$$

$$y_p(k) = \hat{G}(q)\, y(k). \tag{3.21}$$

The error signal $e_p(k)$ is used to control the adaptive process in filters $\hat{F}_1(q)$ and $\hat{H}(q)$. By substituting Eq. (2.31) and Eq. (2.33) into Eq. (3.19) the pre-whitened microphone signal $x_{1p}(k)$ can be reformulated as follows

$$\begin{aligned} x_{1p}(k) &= \hat{G}(q)\left[u_1(k) + \mathbf{f}_1^T \mathbf{y}(k)\right] \\ &= \mathbf{h}^T \mathbf{u}_{2p}(k) + \xi_p(k) + \mathbf{f}_1^T \mathbf{y}_p(k), \end{aligned} \tag{3.22}$$

where $\xi_p(k) = \hat{G}(q)\,\xi(k)$.

Hence, the pre-whitened error signal in Eq. (3.18) can be rewritten as

$$e_p(k) = \mathbf{h}^T \mathbf{u}_{2p}(k) + \xi_p(k) + \left(\mathbf{f}_1^T - \hat{\mathbf{f}}_1^T\right)\mathbf{y}_p(k) - \hat{\mathbf{h}}^T \mathbf{x}_{2p}(k). \tag{3.23}$$

Assuming that the adaptation of $\hat{G}(q)$ is decoupled from the adaptation of $\hat{F}_1(q)$ and $\hat{H}(q)$. The cost function for the PEM-AFC2 is denoted as

$$\begin{aligned} J(\mathbf{a}) &= E\left\{e_p^2(k)\right\} \\ &= E\left\{\left[\mathbf{a}^T \mathbf{z}_{1p}(k) - \left(\mathbf{b}^T \mathbf{z}_{2p}(k) + \xi_p(k)\right)\right]^2\right\}, \end{aligned} \tag{3.24}$$

where $\mathbf{a}$, $\mathbf{b}$ are defined in a manner analogous to those in Section 3.2, and $\mathbf{z}_{1p}(k) = \left[\mathbf{y}_p^T(k) \;\; \mathbf{x}_{2p}^T(k)\right]^T$, $\mathbf{z}_{2p}(k) = \left[\mathbf{y}_p^T(k) \;\; \mathbf{u}_{2p}^T(k)\right]^T$.

Minimizing the cost function in Eq. (3.24) results in the optimal solution

$$\mathbf{a}_o = \begin{bmatrix} \hat{\mathbf{f}}_{1_o} \\ \mathbf{h}_o \end{bmatrix} = \boldsymbol{R}_{\mathbf{z}_{1p}}^{-1} \boldsymbol{R}_{\mathbf{z}_{1p}\mathbf{z}_{2p}} \mathbf{b} + \boldsymbol{R}_{\mathbf{z}_{1p}}^{-1} \boldsymbol{r}_{\mathbf{z}_{1p}\xi_p}. \tag{3.25}$$

The terms $\boldsymbol{R}_{\mathbf{z}_{1p}}^{-1} \boldsymbol{R}_{\mathbf{z}_{1p}\mathbf{z}_{2p}} \mathbf{b}$ and $\boldsymbol{R}_{\mathbf{z}_{1p}}^{-1} \boldsymbol{r}_{\mathbf{z}_{1p}\xi_p}$ are derived in similar way as the terms $\boldsymbol{R}_{\mathbf{z}_1}^{-1} \boldsymbol{R}_{\mathbf{z}_1\mathbf{z}_2} \mathbf{b}$ and $\boldsymbol{R}_{\mathbf{z}_1}^{-1} \boldsymbol{r}_{\mathbf{z}_1\xi}$ (see Appendix A), hence

$$\boldsymbol{R}_{\mathbf{z}_{1p}}^{-1} \boldsymbol{R}_{\mathbf{z}_{1p}\mathbf{z}_{2p}} \mathbf{b} = \begin{bmatrix} \mathbf{f}_1 - \mathbf{f}_{2_\mathbf{h}} \\ \mathbf{h} \end{bmatrix}, \tag{3.26}$$

$$\boldsymbol{R}_{\mathbf{z}_{1p}}^{-1} \boldsymbol{r}_{\mathbf{z}_{1p}\xi_p} = \begin{bmatrix} \tilde{\boldsymbol{B}}_1 \\ \tilde{\boldsymbol{B}}_\mathbf{h} \end{bmatrix}, \tag{3.27}$$

where

$$\tilde{\boldsymbol{B}}_{\mathbf{h}} = \tilde{\boldsymbol{N}}^{T} \boldsymbol{r}_{\mathbf{y}_p \xi_p} + \tilde{\boldsymbol{Q}} \boldsymbol{r}_{\mathbf{x}_{2p} \xi_p}, \tag{3.28}$$

$$\tilde{\boldsymbol{B}}_{1} = \boldsymbol{R}_{\mathbf{y}_p}^{-1} \boldsymbol{r}_{\mathbf{y}_p \xi_p} + \left(\tilde{\boldsymbol{N}} \boldsymbol{r}_{\mathbf{x}_{2p} \xi_p} - \tilde{\boldsymbol{N}} \boldsymbol{R}_{\mathbf{x}_{2p} \mathbf{y}_p} \boldsymbol{R}_{\mathbf{y}_p}^{-1} \boldsymbol{r}_{\mathbf{y}_p \xi_p} \right), \tag{3.29}$$

with $\tilde{\boldsymbol{Q}} = \left(\boldsymbol{R}_{\mathbf{x}_{2p}} - \boldsymbol{R}_{\mathbf{x}_{2p} \mathbf{y}_p} \boldsymbol{R}_{\mathbf{y}_p}^{-1} \boldsymbol{R}_{\mathbf{y}_p \mathbf{x}_{2p}} \right)^{-1}$, $\tilde{\boldsymbol{N}} = -\boldsymbol{R}_{\mathbf{y}_p}^{-1} \boldsymbol{R}_{\mathbf{y}_p \mathbf{x}_{2p}} \tilde{\boldsymbol{Q}}$.

The derivations in Appendix B show that for the case of undermodeling the RTF the following results are obtained

$$\tilde{\boldsymbol{B}}_{\mathbf{h}} = \mathbf{h}_{res}, \tag{3.30}$$

$$\tilde{\boldsymbol{B}}_{1} = -\boldsymbol{R}_{\mathbf{y}_p}^{-1} \boldsymbol{r}_{\mathbf{y}_p \mathbf{x}_{2p}} \mathbf{h}_{res} = -\boldsymbol{R}_{\mathbf{y}_p}^{-1} \boldsymbol{r}_{\mathbf{y}_p \mathbf{x}_{2p}} \tilde{\boldsymbol{B}}_{\mathbf{h}}, \tag{3.31}$$

if the condition $d_k > L_{h_{full}} - 1$ is satisfied.

Therefore, the optimal solution in Eq. (3.25) can be reformulated as

$$\hat{\mathbf{f}}_{1o} = \mathbf{f}_1 - \mathbf{f}_{2_{\mathbf{h}}} - \boldsymbol{R}_{\mathbf{y}_p}^{-1} \boldsymbol{r}_{\mathbf{y}_p \mathbf{x}_{2p}} \mathbf{h}_{res}, \tag{3.32}$$

$$\mathbf{h}_o = \mathbf{h} + \mathbf{h}_{res}. \tag{3.33}$$

For the case of perfect modeling the RTF, $\xi(k) = 0$ (i.e., $\mathbf{h}_{res} = \mathbf{0}$), the following results are obtained

$$\tilde{\boldsymbol{B}}_{\mathbf{h}} = \boldsymbol{B}_{\mathbf{h}} = \mathbf{0}, \tag{3.34}$$

$$\tilde{\boldsymbol{B}}_{1} = \boldsymbol{B}_{1} = \mathbf{0}. \tag{3.35}$$

The Eq. (3.30) in comparison to Eq. (3.7) shows that the proposed PEM-AFC2 results in a better solution for the estimate of $H(q)$ compared to the AFC2 method when $\xi(k) \neq 0$. In fact, in that case the bias in the estimation of $H(q)$ is exactly the residual part $\mathbf{h}_{res}$ as expected for the PEM-AFC2, but that estimation for the AFC2 method depends on a variety of correlations including $\boldsymbol{R}_{\mathbf{y}}$, $\boldsymbol{R}_{\mathbf{x}_2}$, $\boldsymbol{R}_{\mathbf{x}_2 \mathbf{y}}$, $\boldsymbol{r}_{\mathbf{y}\xi}$ and $\boldsymbol{r}_{\mathbf{x}_2 \xi}$. Similarly, a comparison between Eq. (3.31) and Eq. (3.8) shows that the PEM-AFC2 also achieves a better solution for the estimation of $F_1(q)$ compared to the AFC2 method.

For the case $\xi(k) = 0$, the PEM-AFC2 and the AFC2 achieve the same bias for the estimates of $H(q)$ and $F_1(q)$ as shown in Eq. (3.34) and Eq. (3.35). In fact, there is no bias for the estimate of $H(q)$ and the estimate of $F_1(q)$ in this case only depends on the value of $\mathbf{f}_{2_\mathbf{h}}$. These conclusions are verified in experimental results (cf. Section 3.4) which show that the PEM-AFC2 has much better performance than the AFC2 for the case undermodeling the RTF. The reason is that the pre-filters used in the PEM-AFC2 can reduce the bias by pre-whitening the inputs of adaptive filters. For the perfect modeling the RTF both methods will converge to the same level with very low steady-state error.

For the PEM-AFC2, the optimal coefficients $\hat{\mathbf{f}}_{1_o}$, $\mathbf{h}_o$ in Eq. (3.25) can be updated using the NLMS algorithm as follows

$$\hat{\mathbf{f}}_1(k) = \hat{\mathbf{f}}_1(k-1) + \frac{\mu}{\|\mathbf{y}_p(k)\|_2^2 + \delta}\mathbf{y}_p(k)\, e_p(k), \tag{3.36}$$

$$\hat{\mathbf{h}}(k) = \hat{\mathbf{h}}(k-1) + \frac{\mu}{\|\mathbf{x}_{2p}(k)\|_2^2 + \delta}\mathbf{x}_{2p}(k)\, e_p(k), \tag{3.37}$$

with $e_p(k)$ defined in Eq. (3.18).

3.4 Experimental results

In simulations, measured feedback paths for the case without obstacle between loudspeaker and microphones (namely normal feedback paths) as well as for the case a flat object placed very close to the ear (namely closest feedback paths) have been used [3]. Figure 3.2 depicts the amplitude responses of the measured feedback paths. It shows that the closest feedback paths have higher amplitudes than the corresponding normal feedback paths. The normalized misalignment and added stable gain are used to evaluate the adaptive feedback control methods. The normalized misalignments for estimating $F_1(q)$ (namely MIS) and for estimating $H(q)$ (namely MIS_H) are denoted as [49]

$$\mathrm{MIS} = 10\log_{10}\left(\frac{\int_0^\pi \left|F_1(e^{j\omega}) - e^{-j\omega d_{fb}}\hat{F}_1(e^{j\omega})\right|^2 \mathrm{d}\omega}{\int_0^\pi |F_1(e^{j\omega})|^2 \mathrm{d}\omega}\right), \tag{3.38}$$

$$\text{MIS\_H} = 10\log_{10}\left(\frac{\int_0^{\pi}\left|H\left(e^{j\omega}\right)-\hat{H}\left(e^{j\omega}\right)\right|^2 \mathrm{d}\omega}{\int_0^{\pi}\left|H\left(e^{j\omega}\right)\right|^2 \mathrm{d}\omega}\right), \tag{3.39}$$

and the added stable gain is calculated as [49, 118]

$$\begin{aligned}\text{ASG} &= 10\log_{10}\left(\min_{\omega}\frac{1}{\left|F_1\left(e^{j\omega}\right)-e^{-j\omega d_{fb}}\hat{F}_1\left(e^{j\omega}\right)^2\right|}\right)\\ &\quad -10\log_{10}\left(\min_{\omega}\frac{1}{\left|F_1\left(e^{j\omega}\right)\right|^2}\right),\end{aligned} \tag{3.40}$$

where d_{fb} is a delay in the feedback canceler's path; $F_1\left(e^{j\omega}\right)$ and $\hat{F}_1\left(e^{j\omega}\right)$ are frequency responses of the true and the estimated feedback paths at the normalized angular frequency ω, respectively. The following parameters are selected for all simulations: the delay in the forward path $d_k = 32$ samples, the gain in the forward path $|K| = 30\text{dB}$, the delay in the feedback canceller's path $d_{fb} = 16$ samples, the sampling frequency $f_s = 16\text{kHz}$ and $\delta = 10^{-6}$. The lengths of the true and estimated feedback paths are $L_f = 38$ and $L_{\hat{f}} = 22$, respectively. The length $L_h = L_{\hat{h}} = 10$ and $L_{h_{full}} = 20$ are chosen. For all AFC methods using two microphones, the same step-sizes are chosen to update both adaptive filters $\hat{F}_1(q)$ and $\hat{H}(q)$.

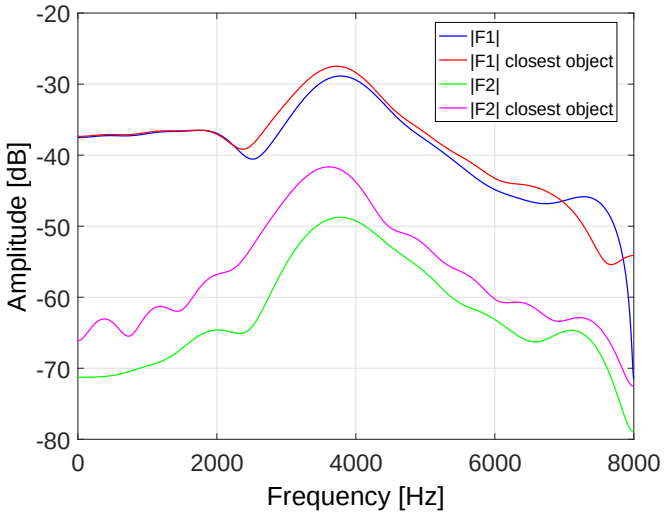

Figure 3.2: Amplitude responses of measured feedback paths.

3.4.1 Evaluate the proposed method for SSN as the incoming signal

In this subsection, synthesized SSN is used as the second incoming signal to verify the theoretical analyses for the cases of undermodeling and perfect mod-

eling the RTF. This SSN is generated by passing a white Gaussian noise (WGN) sequence through an all-pole filter $G^{-1}(q)$ with the filter order of 20. The linear predictor coefficients (LPC) of filter $G^{-1}(q)$ are computed by using the autocorrelation method. The input of the autocorrelation method is clean speech which is constructed by concatenating 26 sentences spoken by 4 different speakers from the TIMIT database [127]. P_s synthesized SSN signals are produced by using P_s random WGN sequences as the input of the all-pole filter $G^{-1}(q)$. For each compared AFC method, simulations are run P_s times for P_s different synthesized SSN signals, then the mean misalignments for MIS (Mean MIS) and for MIS_H (Mean MIS_H) are computed, respectively, i.e.,

$$\text{Mean MIS} = \frac{1}{\mathrm{P_s}} \sum_{i=1}^{\mathrm{P_s}} \mathrm{MIS}_i, \tag{3.41}$$

$$\text{Mean MIS\_H} = \frac{1}{\mathrm{P_s}} \sum_{i=1}^{\mathrm{P_s}} (\mathrm{MIS\_H})_i, \tag{3.42}$$

where P_s is the number of simulation times, MIS_i and $(\mathrm{MIS\_H})_i$ are the normalized misalignments for estimating $F_1(q)$ and for estimating $H(q)$ with the ith SSN as the incoming signal, respectively. MIS_i and $(\mathrm{MIS\_H})_i$ are calculated in a similar way to Eq. (3.38) and Eq. (3.39), respectively. Here $\mathrm{P_s} = 10$ and the normal feedback paths are selected. In this case, the actual $H(q)$ is a random white Gaussian sequence with full length of 20 and a standard deviation of 0.01. Ten random $H(q)$ are generated corresponding to 10 synthesized SSN signals. For the PEM-AFC2 the pre-filter $\hat{G}(q)$ is chosen such that $\hat{G}(q) = G(q)$.

Figure 3.3 depicts the performance of the AFC2 method and the PEM-AFC2 for the case of undermodeling the RTF ($\xi(k) \neq 0$). The same step-size $\mu = 0.001$ is selected for both methods. It can be seen that the PEM-AFC2 has much lower Mean MIS and Mean MIS_H corresponding to significantly lower biases in both estimates of $F_1(q)$ and $H(q)$ compared to the AFC2 method. In fact, the PEM-AFC2 provides more than 15 dB lower Mean MIS_H and approximately 10 dB lower Mean MIS. Moreover, the PEM-AFC2 converges faster than the AFC2 method.

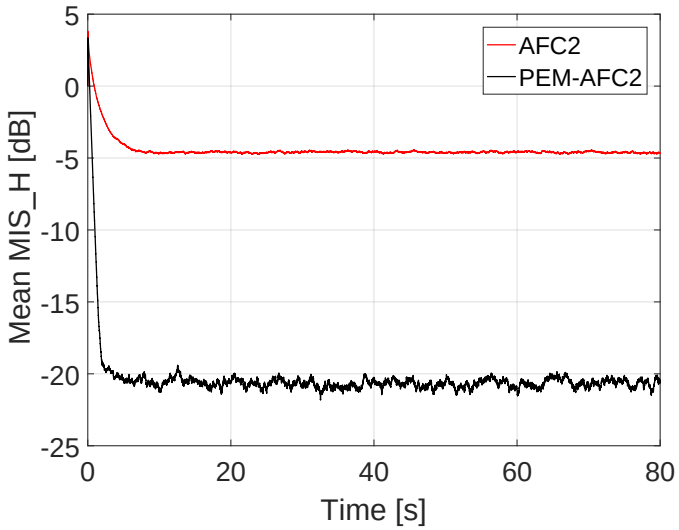

(a)

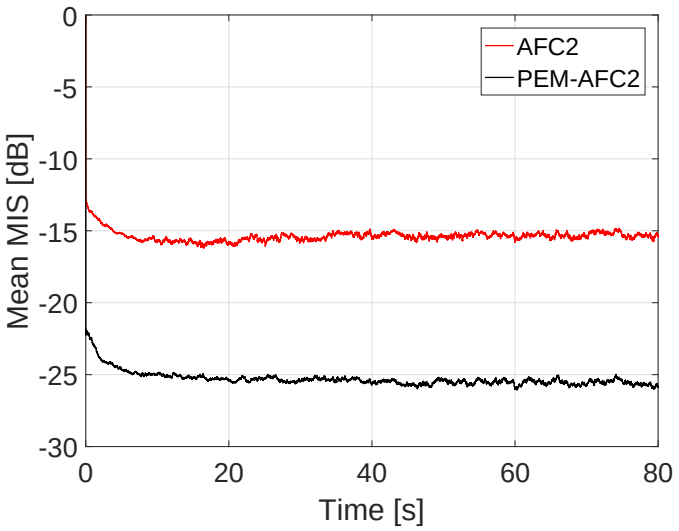

(b)

Figure 3.3: Performance of AFC2 and PEM-AFC2 with normal feedback paths for undermodeling case ($\xi(k) \neq 0$), SSNs are incoming signals, a) mean of MIS_H for 10 generated SSNs, b) mean of MIS for 10 generated SSNs.

Figure 3.4 illustrates the performance of the AFC2 method and the PEM-AFC2 for the case of perfect modeling the RTF ($\xi(k) = 0$). To increase convergence rate the step-size $\mu = 0.005$ is chosen for both methods. Both the AFC2 and the proposed method yield a similar level of Mean MIS_H which reaches to -110 dB when the system converges. This result is consistent with the theoretical analyses in Eq. (3.34) which prove that no bias in the estimate of $H(q)$ is achieved. Figure 3.4b shows that both mentioned methods reach to the same level of Mean MIS when the system converges. This result is also consistent with the theoretical analyses in Eq. (3.35) which show that both methods obtain the same bias for the estimate of $F_1(q)$. The Mean MIS for both methods can reach up to -45 dB, which is much higher than Mean MIS_H. The reason is that the bias in the estimate of $F_1(q)$ is now decided by the term $\mathbf{f}_{2_\mathbf{h}}$.

3.4.2 Evaluate the proposed method for real speech as the incoming signal

In the following scenario 1 and scenario 2, the performance of the PEM-AFC2 in comparison with the PEM-AFC and the AFC2 for real speech sequences as the incoming signals is evaluated. The incoming signals are recorded using two microphones which are designed as in [3]. The speech sources are constructed by using 30 IEEE sentences spoken by 3 male and 3 female speakers from NOIZEUS database [120]. In particular, the concatenated speech signal is generated by concatenating all 30 IEEE sentences together. The male speech signal and the female speech signal are produced by concatenating 15 male speech sentences and 15 female sentences, respectively. To obtain the incoming signals of 80 s length the male speech signal and the female speech signal are repeated several times and then truncated after 80 s. The step-sizes for all AFC methods are selected such that they provide a similar initial convergence rate. For example, the step-size $\mu = 0.001$ is selected for the AFC2 method, whereas $\mu = 0.0005$ is used for both the PEM-AFC and the PEM-AFC2. In all AFC methods using the PEM, a 20-order AR model of the incoming signal is computed for every frame of 160 samples by using the Levinson-Durbin algorithm [128]. To evaluate the quality of the speech signal, the perceptual evaluation of speech quality (PESQ) [120] is used. For the PESQ measures, the incoming signal $u_1(k)$ is chosen for the reference and the error signal $e_1(k)$ is for the test signal. The

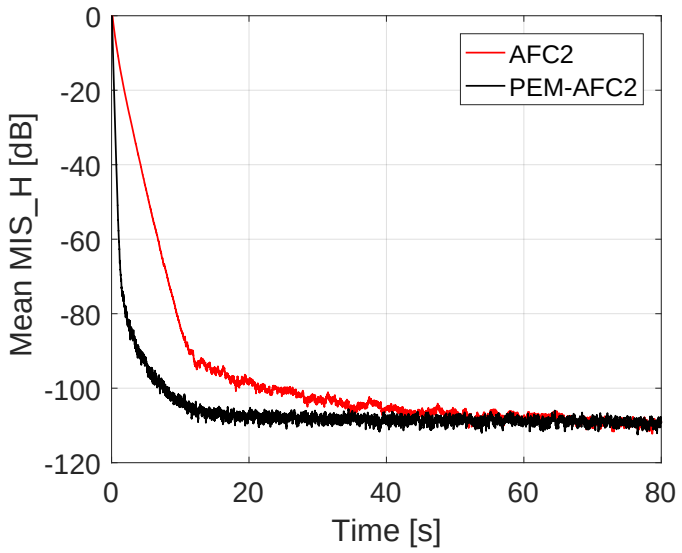

(a)

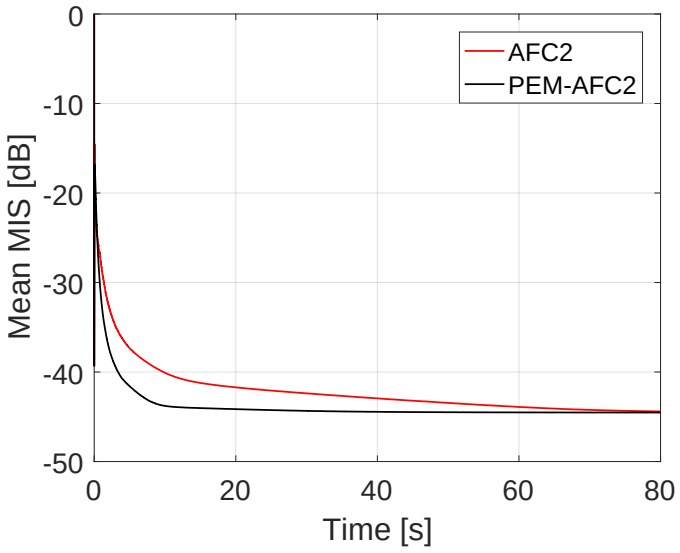

(b)

Figure 3.4: Performance of the AFC2 and PEM-AFC2 with normal feedback paths for perfect modeling ($\xi(k) = 0$), SSNs are incoming signals, a) mean of MIS_H for 10 generated SSNs, b) mean of MIS for 10 generated SSNs.

average misalignment ($\overline{MIS}$) and average added stable gain ($\overline{ASG}$) are also computed over whole 80 s (i.e., 1280000 samples) of each realization.

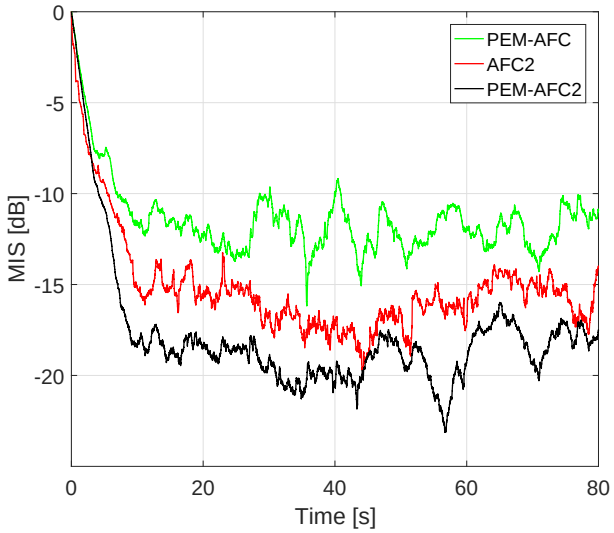

(a) Misalignment

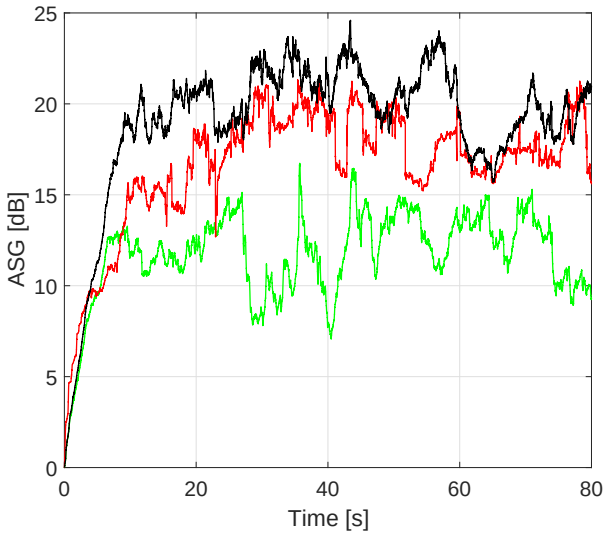

(b) Added Stable Gain

Figure 3.5: Performance of the PEM-AFC, AFC2 and PEM-AFC2 with normal feedback paths, concatenated speech as the incoming signals.

Scenario 1: In this scenario, the feedback paths are normal feedback paths and the incoming signals are concatenated speech.

Figure 3.5 depicts the performance of all considered AFC methods for the second scenario. It can be observed that the AFC2 method outperforms the PEM-AFC and the PEM-AFC2 outperforms the AFC2 method. The variation of the normalized MIS and ASG values over time in case of the PEM-AFC may

come from the model mismatch between $G(q)$ and $\hat{G}(q)$, whereas in the AFC2 method it may come from the model mismatch between the true $H(q)$ and the estimated $\hat{H}(q)$. That variation in the PEM-AFC2 method may be caused by both above reasons.

Table 3.1 shows that all considered AFC methods achieve high perceptual speech quality. The PESQ scores of the AFC2 and the PEM-AFC2 are similar but higher than that of the PEM-AFC. Moreover, the proposed PEM-AFC2 provides much better average misalignment ($\overline{MIS}$) and average added stable gain ($\overline{ASG}$), for instance, approximately 6.4 dB $\overline{MIS}$ gain and 7.3 dB $\overline{ASG}$ gain compared to the PEM-AFC, 2.6 dB $\overline{MIS}$ gain and 2.3 dB $\overline{ASG}$ gain compared to the AFC2 method.

Table 3.1: Evaluate performance of PEM-AFC, AFC2, PEM-AFC2 for concatenated speech as the incoming signals, normal feedback paths.

AFC methods	**PESQ**	$\overline{\textbf{MIS}}$	$\overline{\textbf{ASG}}$
PEM-AFC	4.427	-11.420	11.693
AFC2	4.481	-15.233	16.672
PEM-AFC2	4.466	-17.863	19.028

The PESQ of the HA without using control algorithm is also measured, $PESQ = 3.61$. It demonstrates that the PEM-AFC, the AFC2 method and the PEM-AFC2 provide an improvement of 0.82, 0.87 and 0.86 scores in PESQ compared to the case without control algorithm, respectively. The comparable PESQ scores among three considered AFC methods are expected due to the fact that the maximum stable gain of the system without feedback cancellation is approximately 27-29 dB (the maximum of F1 in Figure 5). With the applied forward path gain of 30 dB, the system is approximately 3 dB overcritical. Hence, once the ASG is larger than approximately 5-6 dB, there will be almost no audible artifacts. Since all considered AFC methods reach this point of 5-6 dB ASG after a very similar time period (approximately 2-3 s) and only this period will contribute distortions that may make a difference in the PESQ scores, the PESQ scores are quite similar among those methods.

To statistically evaluate the differences in the PESQ among compared AFC

methods, the same experiment is repeated for 9 different incoming signals which are produced by concatenating 30 IEEE speech sentences extracted from NOIZEUS database with different order. A one-way analysis of variance (ANOVA) is used to calculate the mean value and the 95 percent confidence interval (CI) over ten above PESQ measures (including the first measure as shown in Table 3.1) for each AFC method. The results are $\{3.616, [3.609, 3.622]\}$, $\{4.418, [4.412, 4.425]\}$, $\{4.481, [4.474, 4.487]\}$ and $\{4.458, [4.451, 4.464]\}$ for the HA without using control algorithm, the PEM-AFC, the AFC2 method, and the PEM-AFC2, respectively, where the first term in the parenthesis indicates the mean value and the second term (bounded by square brackets) indicates the lower and upper limits for 95 percent CIs for the mean. It can be seen that the 95 percent CIs of all mentioned AFC methods are not overlapped. Hence, the mean PESQ is significantly different across measures using those AFC methods. To determine which AFC methods make a difference in the PESQ, a multiple comparison test using the Bonferroni method is performed. The test shows that all obtained p-values are smaller than 0.05, i.e., the mean PESQ measures of all mentioned AFC methods significantly differ across all AFC methods.

Scenario 2: In the second scenario, the feedback paths have been changed from the normal to the closest feedback paths in the middle of simulation time. The performance of the proposed method is evaluated for three types of incoming signals, including concatenated speech, male speech and female speech.

From Figure 3.6 - Figure 3.8, it can be seen that the proposed PEM-AFC2 outperforms the PEM-AFC, even when the feedback paths suddenly change after 40s. It also outperforms the AFC2 method for the normal feedback paths as well as provides lower misalignment and higher added stable gain for the closest feedback paths. Especially, the PEM-AFC2 can track the change of the channels much quicker than both the PEM-AFC and the AFC2 method. In particular, in the first 2 seconds after the change of the feedback paths, the proposed method achieves approximately 3 dB improvement in normalized misalignment compared to the two remaining methods when the incoming signals are male speech. For both cases that concatenated speech and female speech

are used as the incoming signals, those improvements are approximately 5 dB and 3 dB, respectively, compared to the PEM-AFC and the AFC2 method. It is recognized that both the AFC2 and PEM-AFC2 obtain less improvement on MIS and ASG for the closest feedback paths than for the normal feedback paths because now the second feedback paths (corresponding to the closest feedback paths) are strong, i.e., the term $\mathbf{f}_{2_h}$ is high, leading to a large bias in the estimation of the feedback path. These results match well with the theoretical analysis.

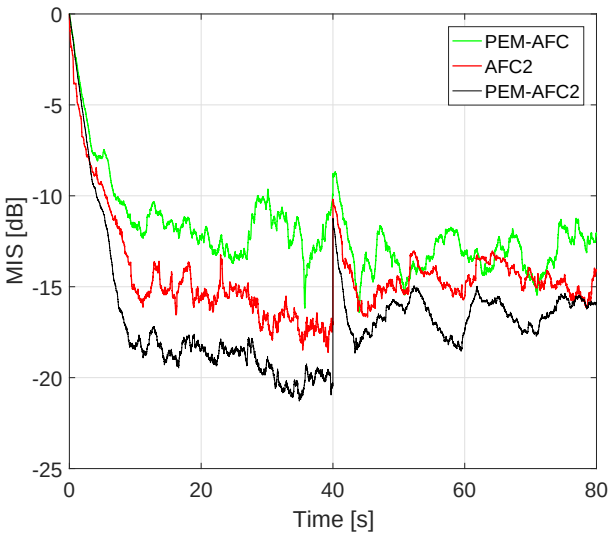

(a) Misalignment

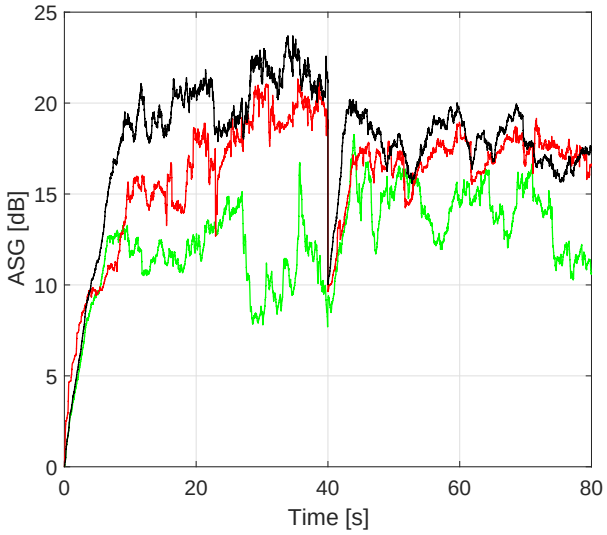

(b) Added Stable Gain

Figure 3.6: Performance of the PEM-AFC, AFC2 and PEM-AFC2 with a sudden change of feedback paths from normal to closest feedback paths after 40 s, concatenated speech as the incoming signal.

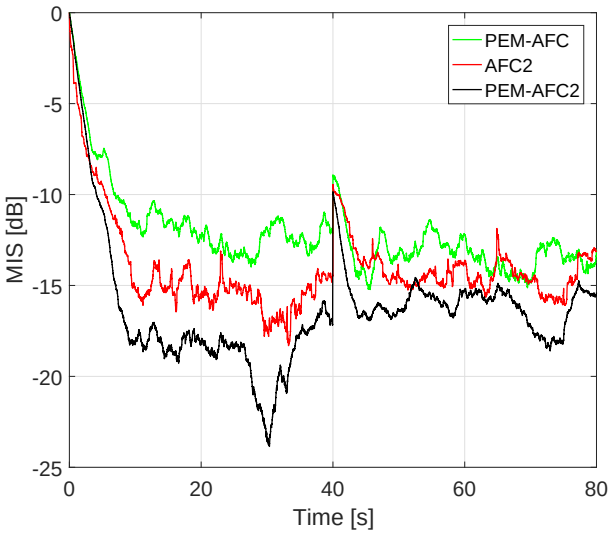

(a) Misalignment

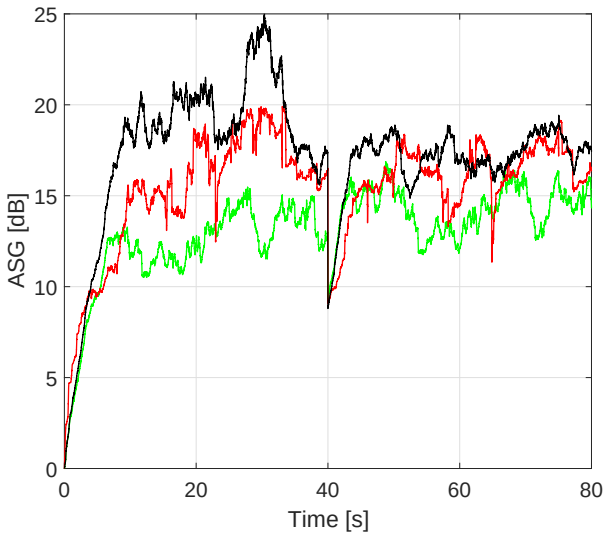

(b) Added Stable Gain

Figure 3.7: Performance of the PEM-AFC, AFC2 and PEM-AFC2 with a sudden change of feedback paths from normal to closest feedback paths after 40 s, male speech as the incoming signal.

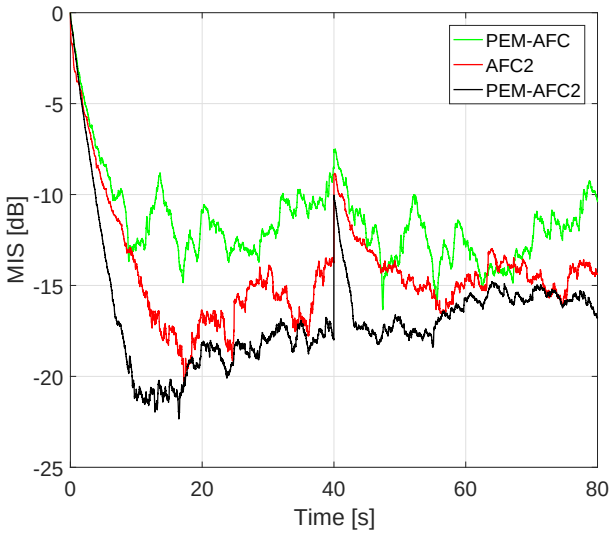

(a) Misalignment

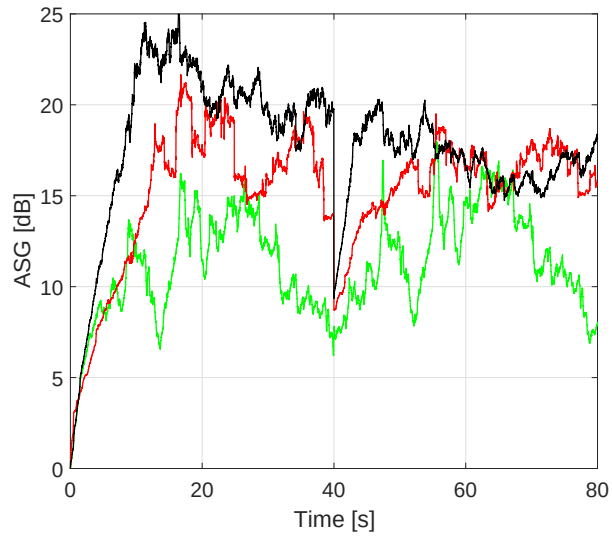

(b) Added Stable Gain

Figure 3.8: Performance of the PEM-AFC, AFC2 and PEM-AFC2 with a sudden change of feedback paths from normal to closest feedback paths after 40 s, female speech as the incoming signal.

Table 3.2: Evaluate performance of PEM-AFC, AFC2, PEM-AFC2 for different types of incoming signals, feedback paths change from normal to closest feedback paths after 40 s.

AFC methods	Incoming signals	PESQ	$\overline{MIS}1$	$\overline{ASG}1$	$\overline{MIS}2$	$\overline{ASG}2$
PEM-AFC	Male speech	4.45	-11.05	11.86	-13.23	14.23
AFC2		4.48	-13.95	14.91	-14.16	15.92
PEM-AFC2		4.47	-16.69	17.51	-15.95	17.01
PEM-AFC	Female speech	4.39	-10.69	10.62	-12.31	11.91
AFC2		4.47	-14.47	14.79	-14.18	15.73
PEM-AFC2		4.46	-17.21	18.59	-16.14	16.87
PEM-AFC	Concatenated speech	4.43	-10.86	10.87	-13.07	13.90
AFC2		4.48	-14.28	15.60	-14.56	16.72
PEM-AFC2		4.47	-17.00	18.11	-16.43	17.65

Table 3.2 summarizes the experimental results of PESQ, average MIS and average ASG for all considered AFC methods. The $\overline{MIS}1$ and $\overline{ASG}1$ present the average MIS and average ASG before the feedback paths change, whereas the $\overline{MIS}2$ and $\overline{ASG}2$ are those values after the change. All methods have PESQ scores larger than 4.4. However, the PEM-AFC2 obtains about 5.6 – 6.5 dB $\overline{MIS}1$ gain and 5.6 – 8.0 dB $\overline{ASG}1$ gain compared to the PEM-AFC as well as approximately 2.7 dB $\overline{MIS}1$ gain and 2.5 – 3.8 dB $\overline{ASG}1$ gain compared to the AFC2 method. After the feedback paths change, the PEM-AFC2 achieves approximately 2.7 – 3.8 dB $\overline{MIS}2$ gain and 2.8 – 5.0 dB $\overline{ASG}2$ gain compared to the PEM-AFC as well as approximately 2 dB $\overline{MIS}2$ gain and 1 dB $\overline{ASG}2$ gain compared to the AFC2 method.

3.4.3 Evaluate the proposed method for real music as the incoming signal

In this subsection, the proposed PEM-AFC2 with music as the incoming signal and with a sudden change of the feedback paths after 40 s is evaluated. The song "Imagine" by John Lennon is selected as the music signal. The same setup that is used in the scenario 3 is chosen, except a 51-order AR model of the incoming signal is selected. Since the music incoming signal is harder to be modeled than the speech incoming signal [129], a higher order is selected for

the AR model in order to improve the modeling accuracy, resulting in an improved system performance. Furthermore, the perceptual evaluation of audio quality (PEAQ) measure [121] is utilized to evaluate the quality of the music signal. For the PEAQ measures, the incoming signal $u_1(k)$ and the error signal $e_1(k)$ are also chosen as the reference and as the test signal, respectively.

Figure 3.9 demonstrates the performance of the proposed method in comparison with the PEM and the AFC2 method for this scenario. It can be seen that the PEM-AFC2 outperforms the two other mentioned methods not only before the feedback paths change, but also after the change. Although the proposed method yields large variations after a sudden change of the feedback paths due to the larger mismatch in modeling the music incoming signal in this situation, it still provides lower misalignment, higher ASG, and quicker tracking rate than the PEM and the AFC2 method.

Table 3.3 compares the average MIS and the average ASG of three mentioned AFC methods before and after the feedback paths change. It shows that the proposed PEM-AFC2 achieves approximately 7 dB gain compared to two remaining AFC methods before the change and 5 dB gain compared to the PEM-AFC, 2 dB gain compared to the AFC2 method after the change.

Table 3.4 evaluates the signal quality of those AFC methods using PEAQ measures. It shows that three AFC methods have the same PEAQ scores for the initial convergence phase (0s-5s). The reason is that the step-sizes are selected such that all the AFC methods have the same initial convergence. However, for the first convergence phase (30s-35s), i.e., before the change of the feedback paths, the proposed method obtains the PEAQ score of -0.59 corresponding to a very good signal quality (almost imperceptible), whereas the PEM-AFC and the AFC2 method get the PEAQ score approximately -2 corresponding to a moderate signal quality (slightly annoying). Similar results are achieved for the reconvergence phase (38s-43s). During the second convergence phase (70s-75s), i.e., after the change of the feedback paths, the PEAQ score of the AFC2 method and the PEM are -1.61 (between perceptible but not annoying and slightly annoying), and -2.17 (slightly annoying), respectively. However, the PEAQ score

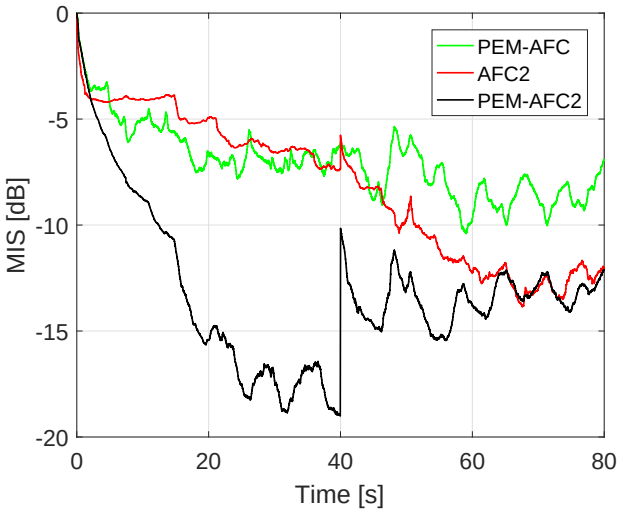

(a) Misalignment

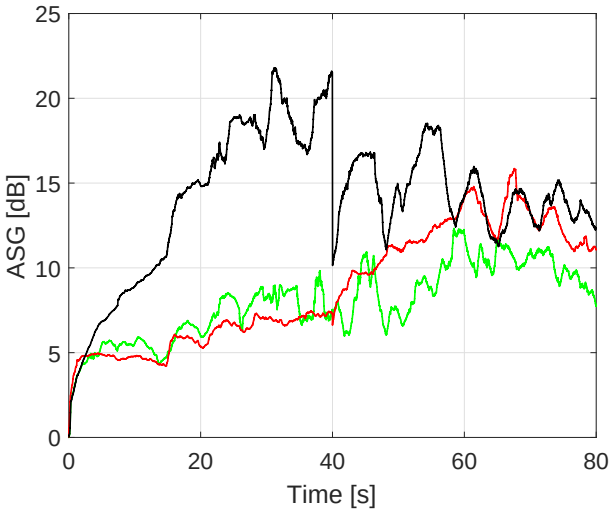

(b) Added Stable Gain

Figure 3.9: Performance of the PEM-AFC, AFC2 and PEM-AFC2 with a sudden change of feedback paths from normal to closest feedback paths after 40 s, music as the incoming signal.

Table 3.3: Evaluate average MIS and average ASG of PEM-AFC, AFC2, PEM-AFC2 for music as the incoming signal, feedback paths change from normal to closest feedback paths after 40 s.

AFC methods	$\overline{MIS}1$	$\overline{ASG}1$	$\overline{MIS}2$	$\overline{ASG}2$
PEM-AFC	-5.99	6.54	-8.10	9.45
AFC2	-5.30	5.82	-11.16	11.95
PEM-AFC2	-13.05	13.73	-13.43	14.35

Table 3.4: Evaluate PEAQ measures of PEM-AFC, AFC2, PEM-AFC2 for music as the incoming signal, feedback paths change from normal to closest feedback paths after 40 s.

AFC methods	PEAQ (0s-5s)	PEAQ (30s-35s)	PEAQ (38s-43s)	PEAQ (70s-75s)
PEM-AFC	-2.20	-2.18	-2.11	-2.17
AFC2	-2.20	-2.20	-2.20	-1.61
PEM-AFC2	-2.20	-0.59	-0.10	-0.14

of the proposed method in this case is -0.1 (almost imperceptible). Overall, the proposed method provides better signal quality than two remaining methods for music incoming signal.

3.4.4 Computational complexity

In this section, a computational complexity comparison among the proposed PEM-AFC2, the PEM-AFC and the AFC2 methods is provided. Table 3.5 summarizes the number of real multiplications per output sample [69] for the three considered AFC methods, where we assume that a real mutiplication and a real division have equal complexity. Generally, the proposed method has a larger computational complexity than either the PEM-AFC or the AFC2 method. In the PEM-AFC2 method $\hat{H}(q)$ as well as the LPC coefficients need to be estimated, whereas in the AFC2 method only the $\hat{H}(q)$ needs to be estimated and in the PEM-AFC method only the LPC coefficients need to be estimated. In particular, the computational complexity for estimating the LPC coefficients using the autocorrelation matrix and the Levinson-Durbin algorithm is $\frac{5P_0^2+2LP_0+P_0}{2L}$ mutiplications, where P_0 is the AR-model order and L is the frame length. In addition, the pre-whitened signal at the output of each pre-filter is computed

Table 3.5: Computational complexity per output sample.

AFC methods	Computational complexity	#
PEM-AFC	$\frac{5P_0^2+2LP_0+P_0}{2L} + 2P_0 + 3L_{\hat{f}} + 2$	134
AFC2	$3\left(L_{\hat{f}} + L_{\hat{h}}\right) + 4$	100
PEM-AFC2	$\frac{5P_0^2+2LP_0+P_0}{2L} + 3P_0 + 3\left(L_{\hat{f}} + L_{\hat{h}}\right) + 4$	186

A numerical value is given for $P_0 = 20$, $L = 160$, $L_{\hat{f}} = 22$, and $L_{\hat{h}} = 10$.

using P_0 mutiplications. The complexity for estimating the adaptive filter coefficients using NLMS algorithm is $3n + 2$ mutiplications, where n is the adaptive filter order [46].

3.5 Conclusions

In this chapter, a new derivation for the AFC2 method, which provides an actual optimal solution to the problem stated in [3], has been investigated. In addition, a novel AFC method based on a combination of the AFC2 method with the widely known PEM has been developed. In the PEM-AFC2, prefilters are used to pre-whiten the input signals of adaptive filters for AFC in two-microphone hearing aids, resulting in further reduction of bias in the estimate of feedback path. The PEM-AFC2 has been theoretically analyzed and improved solutions for the identifications of the feedback path $F_1(q)$ as well as the FIR filter $H(q)$ were obtained when the PEM has been applied for the AFC2 method. The experimental results with correct assumptions match perfectly with the theoretical analyses for both undermodeling the RTF as well as perfect modeling the RTF. The proposed method is also robust against different types of incoming signals as well as against a sudden change in the feedback paths. In fact, the experimental results show that the proposed PEM-AFC2 yields a significant performance improvement in terms of MIS and ASG compared to other widely known methods such as the PEM or the AFC2 methods. Furthermore, it obtains as good signal quality as the two compared methods for speech incoming signals, but better signal quality for music incoming signals. It can also track the sudden change of the feedback paths quicker than the PEM-AFC as well as the AFC2 method.

CHAPTER 4

Fast-Converging Adaptive Filtering Algorithms for Adaptive Feedback Cancellation in Hearing Aids

Chapter's key points:

- PEM-APA
- PEM-PNLMS
- PEM-IPNLMS
- Experimental results

In the previous chapter, the use of the two-microphone AFC method for HAs was considered. A new AFC method, which was a combination of the AFC2 method with the PEM, was proposed to improve the performance of the individual AFC approaches.

In this chapter we investigate the implementation of fast-converging adaptive filtering (FCAF) algorithms such as the APA, the PNLMS and the IPNLMS for the SMSL AFC approaches in HAs. The results of this chapter have been demonstrated in the author's conference papers [35, 130].

4.1 Introduction

The most well-known adaptive filtering algorithm for estimating the coefficients of an adaptive filter is the LMS algorithm. This algorithm is simple and easy for implementation but it is subjected to gradient noise amplification problem if the input of adaptive filter is large. To address this problem the NLMS algorithm which normalizes the input of adaptive filter w.r.t its squared

Euclidean norm [45, 46] is an effective solution. As a result, the NLMS algorithm yields faster convergence compared to the LMS algorithm and becomes the most common adaptive filtering algorithm in practice. A brief review of the LMS, NLMS algorithms can be found in Section 2.4.1. In those algorithms there is a trade-off between fast convergence and low steady-state error. Although the NLMS algorithm provides a convergence improvement compared to the LMS algorithm, its convergence is considerably degraded when the input signal is spectrally coloured [75, 79, 82]. To enhance the convergence whilst maintaining a low steady-state error, many solutions have been proposed in the literature, including variable step-size (VSS) algorithms [74, 75, 77, 79, 81, 80, 82, 84, 90, 131, 132], the affine combination of two adaptive filters using different step-sizes [97, 98, 99, 100, 133, 134, 135] and the FCAF algorithms. The FCAF algorithms include the RLS algorithm [16], the APA [84, 92, 94, 136, 137], and the PNLMS or IPNLMS algorithms [138, 139, 140, 141, 142, 143]. Most of the aforementioned methods are commonly used in the AEC contexts, but a few of them are successfully applied for the AFC contexts due to the high correlation between the loudspeaker and the incoming signal in the AFC contexts.

This chapter only considers the AFC methods using FCAF algorithms for HAs. Those methods provide convergence improvement but they also increase computational complexity. The use of the RLS algorithm for AFC in HAs is not common due to its high computational complexity. In [92] an approximated APA has been applied for the AFC using pre-filter, and in [144] a variable step-size algorithm was used for the approximated APA. Moreover, an inverse gain filter in conjunction with pseudo APA has been used to compensate the delay in the estimate of the linear prediction coefficients [94]. In [95] the VSS-APA based on global speech absence probability (GSAP) has been introduced. By using the APA which updates the weight vector of adaptive filter based on a number of recent input vectors, the mentioned methods can improve the convergence. However, the common features of those mentioned methods include high computational complexity since a large prediction order was used ($P = 4 - 20$), and the incoming signals were SSNs or real speech with added white noise. Note that the added white noise contributes to decorre-

late the loudspeaker and the incoming signal, but the signal quality may be degraded if the power of white noise is large. Other interesting FCAF algorithms were the PNLMS and the IPNLMS algorithms. Variants of the PNLMS algorithm, the Levenberg-Marquardt regularized NLMS (LMR-NLMS) and the Levenberg-Marquardt regularized APA (LMR-APA), have been investigated in [140]. However, those methods were developed for the AEC and the AFC in PAs, not for the AFC in HAs. Note that the length of the feedback paths and the distance between the loudspeaker and the microphone in HAs are much shorter than those in PAs. Thus the acoustic feedback problem in HAs is more severe than that in PAs. In [143] the PNLMS algorithm was employed for the AFC2 method, but the size of HA was increased since the second microphone is added.

The contribution of this chapter is the development of the SMSL AFC methods for HAs based on FCAF algorithms in conjunction with the PEM such that those methods provide not only a fast convergence rate but also maintain a low steady-state error. Unlike the existing methods, the proposed methods are robust toward a variety of incoming signals such as real speech or music without adding white noise as well as toward sudden changes in the acoustic feedback paths. In addition, the proposed methods require no prior knowledge of the feedback paths as well as incoming signal power. Furthermore, the computational complexity only slightly increase since a small projection order of the APA ($P = 2$) is needed.

Figure 4.1 depicts the model of the proposed AFC systems which is similar to the PEM model [16, 31, 49], but uses the APA, or PNLMS or IPNLMS algorithms to compute the coefficients of adaptive filter.

4.2 PEM-APA

This section describes in detail how to apply a classical APA for the PEM to improve the convergence rate while maintaining a low steady-state error. The same model of the PEM for both adaptive filtering algorithms such as the NLMS and the APA is used, c.f Figure 4.1. In this method, the incoming signal

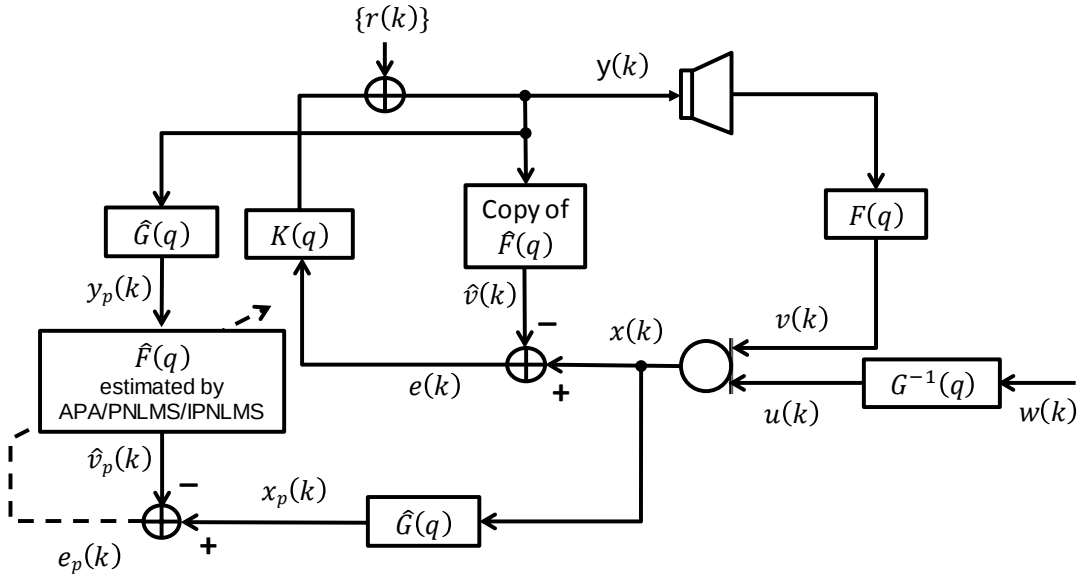

Figure 4.1: PEM model using fast-converging adaptive filtering algorithms.

is assumed to be modeled by an auto-regressive (AR) process, i.e.,

$$u(k) = G^{-1}(q)\, w(k), \tag{4.1}$$

where $G^{-1}(q)$ is an all-pole filter and $w(k)$ is a white Gaussian noise sequence. Normally, the inverse of that filter is an FIR filter whose coefficients are estimated by Levinson-Durbin algorithm [128] or Burg-Lattice algorithm [16, 46]. Then the estimated filter $\hat{G}(q)$ is used to pre-whiten the loudspeaker and microphone signals, i.e.,

$$x_p(k) = \hat{G}(q)\, x(k), \tag{4.2}$$

$$y_p(k) = \hat{G}(q)\, y(k). \tag{4.3}$$

Commonly, the well-known NLMS algorithm is found to be an attractive choice for the PEM due to its simplicity and efficiency, but the convergence rate of the system deteriorates when the incoming signals are spectrally coloured.

The adaptive filter coefficients of the feedback canceller $\hat{F}(q)$ in the case of the PEM-NLMS can be estimated by minimizing the mean-square prediction error, $J_{PEM-NLMS} = E\left\{|e_p(k)|^2\right\}$, as follows

$$\hat{\mathbf{f}}(k) = \hat{\mathbf{f}}(k-1) + \frac{\mu}{(\|\mathbf{y}_p(k)\|_2^2 + \delta)} \mathbf{y}_p(k)\, e_p(k), \tag{4.4}$$

where $\mathbf{y}_p(k) = \left[y_p(k), y_p(k-1), \ldots, y_p\left(k - L_{\hat{f}} + 1\right)\right]^T$ is a vector of the pre-whitened loudspeaker signal.

A classical affine projection algorithm, which provides a superior convergence rate compared to the NLMS algorithm, is employed for the PEM, especially for the case of speech as the incoming signal. In the proposed method, the PEM-APA, P most recent input vectors are used to estimate the coefficients of an adaptive filter, where P is a projection order. Thus, the input vectors of the feedback canceler $\hat{F}(q)$ in the PEM-APA can be defined as

$$\mathbf{Y}_p(k) = \left[\mathbf{y}_p(k), \mathbf{y}_p(k-1), \ldots, \mathbf{y}_p(k-P+1)\right]. \tag{4.5}$$

The vector $\mathbf{e}_p(k) = \left[e_p(k), e_p(k-1), \ldots, e_p(k-P+1)\right]^T$, the pre-whitened error signal, is computed by subtracting the estimated feedback signal from the pre-whitened microphone signal, i.e.,

$$\mathbf{e}_p(k) = \mathbf{x}_p(k) - \mathbf{Y}_p^T(k)\,\hat{\mathbf{f}}(k), \tag{4.6}$$

where $\mathbf{x}_p(k) = \left[x_p(k), x_p(k-1), \ldots, x_p(k-P+1)\right]^T$ is a vector of the pre-whitened microphone signal. By minimizing the mean-square prediction error, $J_{PEM-APA} = E\left\{|\mathbf{e}_p(k)|^2\right\}$, the adaptive filter coefficients of the feedback canceler $\hat{F}(q)$ in the case of the PEM-APA can be estimated as follows

$$\hat{\mathbf{f}}(k) = \hat{\mathbf{f}}(k-1) + \mu\mathbf{Y}_p(k)\left[\mathbf{Y}_p^T(k)\,\mathbf{Y}_p(k) + \mathbf{I}_P\delta\right]^{-1}\mathbf{e}_p(k), \tag{4.7}$$

where $\mathbf{I}_P$ is an $(P \times P)$ identity matrix; δ is a small positive value to avoid division by zero; and μ is a fixed step-size used to control the update of $\hat{\mathbf{f}}(k)$.

By selecting a small projection order P, e.g., $P = 2$, the computational complexity of the proposed method only slightly increases compared to the PEM-NLMS.

Probe noise $r(k)$, which is often a white noise signal, may be added into the loudspeaker signal before the adaptive process in order to further decorrelate

the loudspeaker and the incoming signal, i.e.,

$$y(k) = K(q)\, e(k) + r(k). \tag{4.8}$$

4.3 PEM-PNLMS and PEM-IPNLMS

4.3.1 PEM-PNLMS

The PNLMS algorithm was firstly introduced by Duttweiler for the AEC context [138]. This algorithm uses an adaptive step-size in proportion to the estimated filter coefficient to update each coefficient of the adaptive filter. Therefore, a significant improvement in adaptation speed compared to the NLMS algorithm can be achieved. Note that unlike the AEC systems, the AFC systems suffer from correlation between the loudspeaker signal and the incoming signal. In the proposed PEM-PNLMS for AFC applications, the PEM is used to decorrelate the loudspeaker signal and the incoming signal, resulting in a lower bias in the estimate of the feedback path. Then the pre-whitened signals are used in the PNLMS algorithm to further improve the initial convergence and tracking rate. The proposed PEM-PNLMS is described as

$$\hat{\mathbf{f}}(k) = \hat{\mathbf{f}}(k-1) + \frac{\mu \mathbf{D}(k-1)\, \mathbf{y}_p(k)\, e_p(k)}{\mathbf{y}_p^T(k)\, \mathbf{D}(k-1)\, \mathbf{y}_p(k) + \delta_{PNLMS}}, \tag{4.9}$$

$$\mathbf{D}(k-1) = diag\left\{ d_0(k-1), \ldots, d_{L_{\hat{f}}-1}(k-1) \right\}, \tag{4.10}$$

where δ_{PNLMS} is a regularization parameter and $\mathbf{D}(k-1)$ is a diagonal matrix. This diagonal matrix is used to allocate a step-size to each filter coefficient such that a larger coefficient receives a larger increment and vice versa. Hence, an increase in the convergence of that coefficient is achieved.

In the original PNLMS algorithm [138], the diagonal elements $d_l(k)$ are computed as

$$d_l(k) = \frac{\lambda_l(k)}{\sum_{i=1}^{L_{\hat{f}}-1} \lambda_i(k)}, \tag{4.11}$$

$$\lambda'_{\infty}(k) = \max\left[\kappa, \left|\hat{f}_0(k)\right|, \ldots, \left|\hat{f}_{L_{\hat{f}}-1}(k)\right| \right], \tag{4.12}$$

$$\lambda_l(k) = \max\left\{\rho\lambda'_\infty(k), \left|\hat{f}_l(k)\right|\right\}, \tag{4.13}$$

where ρ, ζ are positive parameters with typical values $\rho = 5/L_{\hat{f}}$, $\zeta = 0.01$. The constant ρ prevents $\hat{f}_l(k)$ from stalling when it is very small and ζ is a regularization parameter.

4.3.2 PEM-IPNLMS

To further improve the convergence of the PNLMS, the improved PNLMS [139, 141] modified the PNLMS by providing new rules to better exploit the shape of the estimated feedback path for calculating the tap-dependent step-size. In [139] the l_1-norm of the adaptive filter was exploited, whereas the l_0-norm was used in [141]. In this subsection the IPNLMS with l_1-norm or l_0-norm is proposed to be employed for the PEM in HAs.

The proposed PEM-IPNLMS (l_1-norm) method uses a smoother choice for the elements in Eq. (4.13), i.e.,

$$\lambda_l(k) = (1-\alpha)\frac{\left\|\hat{\mathbf{f}}(k)\right\|_{l_1}}{L_{\hat{f}}} + (1+\alpha)\left|\hat{f}_l(k)\right|, \tag{4.14}$$

where $-1 \leq \alpha < 1$ and $\left\|\hat{\mathbf{f}}(k)\right\|_{l_1} = \sum_{l=0}^{L_{\hat{f}}-1}\left|\hat{f}_l(k)\right|$, $l = 0, 1, \ldots, L_{\hat{f}} - 1$. Thus the diagonal elements of $\mathbf{D}(k-1)$ in Eq. (4.9) can be recalculated as

$$d_l(k) = \frac{1-\alpha}{2L_{\hat{f}}} + (1+\alpha)\frac{\left|\hat{f}_l(k)\right|}{2\left\|\hat{\mathbf{f}}(k)\right\|_{l_1} + \varepsilon}, \tag{4.15}$$

where ε is a small positive value added to avoid division by zero. If $\alpha = -1$, the IPNLMS becomes the NLMS algorithm. If $\alpha \approx 1$, the IPNLMS is similar to the PNLMS algorithm. In practice, good choices for α are -0.5 or 0. The relation among the regularization parameters of the mentioned algorithms are $\delta_{PNLMS} = \delta_{NLMS}/L_{\hat{f}}$ and $\delta_{IPNLMS} = (1-\alpha)\delta_{NLMS}/2L_{\hat{f}}$ [139].

For the IPNLMS algorithm the l_0-norm can be a good alternative to the l_1-norm [141]. The l_0-norm of a vector is the number of its non-zero components. The

l_0-norm of a L-dimensional vector $\mathbf{b} = [b_0, b_1, \ldots, b_{L-1}]$ is defined as

$$\|\mathbf{b}\|_{l_0} = \sum_{l=0}^{L-1} f(b_l), \tag{4.16}$$

$$f(b_l) = \begin{cases} 1, & b_l \neq 0 \\ 0, & b_l = 0. \end{cases} \tag{4.17}$$

The function $f(b_l)$ can be approximated as [145]

$$f(b_l) \approx 1 - \exp(-\gamma |b_l|), \tag{4.18}$$

where γ is a large positive value. Hence,

$$\|\mathbf{b}\|_{l_0} \approx \sum_{l=0}^{L-1} [1 - \exp(-\gamma |b_l|)]. \tag{4.19}$$

In the PEM-IPNLMS using the l_0-norm the equations Eq. (4.13) and Eq. (4.15) are rewritten as follows

$$\lambda_l(k) = (1-\alpha) \frac{\|\hat{\mathbf{f}}(k)\|_{l_0}}{L_{\hat{f}}} + (1+\alpha) \left[1 - e^{(-\gamma |\hat{f}_l(k)|)}\right], \tag{4.20}$$

$$d_l(k) = \frac{1-\alpha}{2L_{\hat{f}}} + (1+\alpha) \frac{1 - \exp\left(-\gamma \left|\hat{f}_l(k)\right|\right)}{2\|\hat{\mathbf{f}}(k)\|_{l_0} + \varepsilon}. \tag{4.21}$$

4.4 Experimental results

4.4.1 Results for the PEM-APA

In this section, the proposed PEM-APA is evaluated for a real speech as the incoming signal. A dummy head with adjustable ear canals [146] in conjunction with a two-microphone behind-the-ear hearing aid and open-fitting ear molds [147] is used to measure acoustic feedback paths in two scenarios free-field ($F_1(f)$) and with a telephone receiver ($F_2(f)$) placed close to the hearing aid. The sampling frequency is $f_s = 16\text{kHz}$ and the length of the measured feedback paths is $L_f = 100$. Figure 4.2 shows the amplitude and phase characteristics of the measured feedback paths used in simulations. A real speech signal created

by concatenating male and female speech used in [123] is selected as the incoming signal. All simulations are implemented with 50 s long speech as the incoming signal and with a sudden change from the free-field to the telephone-near feedback path at the 25th second. The normalized misalignment (MIS) and the added stable gain (ASG), which are denoted in a manner analogous to Eq. (2.43) and Eq. (2.45), are used for performance evaluation of the AFC methods.

The following settings are used for all simulations. The forward path gain and delay of the hearing aid are set to $|K| = 30\,dB$ and $d_k = 96$ samples, respectively. The feedback canceler path is delayed by 1 sample. The length of adaptive filter $L_{\hat{f}} = 64$, and step-size $\mu = 0.001$ are chosen for the time-domain implementation. The prediction-error filter $G(q)$ is of order 17 and updated using the Levinson-Durbin algorithm every 10 ms in both the PEM-NLMS and the PEM-APA. For the PEM-APA, a small projection order of 2 is chosen to avoid a large increase in computational complexity.

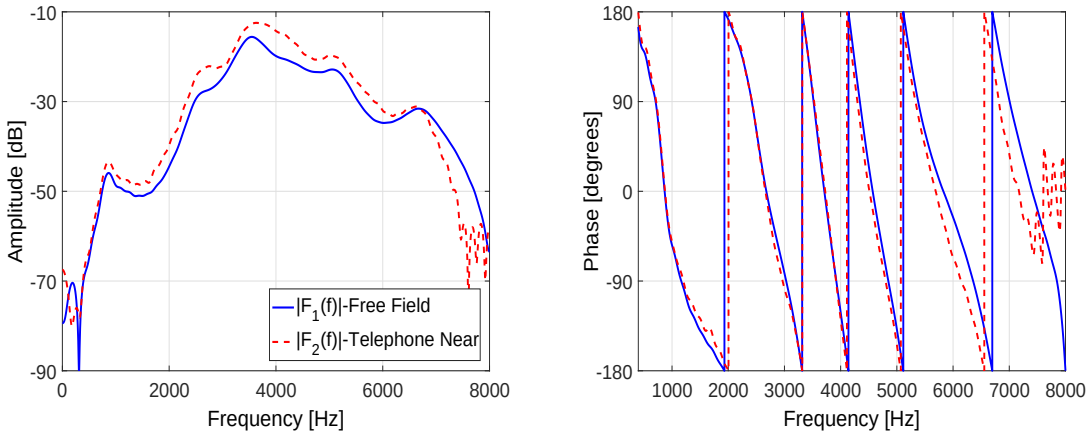

(a) Amplitude response **(b)** Phase response

Figure 4.2: Characteristics of measured feedback paths.

Figure 4.3 demonstrates the simulation results for the PEM using the NLMS algorithm and the APA for the case of no probe noise. The convergence performance of the PEM-APA outperforms that of the PEM-NLMS. When the feedback path changes from free-field feedback path to telephone-near feedback path at the 25th second, the PEM-APA can track that change quicker than the PEM-NLMS.

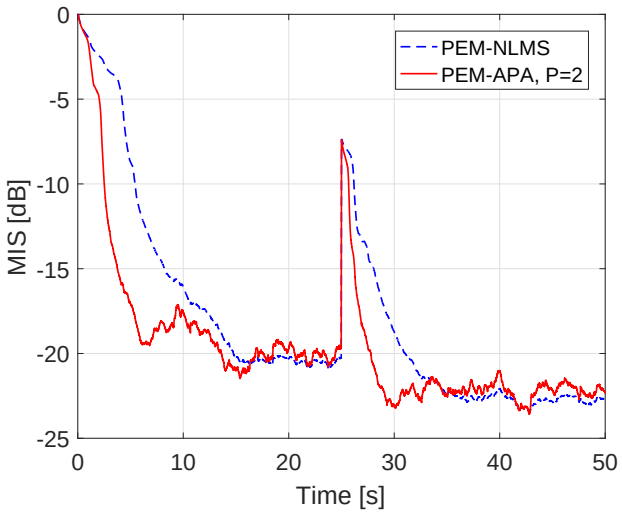

(a) Misalignment

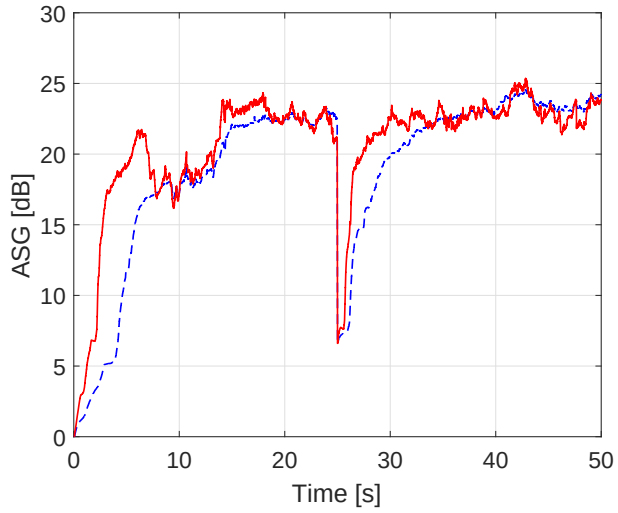

(b) Added Stable Gain

Figure 4.3: Performance of PEM-NLMS, PEM-APA (P=2) with step size $\mu = 0.001$, pre-filter order $L_p = 17$, real speech as the incoming signal.

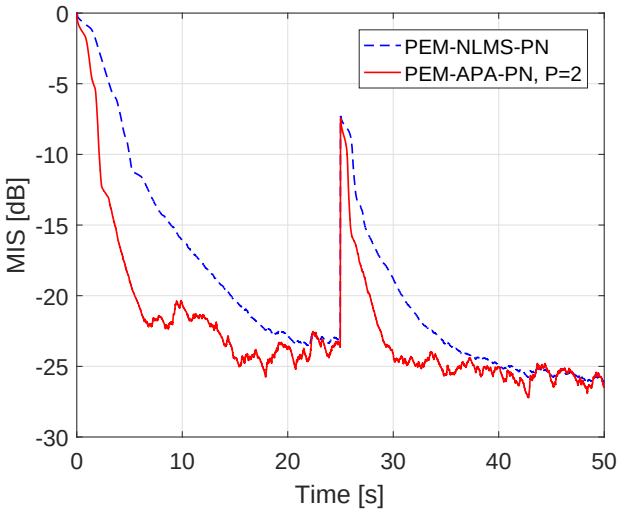

(a) Misalignment

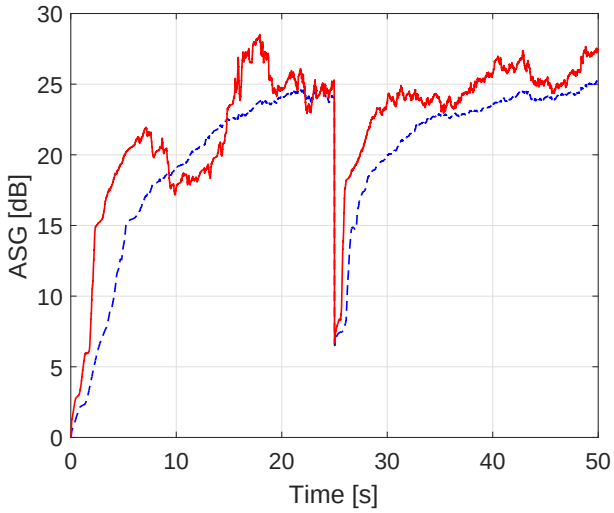

(b) Added Stable Gain

Figure 4.4: Performance of PEM-NLMS, PEM-APA (P=2) in case of using probe noise, SNR = 25 dB, step size μ = 0.001, pre-filter order L_p = 17, real speech as the incoming signal.

Figure 4.4 and Figure 4.5 illustrate the performance of the PEM-NLMS and the PEM-APA in the case of using probe noise (PN). In this case, a white Gaussian noise with SNR = 25 dB and SNR = 20 dB, respectively, are injected into the loudspeaker signal. All other parameters are set the same as the case of no probe noise. The probe noise provides further decorrelation between the loudspeaker and incoming signals, thus the better performance can be achieved for both mentioned systems. However, the PEM-APA-PN still outperforms the PEM-NLMS-PN in both terms of misalignment and added stable gain. It converges quicker and tends to yield lower steady-state error. Futhermore, it also obtains very fast tracking rate when the feedback path changes.

Table 4.1 and Table 4.2 compare the performance evaluation between the PEM-APA and the PEM-NLMS for the cases without and with probe noise, respectively. The $\overline{MIS}1$ and $\overline{ASG}1$ present the average MIS and average ASG before the feedback path changes, whereas the $\overline{MIS}2$ and $\overline{ASG}2$ are those values after the change. The PESQ scores are measured during the periods that the system has converged, e.g., PESQ1 scores are measured during the period of $35s$ – $39s$ (before the change of the feedback path) and PESQ2 scores are measured during the period of $75s$–$79s$ (after the change of the feedback path). The PEM-APA and the PEM-NLMS without probe noise yield similar PESQ scores which are larger than 4.2 both before and after the change of the feedback path (cf. Table 4.1). It is meant that both methods obtain very good signal quality when the system has converged. However, the PEM-APA achieves approximately 2dB $\overline{MIS}1$ gain, 2dB $\overline{ASG}1$ gain as well as approximately 0.8dB $\overline{MIS}2$ gain and 0.8dB $\overline{ASG}2$ gain compared to the PEM-NLMS. Similarly, Table 4.2 shows that the PEM-APA and the PEM-NLMS with probe noise yield similar PESQ scores (larger than 4.2) both before and after the change of the feedback path. However, the PEM-APA achieves approximately 4 – 5dB $\overline{MIS}1$ gain, 2 – 3dB $\overline{ASG}1$ gain as well as approximately 1.8 – 2.4dB $\overline{MIS}2$ gain and 2.2dB $\overline{ASG}2$ gain compared to the PEM-NLMS.

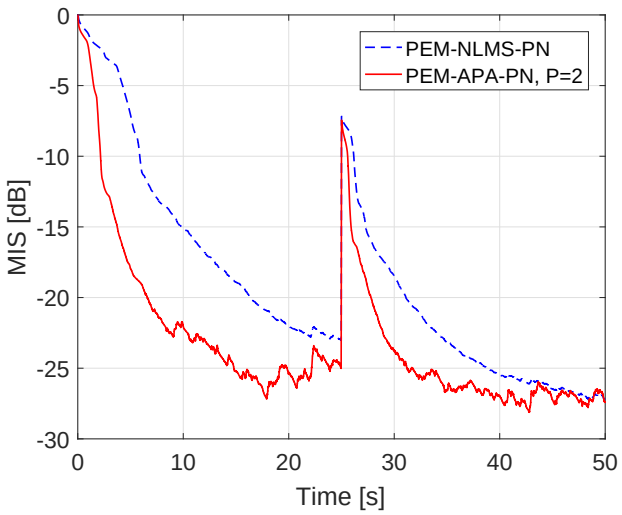

(a) Misalignment

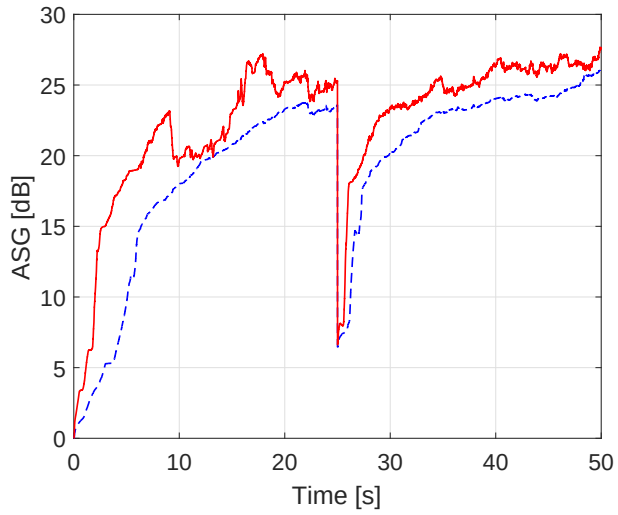

(b) Added Stable Gain

Figure 4.5: Performance of PEM-NLMS, PEM-APA (P=2) in case of using probe noise, SNR = 20 dB, step size μ = 0.001, pre-filter order L_p = 17, real speech as the incoming signal.

Table 4.1: Evaluate performance of PEM-NLMS and PEM-APA with P = 2, μ = 0.001, L_p = 17, and real speech as the incoming signal.

AFC methods	$\overline{MIS}1$	$\overline{ASG}1$	PESQ1	$\overline{MIS}2$	$\overline{ASG}2$	PESQ2
PEM-NLMS	-15.16	16.92	4.45	-20.52	21.15	4.32
PEM-APA	-17.38	19.17	4.39	-21.35	21.93	4.22

Table 4.2: Evaluate performance of PEM-NLMS-PN and PEM-APA-PN with $P = 2$, $\mu = 0.001$, $L_p = 17$, and real speech as the incoming signal.

AFC methods	SNR	$\overline{MIS}1$	$\overline{ASG}1$	PESQ1	$\overline{MIS}2$	$\overline{ASG}2$	PESQ2
PEM-NLMS-PN	25 dB	-16.12	18.30	4.43	-22.16	21.61	4.38
PEM-APA-PN		-20.32	20.39	4.41	-23.95	23.84	4.29
PEM-NLMS-PN	20 dB	-15.10	16.92	4.35	-22.44	21.91	4.37
PEM-APA-PN		-20.96	20.60	4.37	-24.82	24.14	4.23

4.4.2 Results for the PEM-PNLMS and PEM-IPNLMS

The proposed methods, PEM-PNLMS and PEM-IPNLMS, are evaluated for both speech and music as the incoming signals. The speech used as incoming signal is the same concatenated real male and female speech as in [123], while the music used as incoming signal is the song "Imagine" by John Lennon. All simulations are run for 80 s with a sudden change from the free-field to the telephone-near feedback path after 40 s. For the evaluation of all mentioned AFC methods the normalized misalignment (MIS) and the added stable gain (ASG) are defined in an analogous way to Eq. (2.43) and Eq. (2.45), respectively.

The following parameters are set for all simulations. The sampling frequency is $f_s = 16\text{kHz}$. The adaptive filter of length $L_{\hat{f}} = 64$, step-size $\mu = 0.001$, $\delta_{NLMS} = \varepsilon = 10^{-10}$ and $\alpha = 0$, $\gamma = 50$ are chosen. The prediction-error filter $\hat{G}(q)$ of order 20 is updated using the Levinson-Durbin algorithm every 10 ms. The delay in the feedback canceller path is 1 sample, whereas the delay and gain in the forward path are $d_k = 96$ samples and $|K| = 30\,dB$, respectively.

The first feedback path ($\mathbf{f}_1$) and the second feedback path ($\mathbf{f}_2$) were measured in free-field and with a telephone receiver close to the ear, respectively. Figure 4.6 shows the IRs of measured acoustic feedback paths of length $L_f = 100$ with a two-microphone behind-the-ear hearing aid [147] used for the simulations.

Figure 4.7 compares the performance of all mentioned methods for speech as the incoming signal. The proposed PEM-PNLMS outperforms the PEM-NLMS for both initial convergence and tracking rates while retaining a similar steady-

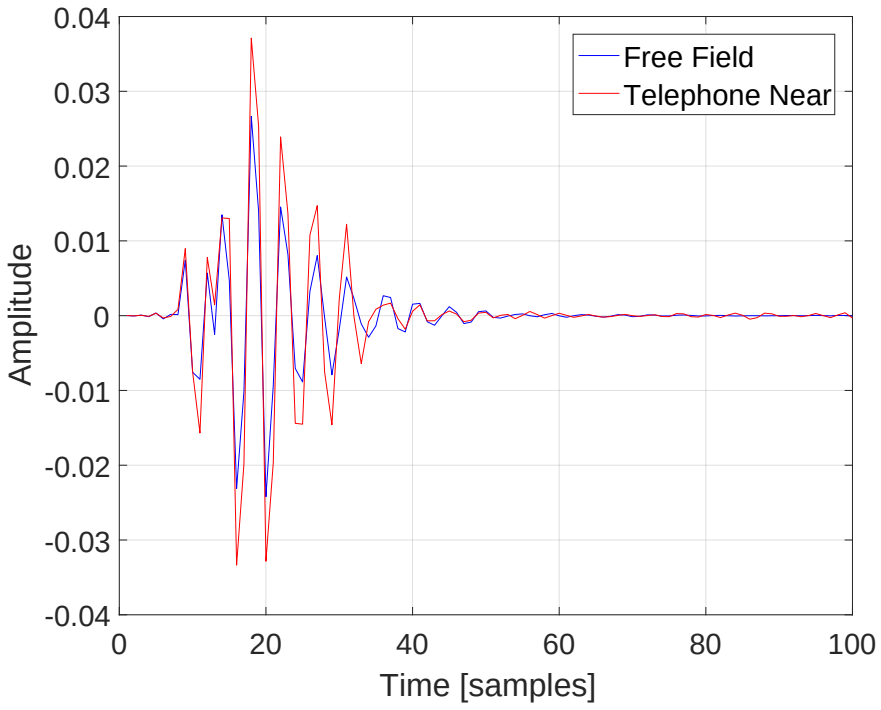

Figure 4.6: Impulse responses of measured feedback paths.

state error. The PEM-IPNLMS provides a further improvement in initial convergence and tracking rate compared to the PEM-PNLMS. The performance of the PEM-IPNLMS using l_0-norm is slightly better than the PEM-IPNLMS using l_1-norm.

Figure 4.8 illustrates the performance of the proposed methods for music as the incoming signal. It can be seen that the proposed PEM-PNLMS and PEM-IPNLMS have slightly faster initial convergence as well as lower misalignment and ASG than the PEM-NLMS for the free-field feedback path. The powerful characteristic of the proposed methods is exposed when the feedback path suddenly changes after 40s, where the tracking of the PEM-PNLMS and PEM-IPNLMS (with l_1-norm/l_0-norm) is quicker than that of the PEM-NLMS.

Table 4.3 and Table 4.4 summarize the performance evaluation of the PEM-NLMS, PEM-PNLMS and PEM-IPNLM for speech and music as the incoming signals, respectively. The $\overline{MIS}1$ and $\overline{ASG}1$ present the average MIS and average ASG before the feedback path changes, whereas the $\overline{MIS}2$ and $\overline{ASG}2$ are those values after the change. The PESQ score (for speech signal) and PEAQ score (for music signal) are measured during the periods that the sys-

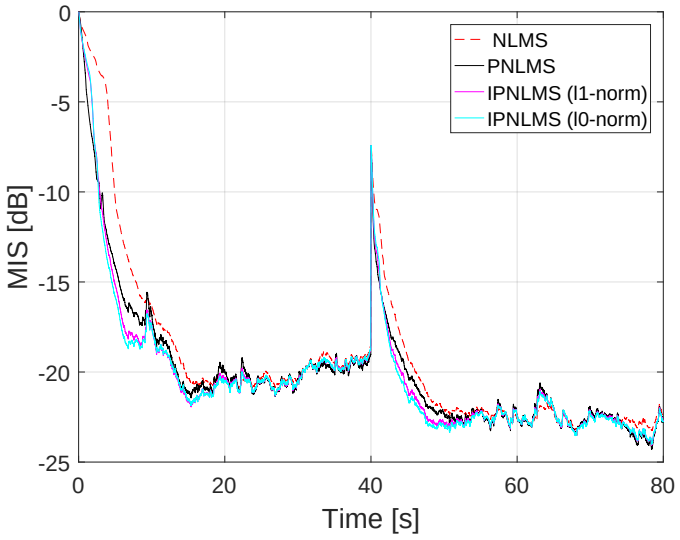

(a)

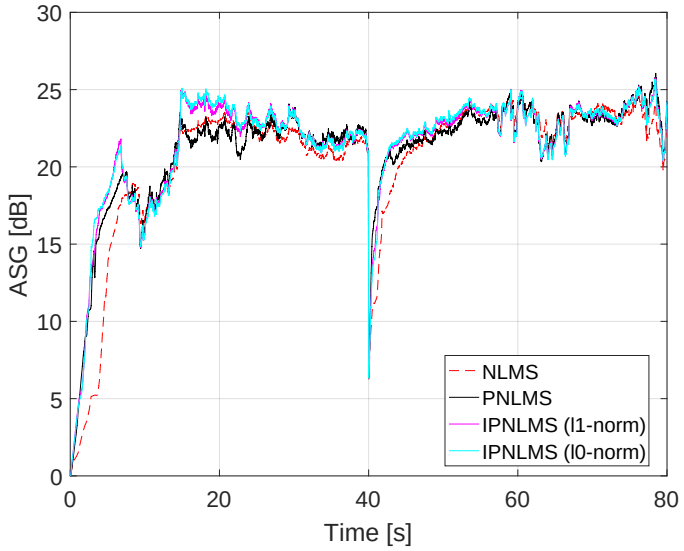

(b)

Figure 4.7: (a) Misalignment, (b) ASG of the PEM using NLMS, PNLMS, IPNLMS algorithms with speech as the incoming signal.

Table 4.3: Evaluate performance of the PEM using NLMS, PNLMS, IPNLMS algorithms with speech as the incoming signal.

AFC methods	$\overline{MIS}1$	$\overline{ASG}1$	PESQ1	$\overline{MIS}2$	$\overline{ASG}2$	PESQ2
PEM-NLMS	-17.04	18.84	4.40	-21.33	22.16	4.32
PEM-PNLMS	-18.12	19.74	4.38	-21.74	22.49	4.35
PEM-IPNLMS (l_1-norm)	-18.33	20.23	4.39	-21.89	22.60	4.37
PEM-IPNLMS (l_0-norm)	-18.42	20.29	4.39	-21.97	22.63	4.37

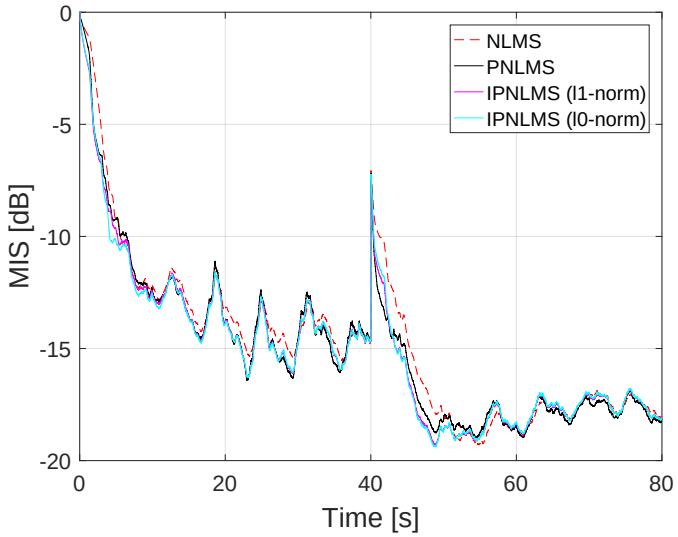

(a)

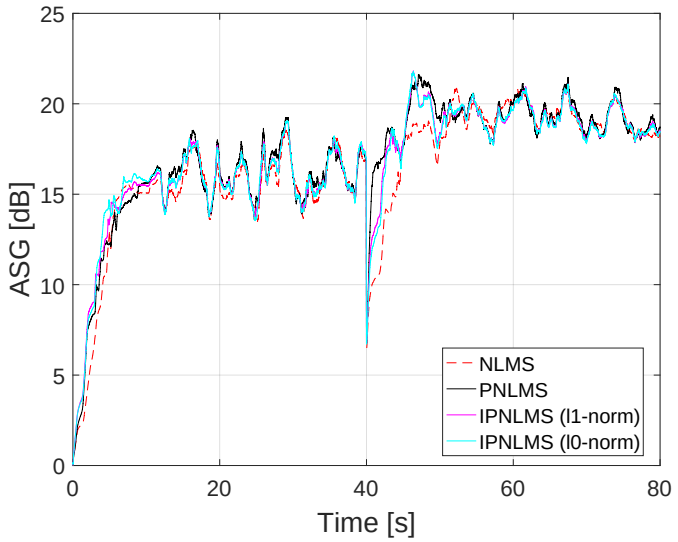

(b)

Figure 4.8: (a) Misalignment, (b) ASG of the PEM using NLMS, PNLMS, IPNLMS algorithms with music as the incoming signal.

Table 4.4: Evaluate performance of the PEM using NLMS, PNLMS, IPNLMS algorithms with music as the incoming signal.

AFC methods	$\overline{MIS}1$	$\overline{ASG}1$	PEAQ1	$\overline{MIS}2$	$\overline{ASG}2$	PEAQ2
PEM-NLMS	-12.26	14.49	-2.00	-17.00	18.35	-2.28
PEM-PNLMS	-12.61	14.90	-1.99	-17.34	19.11	-2.11
PEM-IPNLMS (l_1-norm)	-12.73	14.93	-2.02	-17.36	18.81	-2.2
PEM-IPNLMS (l_0-norm)	-12.79	15.01	-2.00	-17.34	18.75	-2.16

tem has converged, e.g., PESQ1 and PEAQ1 are measured during the period of $35s - 39s$ (before the change of the feedback path) and PESQ2, PEAQ2 are measured during the period of $75s - 79s$ (after the change of the feedback path). All mentioned methods obtain the PESQ1 scores approximately 4.4 and the PESQ2 scores approximately 4.35 for speech as the incoming signal. It is meant that all methods obtain very good signal quality when the system has converged. For music as the incoming signal, the PEAQ1 and PEAQ2 scores are approximately -2 ("slightly annoying"). However, there is a monotonic decrease in the average MIS and monotonic increase in the average ASG of, in ascending order, PEM-NLMS, PEM-PNLMS, PEM-IPNLM using l_1-norm and PEM-IPNLM using l_0-norm for both speech and music as the incoming signals.

4.5 Conclusions

In this chapter, simple but efficient ways to implement the FCAF algorithms such as the APA, the PNLMS and the IPNLMS in conjunction with the PEM have been developed for SMSL AFC in HAs. In the proposed PEM-APA, the PEM is known as a promising method to decorrelate the input signals, whereas the APA provides a superior convergence. The PEM-APA is evaluated for real speech as the incoming signal and for a sudden change of the feedback path. The simulation results show that the proposed method obtains faster convergence, quicker tracking rate, lower $\overline{MIS}$ and higher $\overline{ASG}$ than the PEM-NLMS, while maintaining good signal quality. Moreover, the proposed PEM-APA can work well for AFC in HAs with/without probe noise.

In the proposed PEM-PNLMS and PEM-IPNLMS methods for AFC in HAs, different adaptive algorithms exploiting the shape of the estimated feedback paths to calculate the tap-dependent step-size, which are used for updating the adaptive filter coefficients, have been implemented and evaluated. The quality of the speech and music signals are measured when the system has converged, showing that all compared AFC methods achieve similar signal quality. However, the proposed methods significantly improve the tracking rate compared to the PEM-NLMS for both real speech and music as the incoming signals. Their initial convergence outperforms the PEM-NLMS for the case of speech

as the incoming signal and also has a slight improvement for the case of music as the incoming signal. Morever, the proposed methods do not require prior knowledge of the feedback paths as well as incoming signal power.

CHAPTER 5

New Variable Step-Size Algorithms for Adaptive Feedback Cancellation in Hearing Aids

Chapter's key points:

- PEM-IPVSS-NLMS
- PEM-IPVSS-APA
- PEM-IPVSS-NLMS-FS/PEM-IPVSS-APA-FS
- Experimental results

5.1 Introduction

In adaptive filtering algorithms, the most important parameter is the step-size which is used to control the convergence rate of the algorithm. However, selecting a suitable step-size is a challenge since a large step-size value corresponds to a fast convergence rate but a high steady-state error, whereas a small step-size value yields a slow convergence rate but a low steady-state error. Variable step-size technique is an efficient way to control the step-size of an adaptive filter such that the step-size takes large values when the system is (or close to) unstable and takes small values when the system converges. As a result, the system obtains a fast convergence rate as well as a low steady-state error.

In the literature the applications of the VSS techniques for the AEC are quite common, but their applications for the AFC in HAs are still challenging due to the large correlation between the loudspeaker and the incoming signal. Thus,

in the AFC methods using VSS for HAs, first, different techniques have been used to lower that correlation such as inserting (white) probe noise into loudspeaker signal [90], using pre-filter with adding (white) background noise into the incoming signal [91] or employing a combination of pre-filter, subband and FS techniques [40, 70]. After that, the VSS techniques are applied to the LMS or NLMS adaptive filtering algorithms in order to recursively approximate adaptive filter coefficients such that a quick convergence rate and a low steady-state error are achieved. Although, adding (white) probe noise or (white) background noise can improve the system performance, the signal quality may be degraded if the power of inserting noise is large. Other VSS approaches employed affine projection algorithm [92, 93, 94, 95, 96] instead of the NLMS algorithm, but yielded a high increase in computational complexity since large projection orders were needed. Most existing acoustic feedback cancellation methods using VSS have only considered white noise, speech shaped noise, and real speech with added white noise as incoming signals, while only the approach in [40, 70] has been validated with music as the incoming signals.

This chapter aims at developing a new variable step-size algorithm called improved practical variable step-size (IPVSS) algorithm such that it provides a stable solution for AFC in HAs. In particular, this new VSS algorithm can be applied successfully for different adaptive filtering algorithms such as the NLMS and the APA, namely IPVSS-NLMS and IPVSS-APA, respectively. Moreover, it is robust against different types of incoming signals, e.g., real speech and music without adding white noise, and against sudden changes in the acoustic feedback paths. In the proposed IPVSS-APA, a small projection order is chosen resulting in a slight increase in the computational burden compared to the IPVSS-NLMS, but a fast convergence rate, a quick tracking rate and a low steady-state error are achieved. In fact, the proposed IPVSS algorithm is inspired from the practical variable step-size (PVSS) introduced in [80, 84]. The PVSS algorithm was successfully applied for the AEC contexts, but its application for the AFC contexts has not been investigated. The simulation in Section 5.5.1 shows that the PVSS algorithm seems not to work properly for the AFC applications due to the presence of the high correlation between the loud-

speaker and the incoming signal even when the PEM is employed. Therefore, a modification of the PVSS such that it could work well for the AFC applications is necessary. In the proposed IPVSS-NLMS algorithm and the IPVSS-APA, the variable step-size $\mu(k)$ is restricted between an upper step-size (μ_U) and a lower step-size (μ_L) in order to control the convergence behavior. Then those algorithms are implemented on the PEM for AFC in HAs, forming new AFC methods called the PEM-IPVSS-NLMS and the PEM-IPVSS-APA. In these proposed AFC methods, the well-known PEM is used to reduce the correlation between the loudspeaker and the incoming signal, leading to a lower bias in the feedback path estimate. Then the new IPVSS is implemented in conjunction with the NLMS algorithm or the APA to further improve the performance of the system. Furthermore, frequency shifting which is known as a common technique for reducing the correlation between the loudspeaker and the incoming signal is added into broadband of the proposed AFC methods. By selecting a small amount of frequency shifting, a further performance improvement is achieved while preserving good signal quality. The results of this chapter have been presented in the author's conference papers [89] and [148].

5.2 PEM-IPVSS-NLMS

This section proposes the novel IPVSS-NLMS algorithm and its effective application to the PEM in order to cancel the acoustic feedback in HAs. The proposed system model looks alike the PEM model, but the IPVSS-NLMS algorithm is used for the adaptive filter $\hat{F}(q)$. Figure 5.1 depicts the proposed system model with the IPVSS-NLMS algorithm. The derivation in this section is for the system without FS, i.e., $y(k) = y_{FS}(k)$. For the case of the system using FS, the notation $y(k)$ in all following equations is replaced by $y_{FS}(k)$, where $y_{FS}(k)$ is a version of $y(k)$ after frequency shifting.

Like in the PEM, in the proposed method it is assumed that the incoming signal can be modeled by filtering a white Gaussian noise sequence $w(k)$ via a monic and inversely stable all-pole filter $G^{-1}(q)$, i.e.,

$$u(k) = G^{-1}(q)\, w(k). \tag{5.1}$$

The microphone, error, and loudspeaker signals are defined in the same way as in Eq. (2.3), Eq. (2.9) and Eq. (2.10), respectively, i.e.,

$$x(k) = u(k) + v(k) = u(k) + \mathbf{f}^T \mathbf{y}(k), \tag{5.2}$$

$$e(k) = x(k) - \hat{v}(k) = x(k) - \hat{\mathbf{f}}^T \mathbf{y}(k), \tag{5.3}$$

$$y(k) = K(q)\, e(k), \tag{5.4}$$

where the forward path $K(q)$, the IR of the true feedback path $\mathbf{f}$ are defined in Section 2.2, and the IR of the estimated feedback path $\hat{\mathbf{f}}$ is defined in Section 2.3.2.

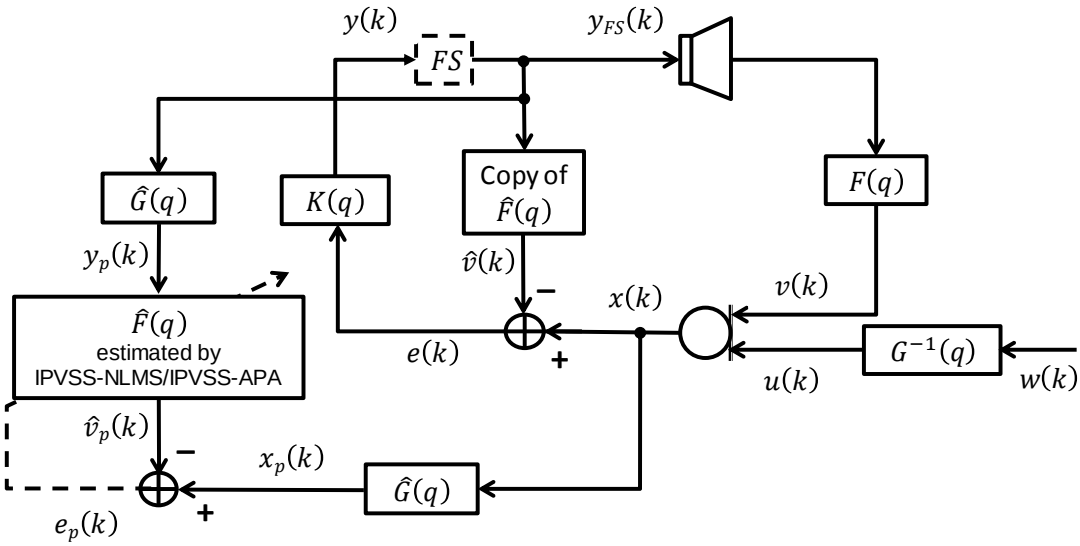

Figure 5.1: PEM model using IPVSS algorithms.

Pre-whitening filters are employed to whiten the loudspeaker and microphone signals before the adaptive process, i.e., $x_p(k) = \hat{G}(q)x(k)$ and $y_p(k) = \hat{G}(q)y(k)$, where $\hat{G}(q)$ is an estimate of $G(q)$. Thus the pre-whitened error signal is computed as

$$e_p(k) = x_p(k) - \hat{v}_p(k) = x_p(k) - \hat{\mathbf{f}}^T \mathbf{y}_p(k), \tag{5.5}$$

where $\mathbf{y}_p(k) = \left[y_p(k), y_p(k-1), \ldots, y_p\left(k - L_{\hat{f}} + 1\right)\right]^T$ is a $L_{\hat{f}}$-dimensional vector representing the pre-whitened loudspeaker signal and $\hat{v}_p(k) = \hat{\mathbf{f}}^T \mathbf{y}_p(k)$ is the pre-whitened estimation of the feedback signal. The coefficients of filter $\hat{G}(q)$ are estimated from the error signal $e(k)$ by using the Levinson-Durbin algo-

rithm [128].

Generally, the estimated feedback path in the PEM is recursively updated using the NLMS algorithm as follows

$$\hat{\mathbf{f}}(k) = \hat{\mathbf{f}}(k-1) + \frac{\mu}{\|\mathbf{y}_p(k)\|_2^2 + \delta_{NLMS}} \mathbf{y}_p(k)\, e_p(k), \tag{5.6}$$

where μ is a fixed step-size and δ_{NLMS} is a positive regularization parameter.

Assuming that Eq. (5.1) is fulfilled, the pre-whitened signals $y_p(k)$ and $u_p(k)$ are uncorrelated [16]. Thus,

$$E\left\{x_p^2(k)\right\} = E\left\{v_p^2(k)\right\} + E\left\{u_p^2(k)\right\}, \tag{5.7}$$

where

$$u_p(k) = \hat{G}(q)u(k), \tag{5.8}$$

$$v_p(k) = \mathbf{f}^T \mathbf{y}_p(k), \tag{5.9}$$

with $\mathbf{y}_p(k) = [y_p(k), y_p(k-1), \ldots, y_p(k-L_f+1)]^T$. When the adaptive filter has converged close to the optimal value, the following condition is fulfilled,

$$E\left\{\hat{v}_p^2(k)\right\} \approx E\left\{v_p^2(k)\right\}. \tag{5.10}$$

As a result, the power of pre-whitened incoming signal can be approximated as

$$\hat{\sigma}_{u_p}^2(k) \approx \hat{\sigma}_{x_p}^2(k) - \hat{\sigma}_{\hat{v}_p}^2(k). \tag{5.11}$$

Practically, the powers of microphone signal, estimated feedback signal and error signal after pre-whitening, respectively, can be recursively calculated as follows

$$\hat{\sigma}_{x_p}^2(k) = \eta\hat{\sigma}_{x_p}^2(k-1) + (1-\eta)\, x_p^2(k), \tag{5.12}$$

$$\hat{\sigma}_{\hat{v}_p}^2(k) = \eta\hat{\sigma}_{\hat{v}_p}^2(k-1) + (1-\eta)\, \hat{v}_p^2(k), \tag{5.13}$$

$$\hat{\sigma}_{e_p}^2(k) = \eta\hat{\sigma}_{e_p}^2(k-1) + (1-\eta)\, e_p^2(k), \tag{5.14}$$

where η is a positive weighting factor which is chosen such that η is close to 1.

In [80, 83], the fixed step-size in Eq. (5.6) was replaced by a practical variable step-size ($\mu_{PVSS-NLMS}(k)$) which was defined as

$$\mu_{PVSS-NLMS}(k) = \left| 1 - \frac{\sqrt{\left|\hat{\sigma}^2_{x_p}(k) - \hat{\sigma}^2_{\hat{v}_p}(k)\right|}}{\hat{\sigma}_{e_p}(k) + \zeta} \right|, \tag{5.15}$$

where ζ is a small positive value added to avoid division by zero. Note that the PVSS algorithm has been only applied for AEC but not for AFC. Our simulations show that the PVSS algorithm does not perform well in AFC contexts (cf. Figure 5.2 in Section 5.5.1). The reason is that the step-size in Eq. (5.15) fluctuates over a large range, resulting in high variations in misalignment and ASG.

To reduce those fluctuations in $\mu_{PVSS-NLMS}(k)$, an improved PVSS algorithm (IPVSS) is proposed. The IPVSS-NLMS algorithm employs a limiter [76, 91] to modify the PVSS-NLMS algorithm. This limiter uses the upper and lower limits on the step-size to control the step-size range. This constraint of the step-size means that the algorithm will have properties that are contained in that set. Thus, if we compare the performance with the upper limit and the lower limit we know that the algorithm falls within that set. The step-size of the proposed IPVSS-NLMS algorithm is defined as follows

$$\mu_{IPVSS-NLMS}(k) = \begin{cases} \mu_U & if \;\; \mu_c(k) > \mu_U \\ \mu_L & if \;\; \mu_c(k) < \mu_L \\ \mu_c(k) & otherwise \end{cases}, \tag{5.16}$$

where μ_U and μ_L are the upper and lower limits of the step-size, respectively and

$$\mu_c(k) = \mu_U * \gamma(k),$$

with $\gamma(k) = \mu_{PVSS-NLMS}(k)$. The estimated feedback path is then computed as

$$\hat{\mathbf{f}}(k) = \hat{\mathbf{f}}(k-1) + \frac{\mu_{IPVSS}(k)}{(\|\mathbf{y}_p(k)\|_2^2 + \delta_{NLMS})} \mathbf{y}_p(k)\, e_p(k).$$

By selecting suitable values for μ_U and μ_L such that $\mu_U > \mu_L$, the variation range of the step-size $\mu_{PVSS}(k)$ is bounded to a smaller range. Thus the fluctuations of the step-size are reduced and as a consequence, less variations in the performance measures are observed, i.e., misalignment and ASG compared to the PVSS-NLMS algorithm. The main difference between the proposed algorithm and the variable step-size modified decorrelation NLMS algorithm (VSS-MDNLMS) [91] is in the definition of the term $\gamma(k)$. In [91] this term was defined as

$$\gamma_{VSS-MDNLMS}(k) = \left| 1 - \frac{\hat{\sigma}_{x_p}(k)}{\hat{\sigma}_{e_p}(k) + \zeta} \right|. \tag{5.17}$$

In the following the effect of this term for the adaptive algorithm performance in two scenarios of with and/or without an added (white) background noise is analyzed. In each scenario, two cases, the adaptive feedback canceler has converged close to the optimal value and the feedback system is (close to) unstable, have been considered.

Scenario 1: No (white) background noise is added into the incoming signal.

Case 1: The feedback cancellation filter has converged close to the optimal value, i.e., $\hat{\mathbf{f}}(k) \to \mathbf{f}(k)$, hence $\hat{\sigma}^2_{e_p}(k) \approx \hat{\sigma}^2_{u_p}(k)$:

The Eq. (5.17) can be rewritten as

$$\gamma_{VSS-MDNLMS}(k) \approx \left| 1 - \sqrt{1 + \frac{\hat{\sigma}^2_{v_p}(k)}{\hat{\sigma}^2_{u_p}(k)}} \right| = \left| 1 - \beta_1(k) \right|, \tag{5.18}$$

where $\beta_1(k) = \sqrt{1 + \frac{\hat{\sigma}^2_{v_p}(k)}{\hat{\sigma}^2_{u_p}(k)}} > 1$. It can be seen that $\gamma_{VSS-MDNLMS}(k)$ (so step-size of the VSS-MDNLMS algorithm, $\mu_{VSS-MDNLMS}(k)$) depends on the feedback to (incoming) signal ratio (FSR). The larger this ratio is, the larger $\beta_1(k)$ and thus the larger value of $\mu_{VSS-MDNLMS}(k)$ is obtained, resulting in a high steady-state error.

In contrast, in the IPVSS-NLMS algorithm $\gamma(k) = \mu_{PVSS-NLMS}(k) = |1 - \beta_2(k)|$, where $\beta_2(k) = \frac{\sqrt{\left|\hat{\sigma}^2_{x_p}(k) - \hat{\sigma}^2_{v_p}(k)\right|}}{\hat{\sigma}_{e_p}(k) + \zeta} \approx 1$, hence $\gamma(k) \approx 0$, and $\mu_{IPVSS-NLMS}(k) = \mu_L$ (the lower bound). As a result, the proposed algorithm achieves a lower steady-state error compared to the VSS-MDNLMS algorithm when the system has con-

verged. Note that the value μ_L can be set such that the desired misalignment is achieved. Without the lower limit the step-size can be zero and the adaptive filter can lockup and be insensitive to learning data.

Case 2: The system is (close to) unstable, e.g., in the initialization phase and when the feedback path changes:

Under this condition, Eq. (5.10) and Eq. (5.11) do not hold. In $\beta_i(k)$, with $i = 1, 2$, the nominator increases faster than the denominator, i.e., $\beta_i(k) > 1$. Therefore, the variable step-sizes of both algorithms tend to take large values, which drive the the weights of the feedback canceler to converge faster.

Scenario 2: A (white) background noise is added into the incoming signal. In this case the incoming signal plus noise ($u^n(k)$) is an addition of the incoming signal ($u(k)$) with white background noise ($n(k)$), i.e.,

$$u^n(k) = u(k) + n(k). \tag{5.19}$$

Then the pre-filtered incoming signal plus noise can be defined as

$$u_p^n(k) = u_p(k) + n_p(k), \tag{5.20}$$

where $n_p(k)$ is the pre-filtered (white) noise. The incoming signal and the added noise are uncorrelated, so that

$$\hat{\sigma}^2_{u_p^n}(k) = \hat{\sigma}^2_{u_p}(k) + \hat{\sigma}^2_{n_p}(k). \tag{5.21}$$

The Eq. (5.2) and Eq. (5.5) can be rewritten as

$$x_p^n(k) = u_p^n(k) + v_p^n(k), \tag{5.22}$$

$$e_p^n(k) = x_p^n(k) - \hat{v}_p^n(k), \tag{5.23}$$

where $v_p^n(k)$ and $\hat{v}_p^n(k)$ are the true and the estimated feedback signals (with noise) after pre-filtering defined in a manner analogous to $v_p(k)$ and $\hat{v}_p(k)$, re-

spectively. The terms $\beta_1(k)$ and $\beta_2(k)$ in scenario 1 can be redefined as follows

$$\beta_1^n(k) = \frac{\hat{\sigma}_{x_p^n}(k)}{\hat{\sigma}^2_{e_p^n}(k)}, \tag{5.24}$$

$$\beta_2^n(k) = \frac{\sqrt{\left|\hat{\sigma}^2_{x_p^n}(k) - \hat{\sigma}^2_{\hat{v}_p^n}(k)\right|}}{\hat{\sigma}_{e_p^n}(k)}. \tag{5.25}$$

Case 1:

For the VSS-MDNLMS algorithm, the term $\beta_1^n(k) = \sqrt{1 + \frac{\hat{\sigma}^2_{v_p^n}(k)}{\hat{\sigma}^2_{u_p}(k)+\hat{\sigma}^2_{n_p}(k)}} > 1$, which depends on the the feedback to (incoming) signal plus noise ratio (FSNR). By selecting background noise with a larger power compared to incoming signals (speech/music) such that $\beta_1^n(k) < \beta_1(k)$, the VSS-MDNLMS algorithm tends to get smaller step-size values, resulting in a lower steady-state error. However, the simulations in [91] showed that with signal to (background) noise ratio $SNR = 20$ dB the $\mu_{VSS-MDNLMS}(k)$ still fluctuates between the values μ_U and μ_L according to the change of FSNR. For the IPVSS-NLMS algorithm, the term $\beta_2^n(k)$ behaves in a similar manner to $\beta_2(k)$ in the case 1 of scenario 1, i.e., the (white) background noise has small or no impact on the result.

Case 2:

In this case, similar conclusions as case 2 (scenario 1) can be drawn. Note that the VSS-MDNLMS algorithm needs a noisy input signal to work and that is not conducive for a well working algorithm.

5.3 PEM-IPVSS-APA

It is known that the convergence and tracking rates of the system using the NLMS algorithm degrade when the incoming signal is spectrally coloured. In this section, an extension of the IPVSS algorithm in the Section 5.2 is developed for the APA, namely IPVSS-APA. The idea is to take advantage of the powerful characteristics of the APA with regards to faster convergence and tracking rates compared to the NLMS algorithm. The system model of the PEM using IPVSS-APA is similar to the PEM-IPVSS-NLMS, except the adaptive filter is now updated by using the IPVSS-APA instead of using the IPVSS-NLMS al-

gorithm, cf. Figure 5.1. In fact, the PEM-IPVSS-NLMS can be considered as a special case of the PEM-IPVSS-APA when the projection order $P = 1$.

Generally, in the proposed approach the PEM is utilized to reduce the bias in the estimation of the acoustic feedback path, while a small projection order of the APA is chosen to improve the convergence and tracking rates [35]. In addition, the IPVSS, which was successfully applied to the PEM using NLMS algorithm [89], is also employed for the APA in order to further enhance the convergence and tracking rates of the system. As a result, the proposed approach achieves significant improvements on convergence rate and tracking rate, while still maintaining a low steady-state misalignment compared to the PEM-IPVSS-NLMS as well as the PEM-APA using either the lower or upper step-size limits. The following derivation in this section is for the system without FS, i.e., $y(k) = y_{FS}(k)$.

In the PEM-IPVSS-APA, the P most recent input vectors are used to estimate the IR of an adaptive filter, where P is the projection order. Therefore, the input matrix of the adaptive filter $\hat{F}(q)$ can be expressed as

$$\mathbf{Y}_p(k) = [\mathbf{y}_p(k), \mathbf{y}_p(k-1), \ldots, \mathbf{y}_p(k-P+1)], \tag{5.26}$$

where $\mathbf{y}_p(k) = \left[y_p(k), y_p(k-1), \ldots, y_p\left(k-L_{\hat{f}}+1\right)\right]^T$ is the $L_{\hat{f}}$-dimensional vector of pre-whitened loudspeaker signal. The microphone signal vector and the vector of estimated feedback signal after pre-whitening are denoted as $\mathbf{x}_p(k) = [x_p(k), x_p(k-1), ..., x_p(k-P+1)]^T$ and $\hat{\mathbf{v}}_p(k) = \mathbf{Y}_p^T(k)\,\hat{\mathbf{f}}(k)$, respectively. Hence, the pre-whitened error vector $\mathbf{e}_p(k)$ is computed as

$$\mathbf{e}_p(k) = \mathbf{x}_p(k) - \hat{\mathbf{v}}_p(k). \tag{5.27}$$

In the IPVSS-APA, the IR of the acoustic feedback path is estimated as follows

$$\hat{\mathbf{f}}(k) = \hat{\mathbf{f}}(k-1) + \mathbf{Y}_p(k)\left[\mathbf{Y}_p^T(k)\,\mathbf{Y}_p(k) + \delta_{APA}\mathbf{I}_P\right]^{-1}\boldsymbol{\mu}_{IPVSS-APA}(k)\,\mathbf{e}_p(k), \tag{5.28}$$

where δ_{APA} is a regularization parameter; $\mathbf{I}_P$ is an $(P\times P)$ identity matrix and

Table 5.1: Regularization parameters for the APA.

Projection order	Regularization parameter
$P = 1$	$\delta_{APA} = 20\hat{\sigma}^2_{y_p}$
$P = 2$	$\delta_{APA} = 50\hat{\sigma}^2_{y_p}$
$P = 4$	$\delta_{APA} = 100\hat{\sigma}^2_{y_p}$
$P = 8$	$\delta_{APA} = 200\hat{\sigma}^2_{y_p}$

$\boldsymbol{\mu}_{IPVSS-APA}(k)$ is the variable step-size for the PEM-IPVSS-APA, i.e.,

$$\boldsymbol{\mu}_{IPVSS-APA}(k) = \text{diag}\left\{\mu_0(k), \ldots, \mu_{P-1}(k)\right\}. \tag{5.29}$$

The regularization parameter is selected such that the lager δ_{APA} is for the lager value of the projection order and vice versa. The reason is that the condition number of the matrix $\mathbf{Y}_p^T(k)\,\mathbf{Y}_p(k)$ increases when the projection order increases. Table 5.1 provides the relationship between the projection order and the regularization parameter [84], where $\hat{\sigma}^2_{y_p}$ denotes the power of the pre-whitened loudspeaker signal. The value of $\hat{\sigma}^2_{y_p}$ is recursively updated, i.e.,

$$\hat{\sigma}^2_{y_p}(k) = \eta\hat{\sigma}^2_{y_p}(k-1) + (1-\eta)\,y_p^2(k). \tag{5.30}$$

The variable step-size for each projection order is computed as

$$\mu_i(k) = \begin{cases} \mu_U & if\ \ \mu_{c,i}(k) > \mu_U \\ \mu_L & if\ \ \mu_{c,i}(k) < \mu_L \\ \mu_{c,i}(k) & otherwise \end{cases}, \tag{5.31}$$

where

$$\mu_{c,i}(k) = \mu_U \left| 1 - \frac{\sqrt{\left|\hat{\sigma}^2_{x_p}(k-i) - \hat{\sigma}^2_{\hat{v}_p}(k-i)\right|}}{\hat{\sigma}_{e_{p,i+1}}(k) + \zeta} \right|. \tag{5.32}$$

The power of pre-whitened error signal corresponding to each projection order is recursively updated as

$$\hat{\sigma}^2_{e_{p,i+1}}(k) = \eta\hat{\sigma}^2_{e_{p,i+1}}(k-1) + (1-\eta)\,e^2_{p,i+1}(k), \tag{5.33}$$

with $i = 0, \ldots, P-1$.

The terms $\hat{\sigma}^2_{x_p}(k)$ and $\hat{\sigma}^2_{\hat{v}_p}(k)$ are also recursively approximated as follows

$$\hat{\sigma}^2_{x_p}(k) = \eta \hat{\sigma}^2_{x_p}(k-1) + (1-\eta) x_p^2(k), \tag{5.34}$$

$$\hat{\sigma}^2_{\hat{v}_p}(k) = \eta \hat{\sigma}^2_{\hat{v}_p}(k-1) + (1-\eta) \hat{v}_p^2(k). \tag{5.35}$$

It can be seen that the PEM-IPVSS-NLMS is a special case of the PEM-IPVSS-APA when $P = 1$.

Table 5.2: PEM-IPVSS-APA.

Initial parameters: $\hat{\mathbf{f}}(0) = \mathbf{0}_{L_{\hat{f}} \times 1}$; $\hat{\sigma}^2_{x_p}(0) = 0$; $\hat{\sigma}^2_{\hat{v}_p}(0) = 0$;

for $i = 0$ to $P-1$

$\hat{\sigma}^2_{e_{p,i+1}}(0) = 0$

end

for $k = 1, 2, \ldots$

$\hat{\mathbf{v}}_p(k) = \mathbf{Y}_p^T(k) \hat{\mathbf{f}}(k)$

$\mathbf{e}_p(k) = \mathbf{x}_p(k) - \hat{\mathbf{v}}_p(k)$

$\hat{\sigma}^2_{x_p}(k) = \eta \hat{\sigma}^2_{x_p}(k-1) + (1-\eta) x_p^2(k)$

$\hat{\sigma}^2_{\hat{v}_p}(k) = \eta \hat{\sigma}^2_{\hat{v}_p}(k-1) + (1-\eta) \hat{v}_p^2(k)$

for $i = 0$ to $P-1$

$\hat{\sigma}^2_{e_{p,i+1}}(k) = \eta \hat{\sigma}^2_{e_{p,i+1}}(k-1) + (1-\eta) e^2_{p,i+1}(k)$

$$\mu_{c,i}(k) = \mu_U \left| 1 - \frac{\sqrt{\left|\hat{\sigma}^2_{x_p}(k-i) - \hat{\sigma}^2_{\hat{v}_p}(k-i)\right|}}{\hat{\sigma}_{e_{p,i+1}}(k) + \zeta} \right|$$

$$\mu_i(k) = \begin{cases} \mu_U & if \ \ \mu_{c,i}(k) > \mu_U \\ \mu_L & if \ \ \mu_{c,i}(k) < \mu_L \\ \mu_{c,i}(k) & otherwise \end{cases}$$

end

$\boldsymbol{\mu}_{IPVSS-APA}(k) = \operatorname{diag}\{\mu_0(k), \ldots, \mu_{P-1}(k)\}$

$$\hat{\mathbf{f}}(k) = \hat{\mathbf{f}}(k-1) + \mathbf{Y}_p(k) \left[\mathbf{Y}_p^T(k) \mathbf{Y}_p(k) + \delta_{APA} \mathbf{I}_P\right]^{-1} \boldsymbol{\mu}_{IPVSS-APA}(k) \mathbf{e}_p(k)$$

end

To avoid a significant increase in computational complexity due to the high projection order of the APA, the smallest projection order is chosen for the proposed approach, i.e., $P = 2$. The proposed approach PEM-IPVSS-APA is summarized in Table 5.2.

5.4 Frequency shifting

The frequency shifting (FS) technique [2, 39, 38, 40, 41] is known as a non-linear operation which contributes to the decorrelation between the loudspeaker signal and the incoming signal. As a result, a lower bias in the estimation of the acoustic feedback path can be obtained. In this section the FS is integrated into the PEM-NLMS, PEM-APA, PEM-IPVSS-NLMS and PEM-IPVSS-APA. Here the FS which is similar to the one proposed in [40] is selected, except the FS now is used for broadband signal, cf. Figure 5.1. The frequency shifting is applied to the signal $y(k)$ representing the output of the hearing aid processing. The analytical representation of the signal $y(k)$ is denoted as

$$y_{\mathrm{a}}(k) = y(k) + j y_{\mathrm{H}}(k), \tag{5.36}$$

where $y_{\mathrm{H}}(k)$ is the Hilbert transform of $y(k)$. The frequency shifting is modeled as a periodically time-varying filter, i.e.,

$$h(k) = \exp\left(j2\pi \frac{f_0}{f_s} k\right), \tag{5.37}$$

where f_s is the sampling frequency and f_0 is the amount of frequency shifting. Now the loudspeaker signal $y_{FS}(k)$, i.e., the output of the FS, can be computed as follows

$$y_{FS}(k) = \mathrm{Re}\{y_{\mathrm{a}}(k)\, h(k)\}. \tag{5.38}$$

Substituting Eq. (5.36) and Eq. (5.37) into Eq. (5.38) yields

$$y_{FS}(k) = y(k)\cos(2\pi f_0 k) - y_{\mathrm{H}}(k)\sin(2\pi f_0 k). \tag{5.39}$$

The FS can significantly reduce the bias in the adaptive process but it also introduces roughness in the signals. Therefore, a small amount of the FS, e.g.,

$0Hz < f_0 \leq 10Hz$, is recommended [42].

5.5 Experimental results

In this section, the proposed PEM-IPVSS-NLMS and PEM-IPVSS-APA with speech and music as the incoming signals and with a sudden change of the feedback path are evaluated. Furthermore, the effect of a small amount of frequency shifting on the performance of those methods is also evaluated.

5.5.1 Results for PEM-IPVSS-NLMS

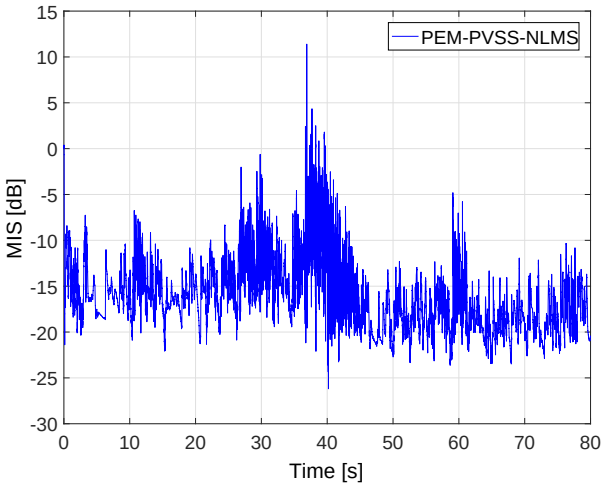

(a)

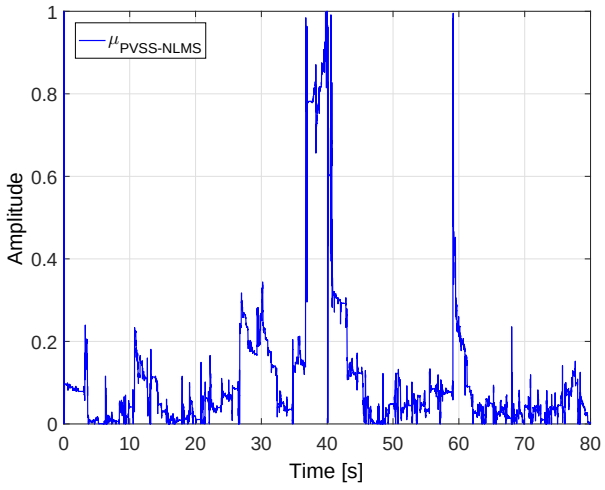

(b)

Figure 5.2: (a) Misalignment of the PEM-PVSS-NLMS; (b) $\mu_{PVSS-NLMS}$, speech as the incoming signal.

In this subsection, the proposed PEM-IPVSS-NLMS without FS is evaluated for both speech and music as the incoming signals and compared with the PEM

using the VSS-MDNLMS algorithm (PEM-VSS-MDNLMS) as well as the PEM using either the upper or lower step-size limits. The same measured acoustic feedback paths with magnitude and phase responses as used in Section 4.4.1 (cf. Figure 4.2) are selected. The length of the measured feedback paths is $L_f = 100$ and the sampling frequency is $f_s = 16$ kHz.

The speech used as incoming signal is concatenated speech which is constructed by concatenating male and female speech patterns extracted from NOIZEUS database [120], while music used as the incoming signal is the song "Imagine" by John Lennon. All simulations have 80 s lengths with a sudden change from the free-field to the telephone-near feedback path after 40 s. No background noise has been added into the incoming signals in all simulations. The normalized misalignment (MIS) and the added stable gain (ASG) which are defined in the same way as in Section 2.5 are utilized to evaluate the performance of all AFC methods.

The following parameters are set for all simulations. The forward path gain and the delay of the hearing aid are $|K| = 30$ dB and $d_k = 6$ ms, respectively. The delay in the feedback canceler path is 1 sample. The length of the adaptive filter $L_{\hat{f}} = 64$, the step-size limits $\mu_U = 0.01$, $\mu_L = 0.001$, and parameters $\eta = 0.9999$, $\zeta = 10^{-6}$, $\delta_{NLMS} = 10^{-10}$ are chosen. The Levinson-Durbin algorithm is used to update the prediction-error filter $\hat{G}(q)$ of order 20 every 10 ms.

Figure 5.3 shows the behavior of $\mu_{VSS-MDNLMS}(k)$ corresponding to speech as the incoming signal and music as the incoming signal with a sudden change of the feedback path after 40 s, respectively. It can be observed that those step-sizes match with the analysis in Scenario 1. When the incoming signal is speech, this step-size seems to get the maximum value almost every time, resulting in high convergence rate and high steady-state error. When the incoming signal is music, this step-size fluctuates quickly in the first 40 s and gets the maximum value after the feedback path changes, thus high variations in the performance of the system are observed. Figure 5.4 and Figure 5.5 illustrate the MIS and ASG of the PEM-VSS-MDNLMS for those incoming signals, respectively. In fact, the PEM-VSS-MDNLMS performance is similar to that of

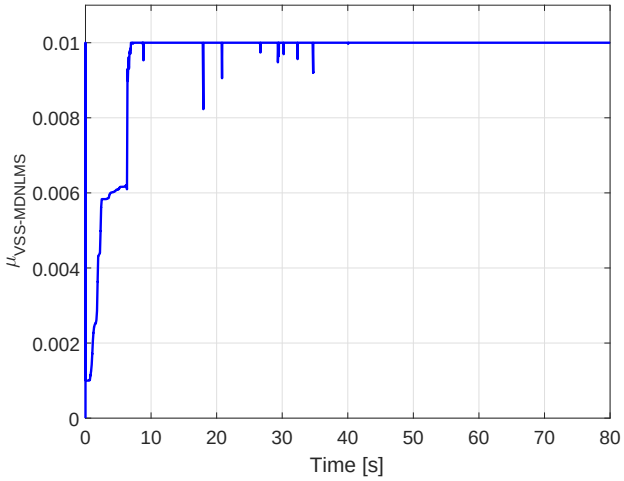

(a)

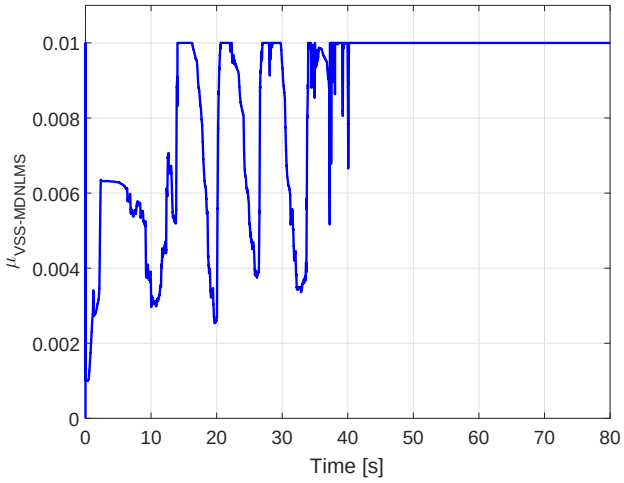

(b)

Figure 5.3: Variable step-sizes of PEM-VSS-MDNLMS with (a) speech, (b) music and a change of the feedback path.

the PEM-NLMS with upper step-size, except it has a slower convergence rate in the initial phase.

Figure 5.6 shows the simulation results for the proposed method with the speech as the incoming signal. The PEM-IPVSS solution outperforms the PEM which only employs either the upper or the lower step-size used in the IPVSS-NLMS algorithm. It also provides much better misalignment and added stable gain than the PEM-VSS-MDNLMS illustrated in Figure 5.4. Especially, when the feedback path changes from the free-field to the telephone-near feedback path, the proposed method tracks the change almost as quickly as the case of the

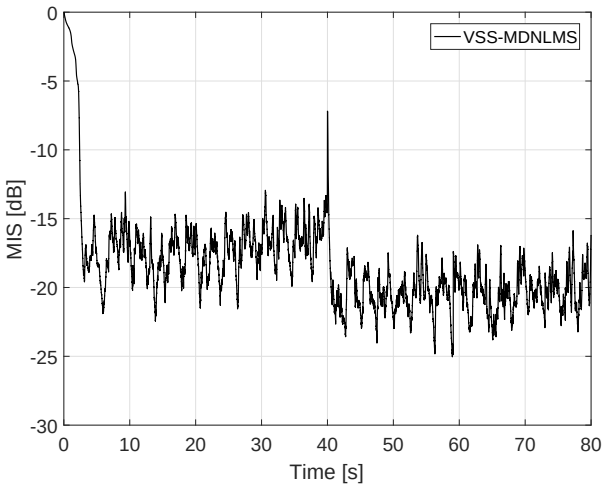

(a)

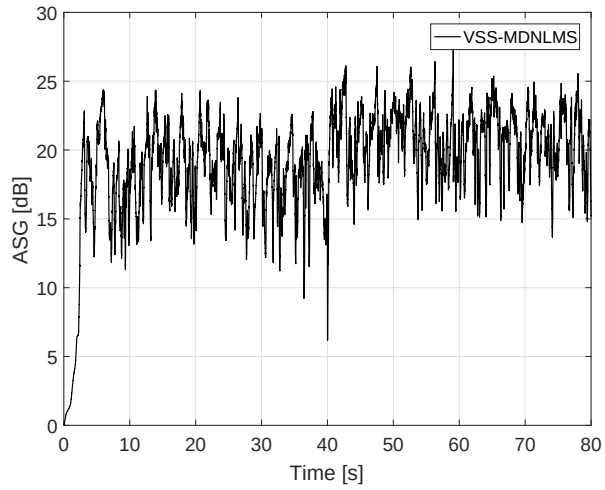

(b)

Figure 5.4: (a) Misalignment, (b) Added Stable Gain of the PEM-VSS-MDNLMS with speech as the incoming signal and a sudden change of the feedback path.

PEM using the upper step-size $\mu_U = 0.01$, while remaining similar steady-state error to the case of the PEM with the lower step-size $\mu_L = 0.001$.

Figure 5.7 demonstrates the results for the proposed method with music as the incoming signal. The simulations show that the PEM-IPVSS-NLMS yields significant improvements in convergence rate as well as tracking rate compared to the PEM with the lower step-size $\mu_L = 0.001$, while providing much lower steady-state error than the PEM with the upper step-size $\mu_U = 0.01$. The proposed method also outperforms the PEM-VSS-MDNLMS presented in Figure 5.5.

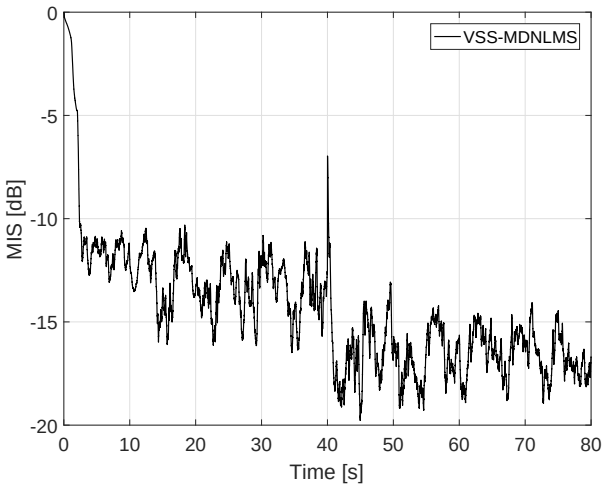

(a)

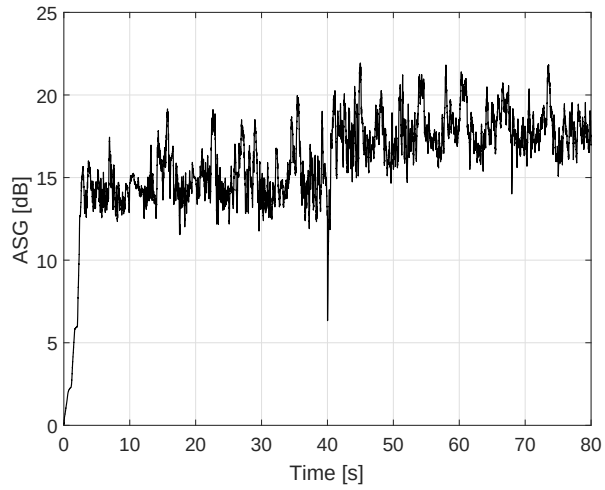

(b)

Figure 5.5: (a) Misalignment, (b) Added Stable Gain of the PEM-VSS-MDNLMS with music as the incoming signal and a sudden change of the feedback path.

Figure 5.8 and Figure 5.9 show that "howling" occurs in the beginning and when the feedback path changes. For the PEM with $\mu_L = 0.001$ the howling periods are much longer than the case of the PEM with $\mu_U = 0.01$. The reason is that the larger step-size makes the system converge faster, i.e., a shorter howling period is observed, but it also provides a larger steady-state error as well as larger variations in the performance and vice versa. For both speech and music as the incoming signals, the proposed method provides a compromise solution, i.e., it can significantly reduce the howling periods, improve convergence rate and tracking rate while lowering steady-state error. Figure 5.8d and Figure 5.9d

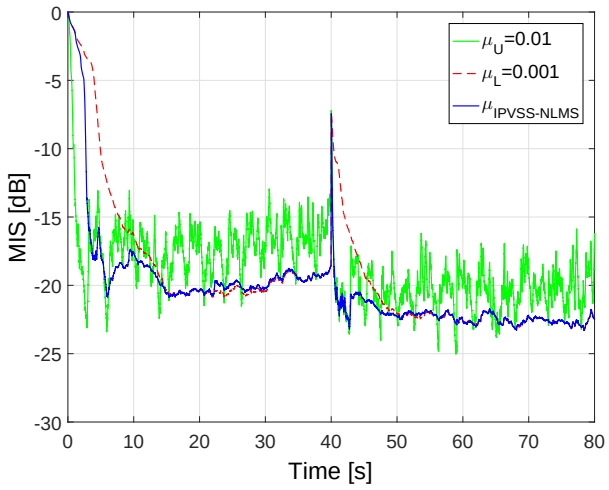

(a)

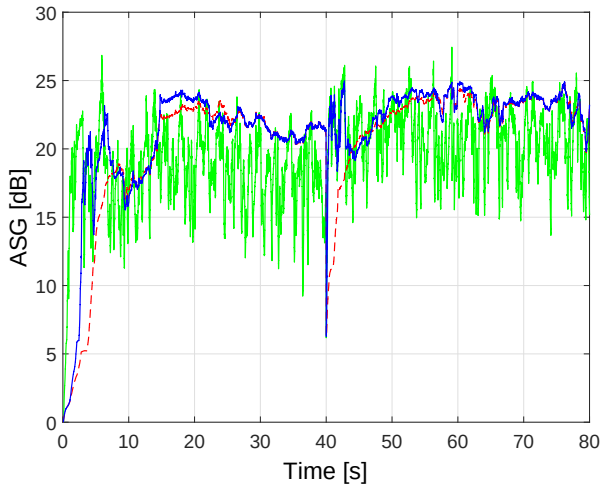

(b)

Figure 5.6: (a) Misalignment, (b) Added Stable Gain of the PEM-NLMS using μ_U, μ_L, and PEM-IPVSS-NLMS with speech as the incoming signal and a sudden change of the feedback path.

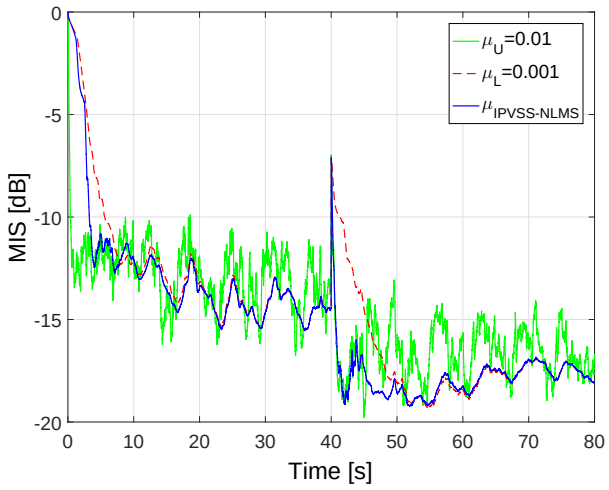

(a)

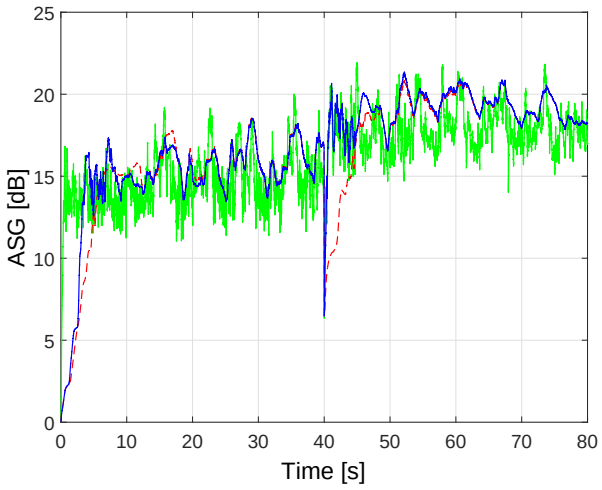

(b)

Figure 5.7: (a) Misalignment, (b) Added Stable Gain of the PEM-NLMS using μ_U, μ_L, and PEM-IPVSS-NLMS with music as the incoming signal and a sudden change of the feedback path.

present the variable step-sizes for the PEM-IPVSS-NLMS with speech and music as the incoming signals, respectively. For both cases, the variations of the step-sizes match with the description in the scenario 1, i.e., they are larger when the system is unstable, e.g., in the beginning of simulation and at the change of the feedback path, and smaller when the system is converged.

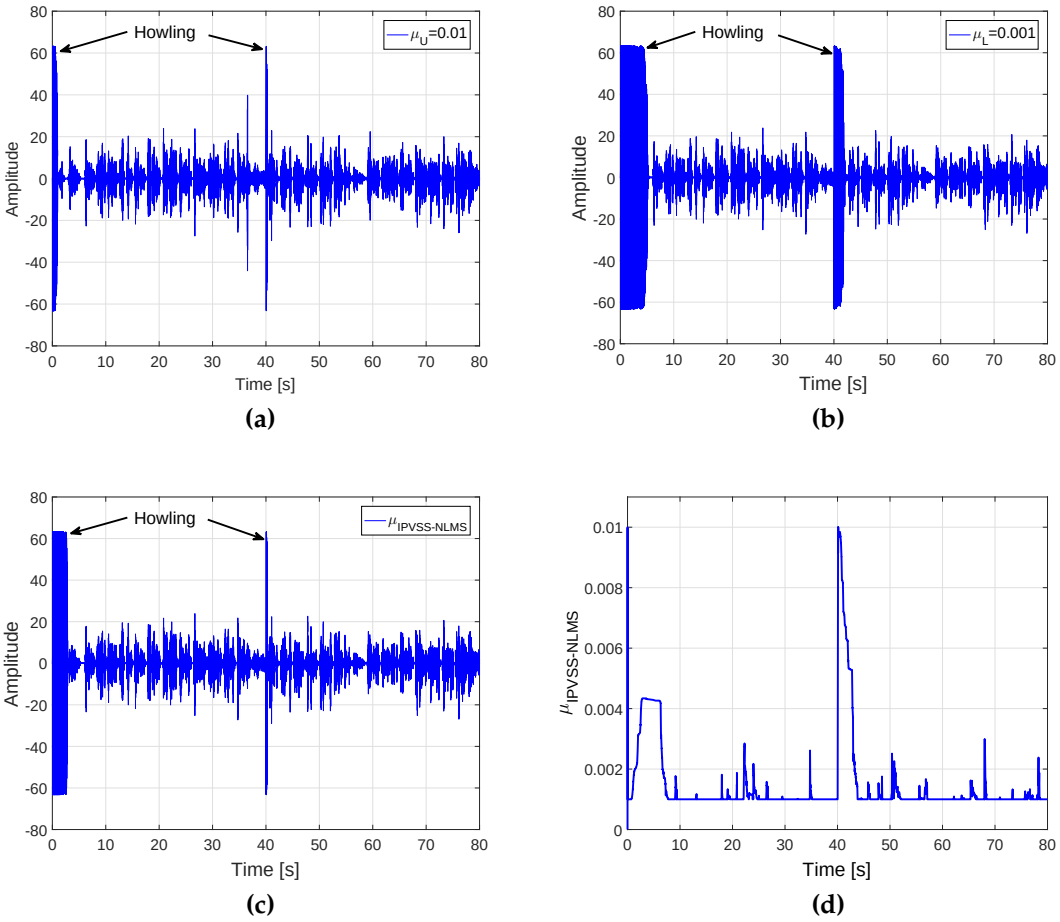

Figure 5.8: Loudspeaker signals for the case of speech as the incoming signal: (a) and (b) PEM-NLMS with μ_U = 0.01, μ_L = 0.001, respectively; (c) PEM-IPVSS-NLMS, and (d) step-size $\mu_{IPVSS-NLMS}$.

For all above simulations, the proposed approach seems to have a slower initial convergence rate and a slower tracking rate than the PEM-NLMS using μ_U since Eq. (5.7) and Eq. (5.10) are biased in these situations [84].

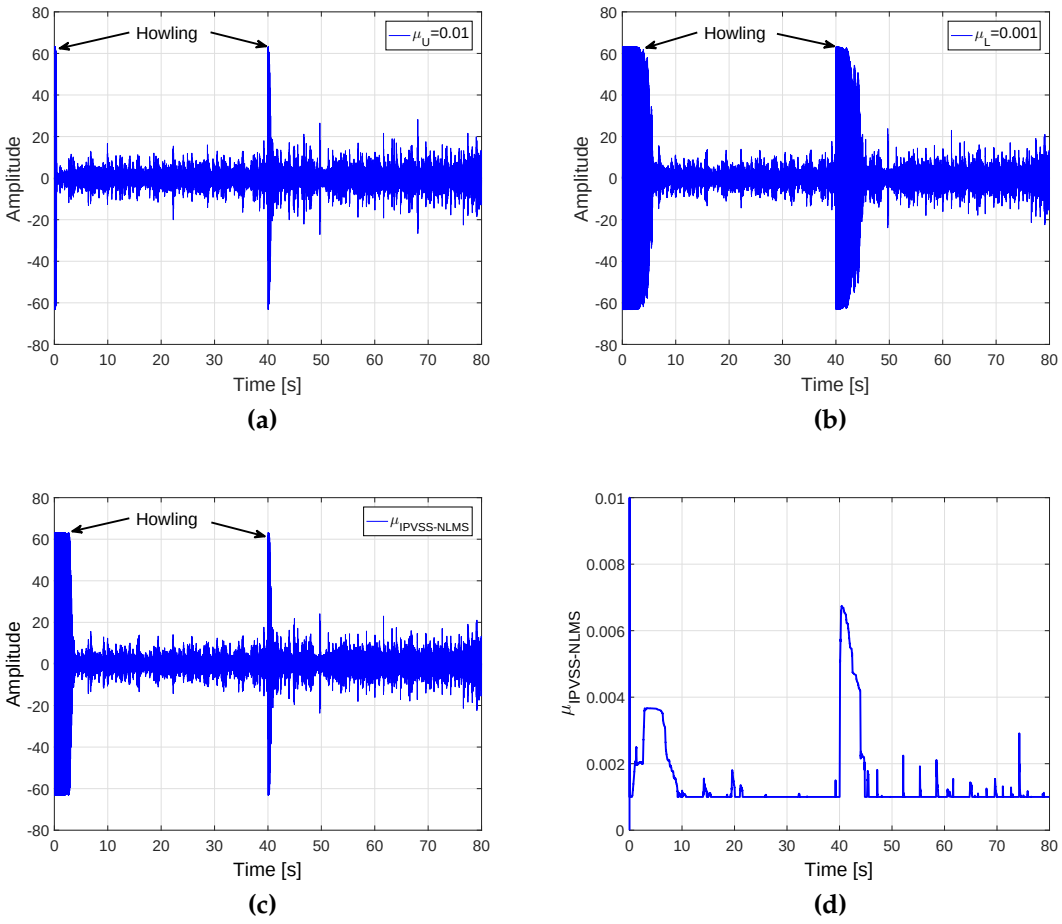

Figure 5.9: Loudspeaker signals for the case of music as the incoming signal: (a) and (b) PEM-NLMS with $\mu_U = 0.01$, $\mu_L = 0.001$, respectively; (c) PEM-IPVSS-NLMS, and (d) step-size $\mu_{IPVSS-NLMS}$.

5.5.2 Results for PEM-IPVSS-APA

In this subsection, the proposed PEM-IPVSS-APA without FS is evaluated for speech and music as the incoming signals and with a sudden change of the feedback path. The same measured acoustic feedback paths and the same speech and music which used in simulations of the PEM-IPVSS-NLMS (cf. Section 5.5.1) are chosen. The acoustic feedback path changes from the free-field feedback path to the telephone-near feedback path after 40 s.

The following parameters are set for all simulations. The lengths of the measured acoustic feedback path and the estimated acoustic feedback path are $L_f = 100$ and $L_{\hat{f}} = 64$, respectively. The sampling frequency $f_s = 16\text{kHz}$, the forward path gain $|K| = 30\,dB$, the delay in the forward path $d_k = 96$ samples,

the delay in the feedback canceller path $d_{fb} = 1$ sample are chosen. The upper and lower bounds of the step-sizes are $\mu_U = 0.005$, $\mu_L = 0.0005$, respectively. The weighting factor $\eta = 0.9999$ and the parameter $\zeta = 10^{-6}$ are also selected. The regularization parameters δ_{APA} are chosen following Table 5.1. The smallest projection order is selected, i.e., $P = 2$ to avoid a large increase in computational complexity. The order of 20 is assigned for the prediction-error filter $\hat{G}(q)$ which is estimated by using the Levinson-Durbin algorithm every 10 ms. For evaluating the performance of mentioned AFC approaches, the normalized misalignment (MIS) and the added stable gain (ASG) defined in a manner analogous to those in Section 2.5 are utilized.

Moreover, the perceptual evaluation of speech quality (PESQ) [120] is also used to evaluate the speech quality. For evaluation of music quality the perceptual evaluation of audio quality (PEAQ) [121] is used. In both PESQ and PEAQ measures the incoming signal $u(k)$ and the error signal $e(k)$ are chosen for the reference signal and the test signal, respectively. Here the PESQ and the PEAQ are measured when the system has converged (during the periods of $35s - 39s$ and $75s - 79s$). Firstly the simulation for the PEM-PVSS-APA with $P = 2$ and speech as the incoming signal is run to show that the PVSS-APA which was introduced in [84] for the AEC contexts seems not to work well for the AFC applications, even when the PEM is employed. The reason is the inherent correlation between the loudspeaker signal and the microphone signal in the AFC contexts. Figure 5.10a shows that the misalignment behavior of the PEM-PVSS-APA is poor due to the frequent fluctuation of the variable step-size $\mu_{PVSS-APA}$ over a large range (cf. Figure 5.10b).

Secondly performance of the proposed PEM-IPVSS-APA with $P = 2$ using speech as the incoming signal is evaluated. Figure 5.11 compares the MIS and ASG of the proposed PEM-IPVSS-APA for speech as the incoming signal and a sudden change of the acoustic feedback path after 40 s to the PEM-IPVSS-NLMS and the PEM-APA using only the upper or the lower step-sizes which is utilized as the boundaries in the IPVSS-APA. It can be seen that the proposed approach outperforms the PEM-APA. In fact, it provides much higher conver-

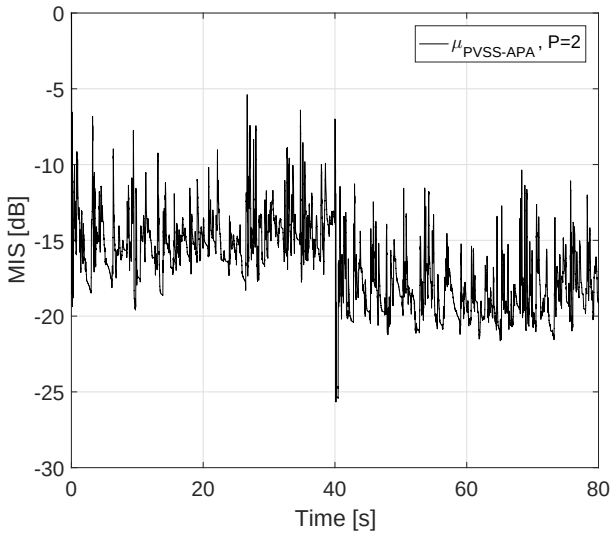

(a)

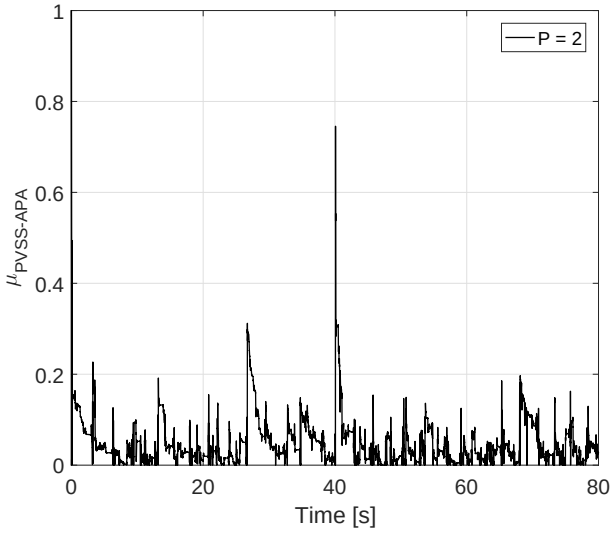

(b)

Figure 5.10: (a) MIS and (b) practical variable step-size results for PEM-PVSS-APA (P=2) with speech as the incoming signal, a sudden change of the acoustic feedback path and without FS.

gence and tracking rate but still maintains a similar steady-state error and a similar ASG level compared to the PEM-APA using μ_L. Moreover, the proposed approach yields a significant improvement in steady-state error while a similar tracking rate compared to the PEM-APA using μ_U is retained. Furthermore, the PEM-IPVSS-APA converges quicker and can track the abrupt change of the acoustic feedback path faster than the PEM-IPVSS-NLMS, while providing a similar steady-state error as well as a similar ASG level when the system converges.

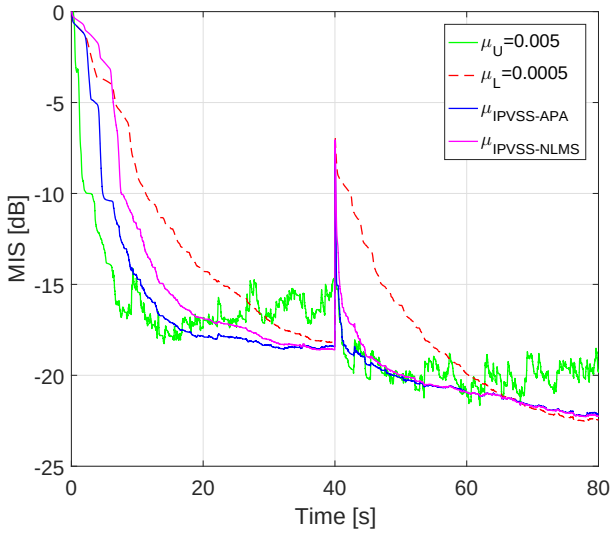

(a)

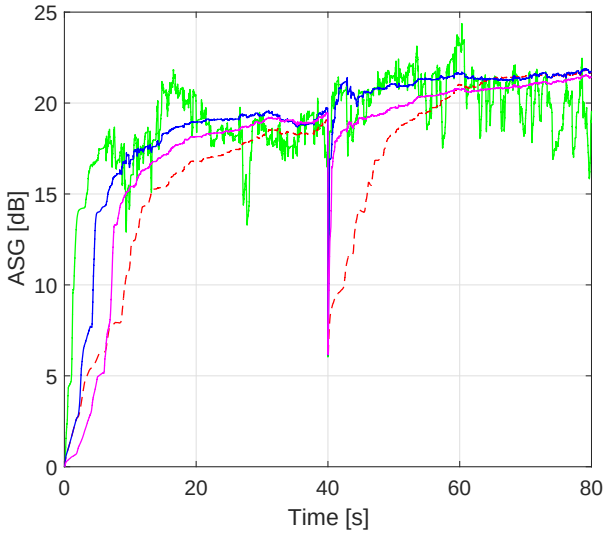

(b)

Figure 5.11: (a) MIS and (b) ASG results for PEM-APA using μ_U, μ_L and PEM-IPVSS-APA with speech as the incoming signal, a sudden change of the acoustic feedback path and without FS.

Figure 5.12 depicts the variable step-size $\mu_{IPVSS-APA}$ for the PEM-IPVSS-APA with speech as the incoming signal. It can be observed that this step-size tends to pick up larger values when the system is unstable, e.g., when the acoustic feedback path changes or at the beginning of simulation, and to get small values when the system has converged. Thus the system will obtain high convergence rate as well as tracking rate while still retaining a low steady-state error.

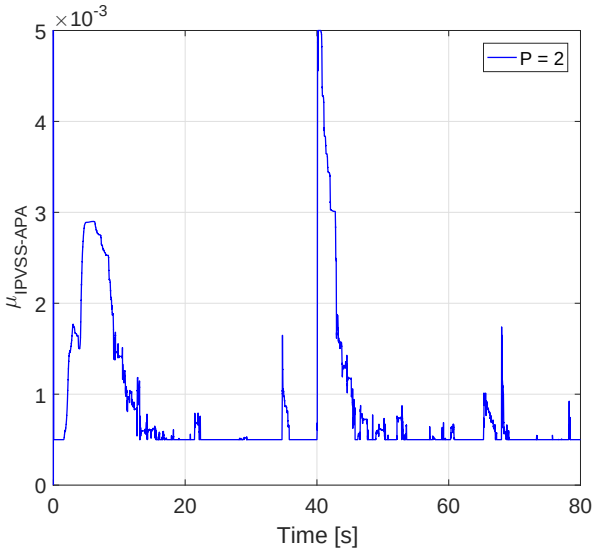

Figure 5.12: Variable step-sizes $\mu_{IPVSS-APA}$ for PEM-IPVSS-APA with speech as the incoming signal and a sudden change of the acoustic feedback path.

Table 5.3 presents the PESQ measures of the above approaches when the system has converged, e.g., the PESQ1 scores are measured during the segment of $35s$–$39s$ (before the change of the feedback path) and the PESQ2 scores are measured during the segment of $75s$ – $79s$ (after the change). It shows that all mentioned approaches yield good PESQ1 and PESQ2 scores, but the proposed approach achieves better PESQ1 and PESQ2 scores compared to the PEM-APA with μ_U while providing similar those scores (approximately 4.4) compared to the other approaches.

Table 5.3: PESQ scores for speech as the incoming signal, a sudden change of the acoustic feedback path and without frequency shifting.

AFC methods	PESQ1	PESQ2
PEM-APA, μ_U = 0.005	4.06	3.99
PEM-APA, μ_L = 0.0005	4.39	4.39
PEM-IPVSS-APA	4.43	4.37
PEM-IPVSS-NLMS	4.45	4.36

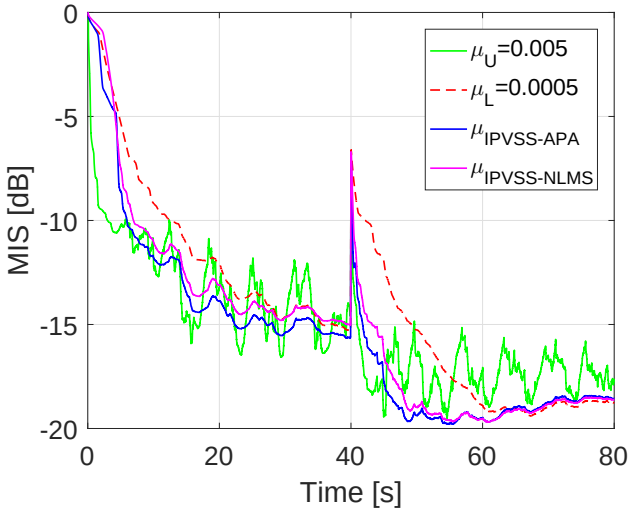

(a)

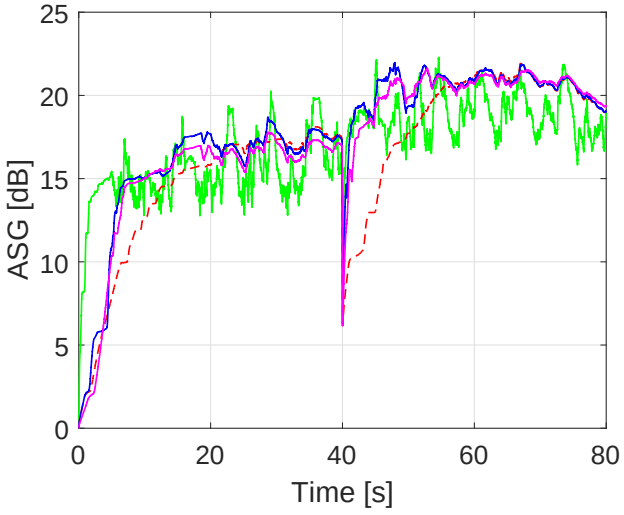

(b)

Figure 5.13: (a) MIS and (b) ASG results for PEM-APA using μ_U, μ_L and PEM-IPVSS-APA with music as the incoming signal, a sudden change of the acoustic feedback path and without FS.

Similar experiment has been pursued for music as the incoming signal. Figure 5.13 demonstrates the misalignment and ASG of all mentioned AFC methods. It can be observed that the proposed PEM-IPVSS-APA outperforms the PEM-APA utilizing either the upper or the lower step-sizes. It also provides better performance than the PEM-IPVSS-NLMS. Figure 5.14 shows that the variable step-sizes of the PEM-IPVSS-APA for music as the incoming signal have similar behavior as the case of speech as the incoming signal above.

Table 5.4 summarizes the PEAQ measures of the mentioned AFC methods for music as the incoming signals when the system has converged, e.g., the PEAQ1 scores are measured during the segment of $35s - 39s$ (before the change of the feedback path) and the PEAQ2 scores are measured during the segment of $75s - 79s$ (after the change). It shows that all mentioned approaches yield similar PEAQ1 scores (approximately -1.8). The proposed method provides a similar PEAQ2 score compared to the PEM-APA using μ_L and the PEM-IPVSS-NLMS, but a better PEAQ2 score compared to the PEM-APA using μ_U.

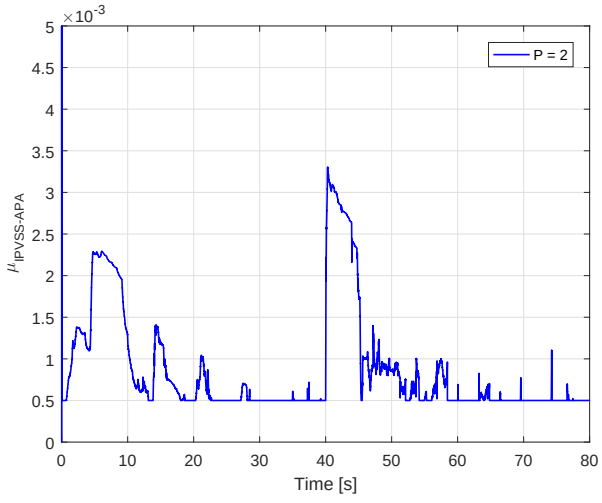

Figure 5.14: Variable step-sizes $\mu_{IPVSS-APA}$ for PEM-IPVSS-APA with music as the incoming signal and a sudden change of acoustic feedback path.

Table 5.4: PEAQ scores for music as the incoming signal, a sudden change of the acoustic feedback path and without frequency shifting.

AFC methods	PEAQ1	PEAQ2
PEM-APA, μ_U = 0.005	-1.81	-2.54
PEM-APA, μ_L = 0.0005	-1.73	-1.98
PEM-IPVSS-APA	-1.80	-1.95
PEM-IPVSS-NLMS	-1.86	-1.96

5.5.3 Results for FS

In this subsection, the proposed approach with FS is evaluated in comparison with the PEM-APA-FS using either μ_U or μ_L and the PEM-IPVSS-NLMS-FS. A small amount of frequency shifting is chosen, i.e., f_0 = 5 Hz, and the FS is applied for the broadband signal. By choosing such small frequency shifting, almost no degradation in the signal quality is noticed.

Figure 5.15 evaluates the convergence rate of the PEM-IPVSS-APA-FS in comparison with the PEM-APA-FS and the PEM-IPVSS-NLMS-FS for the case of speech as the incoming signal and the first acoustic feedback path. It can be observed that the proposed method yields quicker convergence rate compared to both the PEM-IPVSS-NLMS-FS and the PEM-APA-FS with μ_L. In particular, in the first 7 seconds the proposed PEM-IPVSS-APA-FS method achieves approximately 3 dB improvement in normalized misalignment compared to the PEM-IPVSS-NLMS-FS. This improvement is approximately 6 dB compared to the PEM-APA-FS with μ_L. Moreover, three methods including the PEM-APA-FS with μ_L, the PEM-IPVSS-NLMS-FS and the PEM-IPVSS-APA-FS converge to a similar steady-state error (approximately -31 dB) which is much lower than that of the PEM-APA-FS with μ_U.

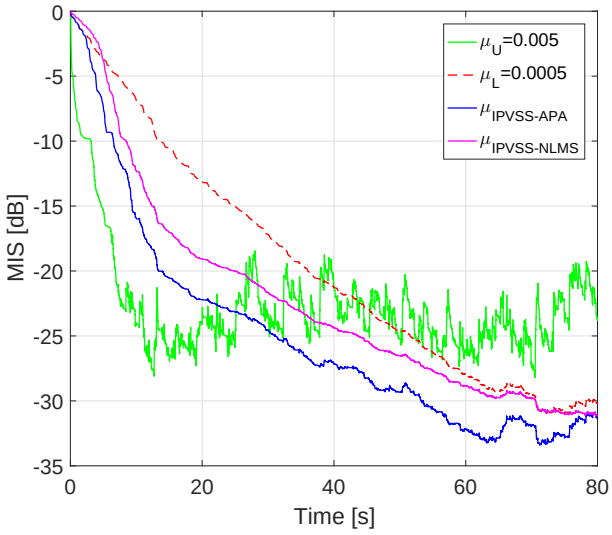

(a)

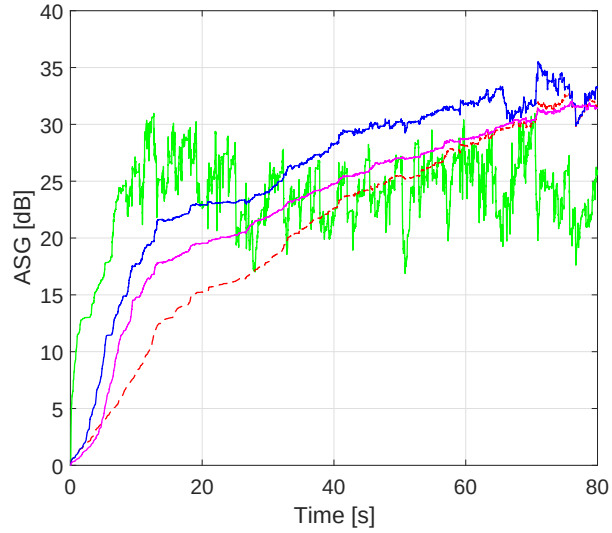

(b)

Figure 5.15: (a) MIS and (b) ASG results for PEM-APA-FS using μ_U, μ_L, PEM-IPVSS-APA-FS and PEM-IPVSS-NLMS-FS with $f_0 = 5Hz$, the first acoustic feedback path and speech as the incoming signal.

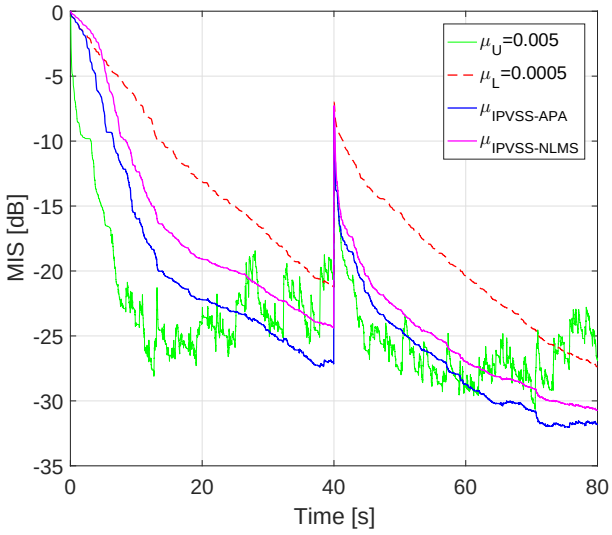

(a)

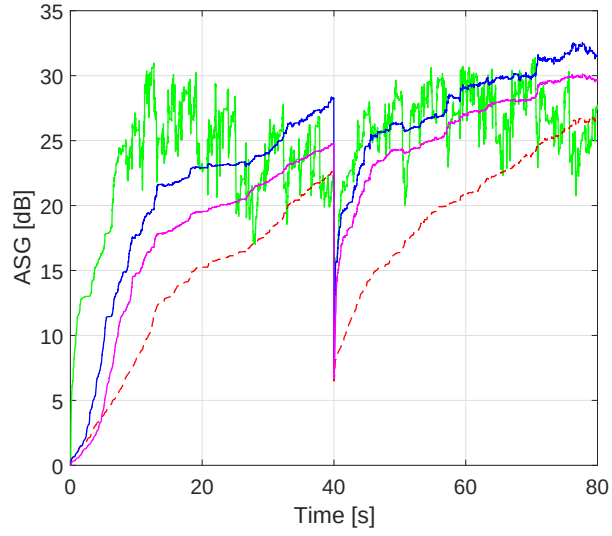

(b)

Figure 5.16: (a) MIS and (b) ASG results for PEM-APA-FS using μ_U, μ_L, PEM-IPVSS-APA-FS and PEM-IPVSS-NLMS-FS with $f_0 = 5Hz$, a sudden change of the acoustic feedback path, and speech as the incoming signal.

Figure 5.16 evaluates the tracking rate of the proposed method for speech as the incoming signal and a sudden change of acoustic feedback path after 40s. It shows that the PEM-IPVSS-APA-FS can track the change of the acoustic feedback path quicker than the PEM-IPVSS-NLMS-FS as well as the PEM-APA-FS with μ_L. By comparing the steady-state level of the PEM-IPVSS-APA-FS to that of the PEM-IPVSS-APA when the system converges, it can be seen that the frequency shifting can provide approximately 9 dB improvement for the MIS as

well as for the ASG.

Table 5.5: PESQ scores for speech as the incoming signal with a frequency shifting of 5 Hz.

AFC methods	Acoustic feedback path	PESQ1	PESQ2
PEM-APA, $\mu_U = 0.005$	does not change	n/a	3.64
PEM-APA, $\mu_L = 0.0005$		n/a	4.34
PEM-IPVSS-APA		n/a	4.35
PEM-IPVSS-NLMS		n/a	4.40
PEM-APA, $\mu_U = 0.005$	changes	4.19	3.64
PEM-APA, $\mu_L = 0.0005$		4.41	4.35
PEM-IPVSS-APA		4.39	4.36
PEM-IPVSS-NLMS		4.42	4.39

Table 5.5 shows that the PESQ2 reduces approximately 0.35 score for the PEM-APA-FS using μ_U compared to the case without FS. For all other methods, similar PESQ scores are obtained compared to those corresponding methods with no FS for both cases with/without a change of the acoustic feedback path.

Figure 5.17 depicts the $\mu_{IPVSS-APA}$ for the PEM-IPVSS-APA-FS for speech as the incoming signal and with/without a change of the acoustic feedback path. The behavior of the $\mu_{IPVSS-APA}$ for the system with FS is similar to that for the system without FS, i.e., it also picks up high values when the system is unstable and low values when the system has converged.

For all above simulations, the proposed approach seems to have a slower initial convergence rate and a slower tracking rate than the PEM-APA using μ_U since Eq. (5.7) and Eq. (5.10) are biased in these situations [84].

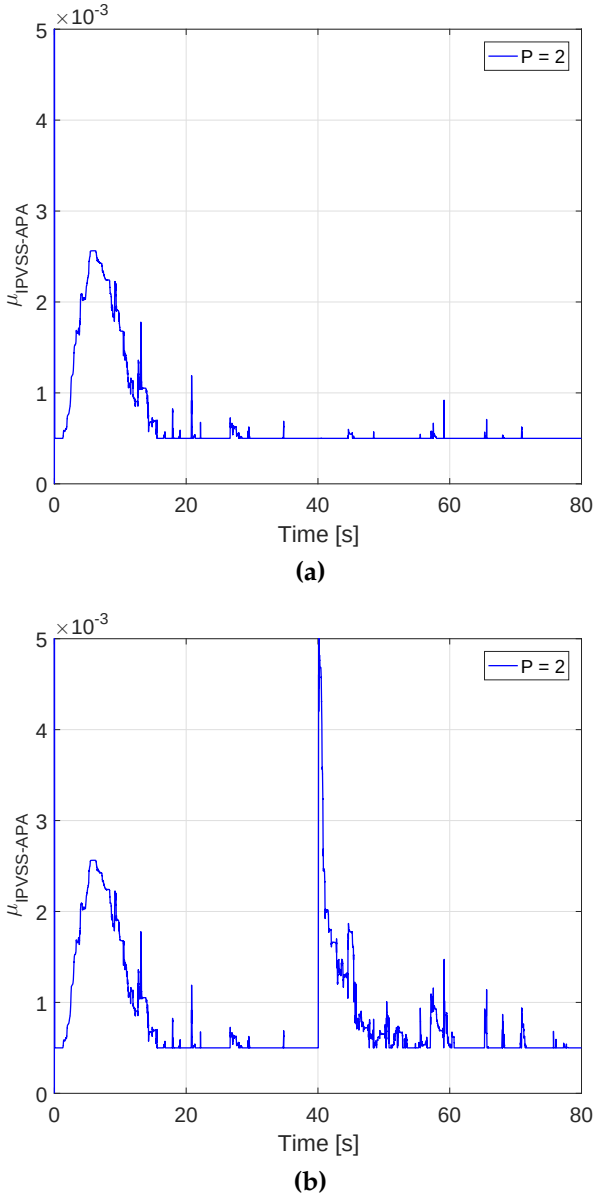

Figure 5.17: Variable step-sizes $\mu_{IPVSS-APA}$ for PEM-IPVSS-APA-FS with speech as the incoming signal (a) without a change of the acoustic feedback path, (b) with a sudden change of the acoustic feedback path.

5.6 Conclusions

In this chapter, a new variable step-size (IPVSS) algorithm has been proposed in the context of adaptive feedback cancellation using the PEM for HAs. This new IPVSS algorithm has been applied and evaluated for different adaptive filtering algorithms such as the NLMS algorithm and the APA. A small projection order for the APA, e.g., $P = 2$, was chosen to ensure that only a small increase in computational complexity compared to the NLMS algorithm [35]. It

has been shown that the proposed PEM-IPVSS-NLMS outperformed the PEM-NLMS when employing either the upper or the lower step-size used as the limits in the IPVSS algorithm, as well as the PEM-VSS-MDNLMS. Similarly, the proposed PEM-IPVSS-APA outperformed the PEM-APA using either the upper or the lower step-size limits. Hence, these proposed methods achieved a reduction in the howling period, while still providing a low steady-state error. In addition, the PEM-IPVSS-APA also obtained significant improvements on the convergence rate and tracking rate while maintaining a similar level of MIS and ASG when the system has converged compared to the PEM-IPVSS-NLMS. Furthermore, the PEM-IPVSS was robust toward different types of the incoming signals (e.g., speech and music) and as well as toward sudden changes in the acoustic feedback paths (e.g., free-field and telephone-near feedback paths), even for the case without added (white) background noise. Finally, a small frequency shifting, e.g., $f_0 = 5$ Hz, was used for broadband signal in order to further improve the MIS and ASG of the proposed approaches for speech as the incoming signal.

CHAPTER 6
Conclusions and Future Work

Chapter's key points:

- Conclusions
- Future work

6.1 Conclusions

This thesis presents novel approaches for acoustic feedback control in hearing aids, which provide better solutions for reducing bias in estimation of the feedback path, and/or improving convergence/tracking rate, while maintaining good signal quality. In addition, these proposed AFC approaches are robust against changes of the incoming signal types and against sudden changes in the feedback paths. The proposed approaches can be classified into three main groups.

The first group presents the combination of two-microphone adaptive feedback cancellation (AFC2) method with the widely known PEM. In the PEM-AFC2, derivations for estimation of the feedback path as well as the relative transfer function (RTF) have been proposed. The derivations demonstrated that the PEM-AFC2 provided an improved solution for identifications of the feedback path and the RTF compared to either the PEM or the AFC2 method due to the whitening effects of the pre-filters on the inputs of adaptive filters. Moreover, a new derivation for optimal filters in the AFC2 method was provided. Experimental results with correct assumptions match perfectly with the theoretical analyses for both undermodeling the RTF as well as perfect modeling the RTF. In fact, the PEM-AFC2 obtained a significant performance improve-

ment in terms of MIS and ASG compared to other popular methods such as the PEM or the AFC2 for different types of the incoming signals as well as with a sudden change in the feedback paths. In addition, the PEM-AFC2 yielded a quicker tracking rate compared to the PEM and the AFC2 method. When the SSN was used as the incoming signal, the PEM-AFC2 outperformed the AFC2 method for the case of undermodeling the RTF, whereas both methods converged to the same solutions for the case of perfect modeling the RTF. Furthermore, the proposed PEM-AFC2 obtains as good signal quality as the two compared methods for speech incoming signals, but better signal quality for music incoming signals.

In the second group, the combination of the PEM and FCAF algorithms for adaptive feedback cancellation in SMSL HAs have been investigated. Three new AFC methods have been developed based on different FCAF algorithms, including the PEM-APA, the PEM-PNLMS and the PEM-IPNLMS. Those methods have been benefited from the superior convergence feature of the APA, the PNLMS and the IPNLMS compared to the NLMS algorithm, resulting in an improvement in convergence rate of the system. Experimental results demonstrated that the PEM with FCAF algorithms converged faster, tracked the sudden change of feedback path quicker while maintaining a low steady-state error compared to the PEM-NLMS. To avoid the high increase in the computational complexity, a small projection order ($P = 2$) was recommended for the PEM-APA.

In the third group, a novel VSS algorithm, the IPVSS, has been proposed for the AFC in HAs. This IPVSS algorithm was developed based on the existing PVSS algorithm, but using a limiter to provide the upper and the lower limits for the variable step-size. Thus, the variable step-size fluctuated in a smaller range, leading to less variations in the system performance. The PVSS algorithm was successfully applied to the AEC contexts, but it provided poor performance for the AFC contexts even when the PEM has been used. In contrast, the proposed IPVSS algorithm performed well for the AFC in HAs. In fact, this algorithm was integrated to the NLMS algorithm or the APA and then applied to the

PEM in order to develop two new AFC methods, the PEM-IPVSS-NLMS and the PEM-IPVSS-APA. Experimental results showed that the PEM-IPVSS-NLMS outperformed the PEM-NLMS using either the upper or the lower step-sizes. A similar conclusion has been obtained for the PEM-IPVSS-APA. Moreover, the PEM-IPVSS-APA had significant performance improvement compared to the PEM-IPVSS-NLMS. In addition, frequency shifting techniques were integrated into the PEM-IPVSS to achieve further performance improvement. A small amount of frequency shift (e.g., $f_0 = 5$ Hz) was recommended to avoid the roughness effect for the signals and a small projection order ($P = 2$) was suggested for the PEM-APA to avoid a large increase in the computational complexity.

6.2 Future work

In the following some potential suggestions for future research in the area of acoustic feedback control are considered.

- Extending the application of the proposed IPVSS algorithm into the PA systems which have multiple-microphones and multiple-loudspeakers (MMML) and longer distances between loudspeakers and microphones. In this dissertation the IPVSS algorithm was investigated only for the AFC in SMSL HAs. It will be interesting when this variable step-size algorithm is further developed for eliminating the acoustic feedback in the MMSL HAs and/or the PA systems.
- Incorporating noise suppression into the AFC2 method in order to have both acoustic feedback cancellation and noise suppression for HAs and/or PA systems.
- Investigating the effect of hearing aid processing (e.g., delay and gain) on the performance of the system. In this dissertation a fixed gain has been used in the forward path.
- The frequency shifting is a potential solution to decorrelate the loudspeaker and the incoming signal, resulting in a bias reduction in the estimate of the feedback path. In this dissertation the frequency shifting (FS) was implemented for speech incoming signals. Therefore, the FS needs

to be further investigated for other types of incoming signals, e.g., strong tones, or music.

- Implementing the proposed AFC methods in real-time systems and evaluating these methods in real acoustic environment.

APPENDIX A

The following derivations show how to compute the terms $\boldsymbol{R}_{\mathbf{z}_1}^{-1}\boldsymbol{R}_{\mathbf{z}_1\mathbf{z}_2}\mathbf{b}$ and $\boldsymbol{R}_{\mathbf{z}_1}^{-1}\boldsymbol{r}_{\mathbf{z}_1\xi}$ in Section 3.2. For simplicity the index "k" is omitted in the following derivations.

Firstly, the auto-correlation matrix $\boldsymbol{R}_{\mathbf{z}_1}$ and the cross-correlation matrix $\boldsymbol{R}_{\mathbf{z}_1\mathbf{z}_2}$ can be computed as

$$\boldsymbol{R}_{\mathbf{z}_1} = \begin{bmatrix} \boldsymbol{R}_{\mathbf{y}} & \boldsymbol{R}_{\mathbf{y}\mathbf{x}_2} \\ \boldsymbol{R}_{\mathbf{x}_2\mathbf{y}} & \boldsymbol{R}_{\mathbf{x}_2} \end{bmatrix} \tag{A.1}$$

and

$$\boldsymbol{R}_{\mathbf{z}_1\mathbf{z}_2} = \begin{bmatrix} \boldsymbol{R}_{\mathbf{y}} & \boldsymbol{R}_{\mathbf{y}\mathbf{u}_2} \\ \boldsymbol{R}_{\mathbf{x}_2\mathbf{y}} & \boldsymbol{R}_{\mathbf{x}_2\mathbf{u}_2} \end{bmatrix}. \tag{A.2}$$

Hence,

$$\boldsymbol{R}_{\mathbf{z}_1}^{-1} = \begin{bmatrix} \boldsymbol{M} & \boldsymbol{N} \\ \boldsymbol{N}^T & \boldsymbol{Q} \end{bmatrix} \tag{A.3}$$

where $\boldsymbol{Q} = \left(\boldsymbol{R}_{\mathbf{x}_2} - \boldsymbol{R}_{\mathbf{x}_2\mathbf{y}}\boldsymbol{R}_{\mathbf{y}}^{-1}\boldsymbol{R}_{\mathbf{y}\mathbf{x}_2}\right)^{-1}$, $\boldsymbol{N} = -\boldsymbol{R}_{\mathbf{y}}^{-1}\boldsymbol{R}_{\mathbf{y}\mathbf{x}_2}\left(\boldsymbol{R}_{\mathbf{x}_2} - \boldsymbol{R}_{\mathbf{x}_2\mathbf{y}}\boldsymbol{R}_{\mathbf{y}}^{-1}\boldsymbol{R}_{\mathbf{y}\mathbf{x}_2}\right)^{-1} = -\boldsymbol{R}_{\mathbf{y}}^{-1}\boldsymbol{R}_{\mathbf{y}\mathbf{x}_2}\boldsymbol{Q}$ and $\boldsymbol{M} = \boldsymbol{R}_{\mathbf{y}}^{-1} - \boldsymbol{N}\boldsymbol{R}_{\mathbf{x}_2\mathbf{y}}\boldsymbol{R}_{\mathbf{y}}^{-1}$.

Then, the term $\boldsymbol{R}_{\mathbf{z}_1\mathbf{z}_2}\mathbf{b}$ is computed as follows

$$\begin{aligned} \boldsymbol{R}_{\mathbf{z}_1\mathbf{z}_2}\mathbf{b} &= \begin{bmatrix} \boldsymbol{R}_{\mathbf{y}} & \boldsymbol{R}_{\mathbf{y}\mathbf{u}_2} \\ \boldsymbol{R}_{\mathbf{x}_2\mathbf{y}} & \boldsymbol{R}_{\mathbf{x}_2\mathbf{u}_2} \end{bmatrix} \begin{bmatrix} \mathbf{f}_1 \\ \mathbf{h} \end{bmatrix} \\ &= \begin{bmatrix} \boldsymbol{R}_{\mathbf{y}}\mathbf{f}_1 + \boldsymbol{R}_{\mathbf{y}\mathbf{u}_2}\mathbf{h} \\ \boldsymbol{R}_{\mathbf{x}_2\mathbf{y}}\mathbf{f}_1 + \boldsymbol{R}_{\mathbf{x}_2\mathbf{u}_2}\mathbf{h} \end{bmatrix}. \end{aligned} \tag{A.4}$$

Let $\boldsymbol{X} = \boldsymbol{R}_{\mathbf{y}}\mathbf{f}_1 + \boldsymbol{R}_{\mathbf{yu}_2}\mathbf{h}$ and $\boldsymbol{Y} = \boldsymbol{R}_{\mathbf{x}_2\mathbf{y}}\mathbf{f}_1 + \boldsymbol{R}_{\mathbf{x}_2\mathbf{u}_2}\mathbf{h}$, resulting in

$$\begin{aligned}\boldsymbol{R}_{\mathbf{z}_1}^{-1}\boldsymbol{R}_{\mathbf{z}_1\mathbf{z}_2}\mathbf{b} &= \begin{bmatrix} \boldsymbol{M} & \boldsymbol{N} \\ \boldsymbol{N}^T & \boldsymbol{Q} \end{bmatrix}\begin{bmatrix} \boldsymbol{X} \\ \boldsymbol{Y} \end{bmatrix} \\ &= \begin{bmatrix} \boldsymbol{M}\boldsymbol{X} + \boldsymbol{N}\boldsymbol{Y} \\ \boldsymbol{N}^T\boldsymbol{X} + \boldsymbol{Q}\boldsymbol{Y} \end{bmatrix}. \end{aligned} \tag{A.5}$$

However,

$$\begin{aligned}\boldsymbol{M}\boldsymbol{X} + \boldsymbol{N}\boldsymbol{Y} = \mathbf{f}_1 &+ \boldsymbol{R}_{\mathbf{y}}^{-1}\boldsymbol{R}_{\mathbf{yu}_2}\mathbf{h} - \boldsymbol{N}\boldsymbol{R}_{\mathbf{x}_2\mathbf{y}}\boldsymbol{R}_{\mathbf{y}}^{-1}\boldsymbol{R}_{\mathbf{yu}_2}\mathbf{h} \\ &+ \boldsymbol{N}\boldsymbol{R}_{\mathbf{x}_2\mathbf{u}_2}\mathbf{h}, \end{aligned} \tag{A.6}$$

and

$$\boldsymbol{N}^T\boldsymbol{X} + \boldsymbol{Q}\boldsymbol{Y} = \boldsymbol{Q}\left(\boldsymbol{R}_{\mathbf{x}_2\mathbf{u}_2}\mathbf{h} - \boldsymbol{R}_{\mathbf{x}_2\mathbf{y}}\boldsymbol{R}_{\mathbf{y}}^{-1}\boldsymbol{R}_{\mathbf{yu}_2}\mathbf{h}\right), \tag{A.7}$$

due to $\boldsymbol{R}_{\mathbf{y}}^T = \boldsymbol{R}_{\mathbf{y}}$, $\boldsymbol{R}_{\mathbf{x}_2}^T = \boldsymbol{R}_{\mathbf{x}_2}$, $\boldsymbol{Q}^T = \boldsymbol{Q}$.

The Eq. (2.32) is reformulated as

$$u_2 = x_2 - F_2(q)\, y, \tag{A.8}$$

then the term $H(q)$ is multiplied with both sides of that equation, i.e.,

$$H(q)\, u_2 = H(q)\, x_2 - H(q)\, F_2(q)\, y,$$

or in vector form

$$\mathbf{h}^T\mathbf{u}_2 = \mathbf{h}^T\mathbf{x}_2 - \mathbf{f}_{2_\mathbf{h}}^T\mathbf{y}, \tag{A.9}$$

where $\mathbf{f}_{2_\mathbf{h}}$ is the coefficient vector of the product $H(q)\, F_2(q)$. Computing the expectation of the vector $\mathbf{x}_2$ with each side of Eq. (A.9) yields

$$E\left\{\mathbf{x}_2\left[\mathbf{h}^T\mathbf{u}_2\right]^T\right\} = E\left\{\mathbf{x}_2\left[\mathbf{h}^T\mathbf{x}_2(k) - \mathbf{f}_{2_\mathbf{h}}^T\mathbf{y}\right]^T\right\},$$

$$\boldsymbol{R}_{\mathbf{x}_2\mathbf{u}_2}\mathbf{h} = \boldsymbol{R}_{\mathbf{x}_2}\mathbf{h} - \boldsymbol{R}_{\mathbf{x}_2\mathbf{y}}\mathbf{f}_{2_\mathbf{h}}. \tag{A.10}$$

Similarly, the following result is obtained

$$E\left\{\mathbf{y}\left[\mathbf{h}^T\mathbf{u}_2\right]^T\right\} = E\left\{\mathbf{y}\left[\mathbf{h}^T\mathbf{x}_2 - \mathbf{f}_{2_\mathbf{h}}^T\mathbf{y}\right]^T\right\},$$

$$\boldsymbol{R}_{\mathbf{y}\mathbf{u}_2}\mathbf{h} = \boldsymbol{R}_{\mathbf{y}\mathbf{x}_2}\mathbf{h} - \boldsymbol{R}_{\mathbf{y}}\mathbf{f}_{2_\mathbf{h}}. \tag{A.11}$$

Substituting Eq. (A.10) and Eq. (A.11) into Eq. (A.6) and Eq. (A.7) yields

$$\boldsymbol{M}\boldsymbol{X} + \boldsymbol{N}\boldsymbol{Y} = \mathbf{f}_1 - \mathbf{f}_{2_\mathbf{h}}, \tag{A.12}$$

$$\boldsymbol{N}^T\boldsymbol{X} + \boldsymbol{Q}\boldsymbol{Y} = \mathbf{h}. \tag{A.13}$$

Moreover,

$$\begin{aligned}\boldsymbol{R}_{\mathbf{z}_1}^{-1}\boldsymbol{r}_{\mathbf{z}_1\xi} &= \begin{bmatrix}\boldsymbol{M} & \boldsymbol{N}\\ \boldsymbol{N}^T & \boldsymbol{Q}\end{bmatrix}\begin{bmatrix}\boldsymbol{r}_{\mathbf{y}\xi}\\ \boldsymbol{r}_{\mathbf{x}_2\xi}\end{bmatrix}\\ &= \begin{bmatrix}\boldsymbol{M}\boldsymbol{r}_{\mathbf{y}\xi} + \boldsymbol{N}\boldsymbol{r}_{\mathbf{x}_2\xi}\\ \boldsymbol{N}^T\boldsymbol{r}_{\mathbf{y}\xi} + \boldsymbol{Q}\boldsymbol{r}_{\mathbf{x}_2\xi}\end{bmatrix}\\ &= \begin{bmatrix}\boldsymbol{B}_1\\ \boldsymbol{B}_\mathbf{h}\end{bmatrix},\end{aligned} \tag{A.14}$$

where

$$\boldsymbol{B}_1 = \boldsymbol{M}\boldsymbol{r}_{\mathbf{y}\xi} + \boldsymbol{N}\boldsymbol{r}_{\mathbf{x}_2\xi}, \tag{A.15}$$

$$\boldsymbol{B}_\mathbf{h} = \boldsymbol{N}^T\boldsymbol{r}_{\mathbf{y}\xi} + \boldsymbol{Q}\boldsymbol{r}_{\mathbf{x}_2\xi}. \tag{A.16}$$

APPENDIX B

This appendix provides proofs for the equality in Eq. (3.30) and Eq. (3.31). Due to the assumption in Eq. (3.17) and if $\hat{G}(q) = G(q)$, then

$$u_{2p}(k) = \hat{G}(q)\, G^{-1}(q)\, w(k) = w(k). \tag{B.1}$$

Thus the cross-correlation between the whitened loudspeaker signal vector $\mathbf{y}_p(k)$ and the whitened second incoming signal vector $\mathbf{u}_{2p}(k) = \mathbf{w}(k)$ is zero if the condition $d_k > L_{\hat{h}} - 1$ is fulfilled, i.e.,

$$\begin{aligned} \boldsymbol{R}_{\mathbf{y}_p\mathbf{u}_{2p}} &= E\left\{\mathbf{y}_p(k)\,\mathbf{u}_{2p}^T(k)\right\} \\ &= E\left\{\mathbf{y}_p(k)\,\mathbf{w}^T(k)\right\} = \mathbf{0}. \end{aligned} \tag{B.2}$$

Moreover, from Eq. (2.32) and Eq. (3.20), we obtain $x_{2p}(k) = w(k) + F_2(q)\, y_p(k)$. Hence,

$$\begin{aligned} \boldsymbol{R}_{\mathbf{x}_{2p}\mathbf{u}_{2p}} &= E\left\{\mathbf{x}_{2p}(k)\,\mathbf{u}_{2p}^T(k)\right\} \\ &= E\left\{\mathbf{x}_{2p}(k)\,\mathbf{w}^T(k)\right\} = \boldsymbol{R}_{\mathbf{w}}. \end{aligned} \tag{B.3}$$

By using the pre-filter $\hat{G}(q)$ in the PEM-AFC2 model, the Eq. (A.10) and Eq. (A.11) in Appendix A can be reformulated as follows

$$\boldsymbol{R}_{\mathbf{w}}\mathbf{h} = \boldsymbol{R}_{\mathbf{x}_{2p}}\mathbf{h} - \boldsymbol{R}_{\mathbf{x}_{2p}\mathbf{y}_p}\mathbf{f}_{2_\mathbf{h}}, \tag{B.4}$$

$$\boldsymbol{R}_{\mathbf{y}_p\mathbf{u}_{2p}}\mathbf{h} = \boldsymbol{R}_{\mathbf{y}_p\mathbf{x}_{2p}}\mathbf{h} - \boldsymbol{R}_{\mathbf{y}_p}\mathbf{f}_{2_\mathbf{h}}. \tag{B.5}$$

Substituting Eq. (B.2) and Eq. (B.3) into Eq. (B.4) and Eq. (B.5) results in

$$\left(\boldsymbol{R}_{\mathbf{x}_{2p}} - \boldsymbol{R}_{\mathbf{w}}\right)\mathbf{h} = \boldsymbol{R}_{\mathbf{x}_{2p}\mathbf{y}_p}\mathbf{f}_{2_{\mathbf{h}}},$$

$$\boldsymbol{R}_{\mathbf{y}_p\mathbf{x}_{2p}}\mathbf{h} = \boldsymbol{R}_{\mathbf{y}_p}\mathbf{f}_{2_{\mathbf{h}}}.$$

Hence,

$$\mathbf{h} = \left(\boldsymbol{R}_{\mathbf{x}_{2p}} - \boldsymbol{R}_{\mathbf{w}}\right)^{-1}\boldsymbol{R}_{\mathbf{x}_{2p}\mathbf{y}_p}\mathbf{f}_{2_{\mathbf{h}}}, \tag{B.6}$$

$$\mathbf{f}_{2_{\mathbf{h}}} = \boldsymbol{R}_{\mathbf{y}_p}^{-1}\boldsymbol{R}_{\mathbf{y}_p\mathbf{x}_{2p}}\mathbf{h}. \tag{B.7}$$

Moreover, substituting Eq. (B.7) into Eq. (B.6) yields

$$\mathbf{h} = \left(\boldsymbol{R}_{\mathbf{x}_{2p}} - \boldsymbol{R}_{\mathbf{w}}\right)^{-1}\boldsymbol{R}_{\mathbf{x}_{2p}\mathbf{y}_p}\boldsymbol{R}_{\mathbf{y}_p}^{-1}\boldsymbol{R}_{\mathbf{y}_p\mathbf{x}_{2p}}\mathbf{h},$$

leading to

$$\left(\boldsymbol{R}_{\mathbf{x}_{2p}} - \boldsymbol{R}_{\mathbf{w}}\right)^{-1}\boldsymbol{R}_{\mathbf{x}_{2p}\mathbf{y}_p}\boldsymbol{R}_{\mathbf{y}_p}^{-1}\boldsymbol{R}_{\mathbf{y}_p\mathbf{x}_{2p}} = \mathbf{I},$$

where $\mathbf{I}$ is the $(L_h \times L_h)$ identity matrix.

As a result,

$$\boldsymbol{R}_{\mathbf{x}_{2p}} - \boldsymbol{R}_{\mathbf{w}} = \boldsymbol{R}_{\mathbf{x}_{2p}\mathbf{y}_p}\boldsymbol{R}_{\mathbf{y}_p}^{-1}\boldsymbol{R}_{\mathbf{y}_p\mathbf{x}_{2p}}. \tag{B.8}$$

Furthermore, $\boldsymbol{R}_{\mathbf{y}_p}^{T} = \boldsymbol{R}_{\mathbf{y}_p}$, $\boldsymbol{R}_{\mathbf{x}_{2p}}^{T} = \boldsymbol{R}_{\mathbf{x}_{2p}}$, $\tilde{\boldsymbol{Q}}^{T} = \tilde{\boldsymbol{Q}}$.

From the equation Eq. (B.8) and the definitions of $\tilde{\boldsymbol{Q}}$ and $\tilde{\boldsymbol{N}}$ in Section 3.3 we obtain

$$\tilde{\boldsymbol{Q}} = \boldsymbol{R}_{\mathbf{w}}^{-1}, \tag{B.9}$$

$$\tilde{\boldsymbol{N}} = -\boldsymbol{R}_{\mathbf{y}_p}^{-1}\boldsymbol{R}_{\mathbf{y}_p\mathbf{x}_{2p}}\boldsymbol{R}_{\mathbf{w}}^{-1} \tag{B.10}$$

If the RTF is undermodeled ($\xi(k) \neq 0$), the term $\xi_p(k)$ is rewritten as follows

$$\begin{aligned}\xi_p(k) &= \mathbf{h}_{res}^{T}\mathbf{u}_{2p}(k)\\ &= \mathbf{h}_{res}^{T}\mathbf{w}(k).\end{aligned} \tag{B.11}$$

The cross-correlations $\boldsymbol{r}_{\mathbf{y}_p\xi_p}$ and $\boldsymbol{r}_{\mathbf{x}_{2p}\xi_p}$ are calculated as

$$\boldsymbol{r}_{\mathbf{y}_p\xi_p} = \boldsymbol{R}_{\mathbf{y}_p\mathbf{w}}\mathbf{h}_{res} = \mathbf{0}, \tag{B.12}$$

$$\boldsymbol{r}_{\mathbf{x}_{2p}\xi_p} = \boldsymbol{r}_{\mathbf{w}\xi_p} = \boldsymbol{R}_{\mathbf{w}}\mathbf{h}_{res}, \tag{B.13}$$

due to $\boldsymbol{R}_{\mathbf{y}_p\mathbf{w}} = \mathbf{0}$ if $d_k > L_{h_{full}} - 1$.

Substituting Eq. (B.12), Eq. (B.13) and Eq. (B.9), Eq. (B.10) into Eq. (3.28) and Eq. (3.29) results in

$$\tilde{\boldsymbol{B}}_{\mathbf{h}} = \mathbf{h}_{res}, \tag{B.14}$$

$$\tilde{\boldsymbol{B}}_1 = -\boldsymbol{R}_{\mathbf{y}_p}^{-1}\boldsymbol{R}_{\mathbf{y}_p\mathbf{x}_{2p}}\mathbf{h}_{res}. \tag{B.15}$$

For perfect modeling case, $\xi(k) = 0$, i.e., $\mathbf{h}_{res} = \mathbf{0}$, we obtain

$$\tilde{\boldsymbol{B}}_{\mathbf{h}} = \mathbf{0}, \tag{B.16}$$

$$\tilde{\boldsymbol{B}}_1 = \mathbf{0}. \tag{B.17}$$

BIBLIOGRAPHY

[1] R. J. Smith, A. E. Shearer, M. S. Hildebrand, and G. Van Camp, "Deafness and hereditary hearing loss overview," 2014. (Cited on pages xiii, 10, and 11)

[2] T. van Waterschoot and M. Moonen, "Fifty Years of Acoustic Feedback Control: State of the Art and Future Challenges," *Proc. IEEE*, vol. 99, no. 2, pp. 288–327, 2011. (Cited on pages 1, 14, 16, 38, and 93)

[3] C. R. C. Nakagawa, S. Nordholm, and W.-Y. Yan, "Analysis of two microphone method for feedback cancellation," *IEEE Signal Process. Lett.*, vol. 22, pp. 35–39, 2015. (Cited on pages 2, 5, 28, 29, 31, 45, 49, and 61)

[4] T. E. of Encyclopædia Britannica, "Deafness," *Encyclopædia Britannica, inc.*, 2017. (Cited on page 10)

[5] W. fact sheet, "Deafness and hearing loss," *http://www.who.int/mediacentre/factsheets/fs300/en/*, 2017. (Cited on page 10)

[6] T. Lancet, "Global elderly care in crisis," *The Lancet, vol. 383, no. 9921, pp. 927, Mar. 2014.* (Cited on page 10)

[7] I. LU, A. TIO, and U. LE, "Hearing loss in older adults," *Am. Fam. Physician*, vol. 85, no. 12, pp. 1150–1156, 2012. (Cited on page 10)

[8] H. net online, "Hearing aids," *Hear net online, https://hearnet.org.au/hearing-technology/hearing-aids.* (Cited on page 11)

[9] H. Nyquist, "Regeneration theory," *Bell Syst. Tech. J., vol. 11, pp.126-147*, vol. 11, no. 1, pp. 126–147, 1932. (Cited on page 14)

[10] C. Chen, "Detection of acoustical feedback in a public address system," in *Proc. IEEE Int. Conf. Acoust., Speech, and Signal Process. (ICASSP)*, vol. 2, pp. 385–388, IEEE, 1977. (Cited on page 14)

[11] M. Schroeder, "Improvement of acoustic-feedback stability by frequency shifting," *J. Acoust. Soc. Am.*, vol. 36, no. 9, pp. 1718–1724, 1964. (Cited on pages 14 and 16)

[12] C. Boner and C. R. Boner, "Minimizing feedback in sound systems and room-ring modes with passive networks," *J. Acoust. Soc. Am.*, vol. 37, no. 1, pp. 131–135, 1965. (Cited on page 14)

[13] F. van der Meulen, S. Kamerling, and C. Janse, "A new way of acoustic feedback suppression," in *104th Audio Engin. Soc. Convention, Amsterdam, Netherlands*, Audio Engineering Society, 1998. (Cited on page 14)

[14] J. M. Kates, "Feedback cancellation in hearing aids: Results from a computer simulation," *IEEE Trans. Signal Process.*, vol. 39, no. 3, pp. 553–562, 1991. (Cited on page 14)

[15] J. A. Maxwell and P. M. Zurek, "Reducing acoustic feedback in hearing aids," *IEEE Trans. Speech, Audio Process.*, vol. 3, no. 4, pp. 304–313, 1995. (Cited on pages 14, 16, 18, and 37)

[16] A. Spriet, I. Proudler, M. Moonen, and J. Wouters, "Adaptive feedback cancellation in hearing aids with linear prediction of the desired signal," *IEEE Trans. Signal Process.*, vol. 53, no. 10, pp. 3749–3763, 2005. (Cited on pages 14, 21, 25, 37, 41, 63, 64, 65, and 85)

[17] M. Guo, S. H. Jensen, and J. Jensen, "Novel acoustic feedback cancellation approaches in hearing aid applications using probe noise and probe noise enhancement," *IEEE Trans. Audio, Speech, Lang. Process.*, vol. 20, no. 9, pp. 2549–2563, 2012. (Cited on pages 14 and 16)

[18] A. Pandey and V. J. Mathews, "Adaptive gain processing with offending frequency suppression for digital hearing aids," *IEEE Trans. Acoust. Speech and Signal Process.*, vol. 20, no. 3, pp. 1043–1055, 2012. (Cited on page 14)

[19] C. R. C. Nakagawa, S. Nordholm, and W.-Y. Yan, "Feedback cancellation with probe shaping compensation," *IEEE Signal Process. Lett.*, vol. 21, no. 3, pp. 365–369, 2014. (Cited on pages 14 and 16)

[20] M. G. Siqueira and A. Alwan, "Steady-state analysis of continuous adaptation in acoustic feedback reduction systems for hearing-aids," *IEEE Trans. Speech, Audio Process.*, vol. 8, no. 4, pp. 443–453, 2000. (Cited on pages 15, 19, and 37)

[21] S. Laugesen, K. Hansen, and J. Hellgren, "Acceptable delays in hearing aids and implications for feedback cancellation," *J. Acoust. Soc. Am.*, vol. 105, no. 2, pp. 1211–1212, 1999. (Cited on page 15)

[22] R. Porayath and D. J. Mapes-Riordan, "Acoustic feedback elimination using adaptive notch filter algorithm," Dec. 1999. US Patent 5 999 631. (Cited on page 16)

[23] W. Leotwassana, R. Punchalard, and W. Silaphan, "Adaptive howling canceller using adaptive IIR notch filter: Simulation and implementation," in *Proc. Int. Conf. Neural Netw., Signal Process.*, vol. 1, pp. 848–851, IEEE, 2003. (Cited on page 16)

[24] J. Wei, L. Du, Z. Chen, and F. Yin, "A new algorithm for howling detection," in *Proc. IEEE Int. Symp. Circuits Syst., (ISCAS)*, vol. 4, pp. IV–IV, IEEE, 2003. (Cited on page 16)

[25] P. R. Williams, "System for elimination of acoustic feedback," Jan. 21 2014. US Patent 8,634,575. (Cited on page 16)

[26] M. Borsch, "Method for suppressing electroacoustic feedback," Feb. 7 2005. US Patent App. 11/052,398. (Cited on page 16)

[27] G. Rombouts, T. van Waterschoot, and M. Moonen, "Proactive notch filtering for acoustic feedback cancellation," *Proc. 2nd Annu. IEEE Benelux/DSP Valley Signal Process. Symp.*, 2006. (Cited on page 16)

[28] P. Gil-Cacho, T. Van Waterschoot, M. Moonen, and S. H. Jensen, "Regularized adaptive notch filters for acoustic howling suppression," in *Proc. 17th Eur. Signal Process. Conf. (EUSIPCO)*, pp. 2574–2578, IEEE, 2009. (Cited on page 16)

[29] T. Kawamura and T. Kanamori, "Howling detection device and method," Mar. 22 2011. US Patent 7,912,230. (Cited on page 16)

[30] D. K. Bustamante, T. L. Worrall, and M. J. Williamson, "Measurement and adaptive suppression of acoustic feedback in hearing aids," in *Proc. IEEE Int. Conf. Acoust., Speech, Signal Process., (ICASSP)*, pp. 2017–2020, IEEE, 1989. (Cited on page 16)

[31] A. Spriet, S. Doclo, M. Moonen, and J. Wouters, "Feedback control in hearing aids," in *Springer Handbook Speech Process.*, pp. 979–1000, Springer, 2008. (Cited on pages 16, 19, 21, 37, and 64)

[32] A. M. Engebretson and M. French-St George, "Properties of an adaptive feedback equalization algorithm," *J. Rehab. Res. Dev.*, vol. 30, no. 1, p. 8, 1993. (Cited on page 16)

[33] J. Kates, "Feedback cancellation in hearing aids," in *Proc. IEEE Int. Conf. Acoust., Speech, and Signal Process. (ICASSP)*, pp. 1125–1128, 1990. (Cited on page 16)

[34] M. Guo, T. B. Elmedyb, S. H. Jensen, and J. Jensen, "On acoustic feedback cancellation using probe noise in multiple-microphone and single-loudspeaker systems," *IEEE Signal Process. Lett.*, vol. 19, no. 5, pp. 283–286, 2012. (Cited on page 16)

[35] L. T. T. Tran, H. H. Dam, and S. Nordholm, "Affine projection algorithm for acoustic feedback cancellation using prediction error method in hearing aids," *Proc. IEEE Int. Workshop Acoust. Signal Enhan. (IWAENC)*, 2016. (Cited on pages 16, 62, 90, and 113)

[36] J. L. Nielsen and U. P. Svensson, "Performance of some linear time-varying systems in control of acoustic feedback," *J. Acoust. Soc. Am.*, vol. 106, no. 1, pp. 240–254, 1999. (Cited on page 16)

[37] P. U. Svensson, "Computer simulations of periodically time-varying filters for acoustic feedback control," *J. Audio Eng. Soc.*, vol. 43, no. 9, pp. 667–677, 1995. (Cited on page 16)

[38] M. Guo, S. H. Jensen, J. Jensen, and S. L. Grant, "On the use of a phase modulation method for decorrelation in acoustic feedback cancellation," in *Proc. Eur. Signal Process. Conf. (EUSIPCO)*, pp. 2000–2004, 2012. (Cited on pages 16 and 93)

[39] H. A. L. Joson, F. Asano, Y. Suzuki, and T. Sone, "Adaptive feedback cancellation with frequency compression for hearing aids," *J. Acoust. Soc. Am.*, vol. 94, no. 6, pp. 3248–3254, 1993. (Cited on pages 16 and 93)

[40] F. Strasser and H. Puder, "Adaptive feedback cancellation for realistic hearing aid applications," *IEEE/ACM Trans. Audio, Speech, Lang. Process.*, vol. 23, no. 12, pp. 2322–2333, 2015. (Cited on pages 16, 27, 38, 82, and 93)

[41] M. Guo and B. Kuenzle, "On the periodically time-varying bias in adaptive feedback cancellation systems with frequency shifting," in *Proc. Int. Conf. Acoust., Speech and Signal Process. (ICASSP)*, pp. 539–543, IEEE, 2016. (Cited on pages 16 and 93)

[42] T. Van Waterschoot and M. Moonen, "Assessing the acoustic feedback control performance of adaptive feedback cancellation in sound reinforcement systems," in *Proc. 17th Eur. Signal Process. Conf.*, pp. 1997–2001, IEEE, 2009. (Cited on pages 16 and 94)

[43] J. E. Greenberg, P. M. Zurek, and M. Brantley, "Evaluation of feedback-reduction algorithms for hearing aids," *J. Acoust. Soc. Am.*, vol. 108, no. 5, pp. 2366–2376, 2000. (Cited on page 18)

[44] J. M. Kates, "Adaptive feedback cancellation in hearing aids," in *Adaptive Signal Process.: Application to Real-Word Problem, ed. by J. Benesty, Y. Huang*, pp. 23–57, Springer, Berlin, Heidelberg, 2003. (Cited on page 18)

[45] S. Haykin, *Adaptive Filter Theory*. Prentice-Hall, 2002. (Cited on pages 19, 20, 25, and 63)

[46] A. H. Sayed, *Fundamental adaptive filtering*. John Wiley & Sons, 2003. (Cited on pages 19, 20, 61, 63, and 65)

[47] J. Hellgren and U. Forssell, "Bias of feedback cancellation algorithms in hearing aids based on direct closed loop identification," *IEEE Trans. Speech, Audio Process.*, vol. 9, no. 8, pp. 906–913, 2001. (Cited on pages 21 and 23)

[48] J. Hellgren, "Analysis of feedback cancellation in hearing aids with filtered-X LMS and the direct method of closed loop identification," *IEEE Trans. Speech and Audio Process.*, vol. 10, no. 2, pp. 119–131, 2002. (Cited on pages 21 and 37)

[49] A. Spriet, G. Rombouts, M. Moonen, and J. Wouters, "Adaptive feedback cancellation in hearing aids," *Elsevier J. Franklin Inst.*, vol. 343, no. 6, pp. 545–573, 2006. (Cited on pages 21, 23, 34, 35, 45, 46, and 64)

[50] G. Rombouts, T. Van Waterschoot, and M. Moonen, "Robust and Efficient Implementation of the PEM-AFROW Algorithm for Acousic Feedback Cancellation," *J. Audio Eng. Soc.*, vol. 55, no. 11, pp. 955–966, 2007. (Cited on page 21)

[51] G. Bernardi, T. van Waterschoot, J. Wouters, and M. Moonen, "An all-frequency-domain adaptive filter with PEM-based decorrelation for acoustic feedback control," in *Proc. Workshop Appl. Signal Process. Audio and Acoust. (WASPAA)*, pp. 1–5, IEEE, 2015. (Cited on page 21)

[52] K. Ngo, T. van Waterschoot, M. G. Christensen, M. Moonen, S. H. Jensen, and J. Wouters, "Prediction-error-method-based adaptive feedback cancellation in hearing aids using pitch estimation," in *Proc. Eur. Signal Process. Conf. (EUSIPCO)*, 2010. (Cited on page 21)

[53] G. Bernardi, T. van Waterschoot, J. Wouters, M. Hillbratt, and M. Moonen, "A PEM-based frequency-domain Kalman filter for adaptive feedback cancellation," in *Proc. 23rd Eur. Signal Proces. Conf. (EUSIPCO)*, pp. 270–274, IEEE, 2015. (Cited on page 21)

[54] A. Gilloire, "Experiments with sub-band acoustic echo cancellers for teleconferencing," in *Proc. IEEE Conf. Int. Acoust., Speech, Signal Process. (ICASSP)*, vol. 12, pp. 2141–2144, IEEE, 1987. (Cited on pages 23 and 37)

[55] A. Gilloire and M. Vetterli, "Adaptive filtering in subbands with critical sampling: analysis, experiments, and application to acoustic echo cancellation," *IEEE trans. signal process.*, vol. 40, no. 8, pp. 1862–1875, 1992. (Cited on page 23)

[56] W. Kellermann, "Analysis and design of multirate systems for cancellation of acoustical echoes," in *Proc. IEEE Int. Conf. Acoust., Speech, Signal Process. (ICASSP)*, pp. 2570–2573, IEEE, 1988. (Cited on page 23)

[57] P. P. Vaidyanathan, "Multirate digital filters, filter banks, polyphase networks, and applications: A tutorial," *Proc. IEEE*, vol. 78, no. 1, pp. 56–93, 1990. (Cited on page 24)

[58] K.-A. Lee, W.-S. Gan, and S. M. Kuo, *Subband adaptive filtering: theory and implementation*. John Wiley & Sons, 2009. (Cited on pages 24, 25, and 37)

[59] D. R. Morgan and J. C. Thi, "A delayless subband adaptive filter architecture," *IEEE Trans. on Signal Process.*, vol. 43, no. 8, pp. 1819–1830, 1995. (Cited on pages 24, 25, and 38)

[60] J. Huo, S. Nordholm, and Z. Zang, "New weight transform schemes for delayless subband adaptive filtering," in *Global Telecommunications Conf., 2001. GLOBECOM'01. IEEE*, vol. 1, pp. 197–201, IEEE, 2001. (Cited on page 24)

[61] K. Nishikawa and H. Kiya, "Conditions for convergence of a delayless subband adaptive filter and its efficient implementation," *IEEE trans. signal process.*, vol. 46, no. 4, pp. 1158–1167, 1998. (Cited on page 24)

[62] S. Ohno and H. Sakai, "On delayless subband adaptive filtering by subband/fullband transforms," *IEEE Signal Process. Lett.*, vol. 6, no. 9, pp. 236–239, 1999. (Cited on page 24)

[63] R. Merched, P. S. Diniz, and M. R. Petraglia, "A new delayless subband adaptive filter structure," *IEEE trans. Signal Process.*, vol. 47, no. 6, pp. 1580–1591, 1999. (Cited on page 24)

[64] N. Hirayama, H. Sakai, and S. Miyagi, "Delayless subband adaptive filtering using the hadamard transform," *IEEE trans. signal process.*, vol. 47, no. 6, pp. 1731–1734, 1999. (Cited on page 24)

[65] K.-A. Lee and W.-S. Gan, "On delayless architecture for the normalized subband adaptive filter," in *2007 IEEE Inter. Conf. on Multimedia and Expo*, pp. 1595–1598, IEEE, 2007. (Cited on pages 24, 25, and 38)

[66] J. M. Gil-Cacho, T. van Waterschoot, M. Moonen, and S. H. Jensen, "Transform domain prediction error method for improved acoustic echo and feedback cancellation," in *Proc. Eur. Signal Process. Conf. (EUSIPCO)*, pp. 2422–2426, IEEE, 2012. (Cited on pages 24, 25, 33, 37, and 38)

[67] B. Farhang-Boroujeny and S. Gazor, "Selection of orthonormal transforms for improving the performance of the transform domain normalised lms algorithm," in *IEE Proceedings-F (Radar and Signal Process.)*, vol. 139, pp. 327–335, IET, 1992. (Cited on pages 24 and 25)

[68] C. R. C. Nakagawa, S. Nordholm, F. Albu, and W.-Y. Yan, "Closed-loop feedback cancellation utilizing two microphones and transform domain processing," in *Proc. Int. Conf. Acoust., Speech and Signal Process. (ICASSP)*, pp. 3645–3649, IEEE, 2014. (Cited on pages 24, 25, 37, and 38)

[69] J. J. Shynk *et al.*, "Frequency-domain and multirate adaptive filtering," *IEEE Signal Process. Mag.*, vol. 9, no. 1, pp. 14–37, 1992. (Cited on pages 25, 38, and 60)

[70] F. Strasser and H. Puder, "Sub-band feedback cancellation with variable step sizes for music signals in hearing aids," in *Proc. IEEE Int. Conf. Acoust., Speech and Signal Process. (ICASSP)*, pp. 8207–8211, IEEE, 2014. (Cited on pages 25, 27, 37, 38, and 82)

[71] S. A. Khoubrouy and I. M. Panahi, "An efficient delayless sub-band filtering for adaptive feedback compensation in hearing aid," *J. Signal Process. Syst.*, pp. 1–9, 2016. (Cited on pages 25, 37, and 38)

[72] A. A. Milani, I. M. Panahi, and P. C. Loizou, "A new delayless subband adaptive filtering algorithm for active noise control system," *IEEE Trans. Audio, Speech & Language Process.*, vol. 17, no. 5, pp. 1038–1045, 2009. (Cited on pages 25 and 38)

[73] S. Pradhan, V. Patel, D. Somani, and N. V. George, "An improved proportionate delayless multiband-structured subband adaptive feedback canceller for digital hearing aids," *IEEE/ACM Trans. Audio, Speech, Lang. Process.*, 2017. (Cited on page 25)

[74] R. H. Kwong and E. W. Johnston, "A variable step size LMS algorithm," *IEEE Trans. Signal Process.*, vol. 40, no. 7, pp. 1633–1642, 1992. (Cited on pages 26 and 63)

[75] A. Mader, H. Puder, and G. U. Schmidt, "Step-size control for acoustic echo cancellation filters–an overview," *Signal Process.*, vol. 80, no. 9, pp. 1697–1719, 2000. (Cited on pages 26 and 63)

[76] A. I. Sulyman and A. Zerguine, "Convergence and steady-state analysis of a variable step-size nlms algorithm," *Signal Process.*, vol. 83, no. 6, pp. 1255–1273, 2003. (Cited on pages 26 and 86)

[77] H.-C. Shin, A. H. Sayed, and W.-J. Song, "Variable step-size NLMS and affine projection algorithms," *IEEE Signal Process. Lett.*, vol. 11, no. 2, pp. 132–135, 2004. (Cited on pages 26, 27, 37, and 63)

[78] D. P. Mandic, "A generalized normalized gradient descent algorithm," *Signal Process. Lett., IEEE*, vol. 11, no. 2, pp. 115–118, 2004. (Cited on page 26)

[79] J. Benesty, H. Rey, L. Rey Vega, and S. Tressens, "A nonparametric VSS NLMS algorithm," *IEEE Signal Process. Lett.*, vol. 13, no. 10, pp. 581–584, 2006. (Cited on pages 26 and 63)

[80] C. Paleologu, S. Ciochină, and J. Benesty, "Variable step-size NLMS algorithm for under-modeling acoustic echo cancellation," *IEEE Signal Process. Lett.*, vol. 15, pp. 5–8, 2008. (Cited on pages 26, 63, 82, and 86)

[81] M. A. Iqbal and S. L. Grant, "Novel variable step size NLMS algorithms for echo cancellation," in *Proc. 2008 IEEE Int. Conf. Acoust., Speech, Signal Process. (ICASSP)*, pp. 241–244, IEEE, 2008. (Cited on pages 26 and 63)

[82] H.-C. Huang and J. Lee, "A new variable step-size NLMS algorithm and its performance analysis," *IEEE Trans. Signal Process.*, vol. 60, no. 4, pp. 2055–2060, 2012. (Cited on pages 26 and 63)

[83] C. Paleologu, J. Benesty, S. L. Grant, and C. Osterwise, "Variable step-size NLMS algorithms designed for echo cancellation," in *Conf. Record of the Forty-Third Asilomar Signals, Syst., Comput.*, pp. 633–637, IEEE, 2009. (Cited on pages 26 and 86)

[84] C. Paleologu, J. Benesty, and S. Ciochina, "A variable step-size affine projection algorithm designed for acoustic echo cancellation," *IEEE Trans. Audio, Speech, Lang. Process.*, vol. 16, no. 8, pp. 1466–1478, 2008. (Cited on pages 27, 63, 82, 91, 101, 103, and 112)

[85] K. Mayyas, "A variable step-size affine projection algorithm," *Elsevier J. Digit. Signal Process.*, vol. 20, no. 2, pp. 502–510, 2010. (Cited on page 27)

[86] L. R. Vega, H. Rey, and J. Benesty, "A robust variable step-size affine projection algorithm," *Elsevier J. Signal Process.*, vol. 90, no. 9, pp. 2806–2810, 2010. (Cited on page 27)

[87] F. Huang, J. Zhang, and S. Zhang, "Combined-step-size affine projection sign algorithm for robust adaptive filtering in impulsive interference environments," *IEEE Trans. Circuits and Syst. II: Express Briefs*, vol. 63, no. 5, pp. 493–497, 2016. (Cited on page 27)

[88] O. Hoshuyama, R. A. Goubran, and A. Sugiyama, "A generalized proportionate variable step-size algorithm for fast changing acoustic environments," in *Proc. IEEE Int. Conf. Acoust., Speech, Signal Process. (ICASSP)*, vol. 4, pp. iv–161, IEEE, 2004. (Cited on page 27)

[89] L. T. T. Tran, H. Schepker, S. Doclo, H. H. Dam, and S. Nordholm, "Improved practical variable step-size algorithm for adaptive feedback control in hearing aids," in *Proc. IEEE Int. Conf. Signal Process. and Commun. Syst. (ICSPCS)*, 2016. (Cited on pages 27, 83, and 90)

[90] S. Thipphayathetthana and C. Chinrungrueng, "Variable step-size of the least-mean-square algorithm for reducing acoustic feedback in hearing aids," in *Proc. IEEE Asia-Pacific Conf. Circuits and Syst. (APCCAS)*, pp. 407–410, 2000. (Cited on pages 27, 37, 63, and 82)

[91] M. Rotaru, F. Albu, and H. Coanda, "A variable step size modified decorrelated NLMS algorithm for adaptive feedback cancellation in hearing aids," *Proc. ISETC. Timisoara*, pp. 263–266, 2012. (Cited on pages 27, 82, 86, 87, and 89)

[92] S. Lee, I.-Y. Kim, and Y.-C. Park, "Approximated affine projection algorithm for feedback cancellation in hearing aids," *Comp. methods and programs in biomed.*, vol. 87, no. 3, pp. 254–261, 2007. (Cited on pages 27, 63, and 82)

[93] S. Nikjoo, A. Seyedi, A. S. Tehrani, *et al.*, "Performance analysis of approximate affine projection algorithm in acoustic feedback cancellation," in *30th Annual Int. Conf. of the IEEE Engineering in Medicine and Biology Soc.*, pp. 258–261, IEEE, 2008. (Cited on pages 27, 37, and 82)

[94] K. Lee, Y.-h. Baik, Y. Park, D. Kim, and J. Sohn, "Robust adaptive feedback canceller based on modified pseudo affine projection algorithm," in *Proc. IEEE Annual Int. Conf. Engin. in Medicine, Biology Soc.*, pp. 3760–3763, 2011. (Cited on pages 27, 63, and 82)

[95] Y.-S. Kim, J.-h. Song, S.-K. Kim, and S. Lee, "Variable step-size affine projection algorithm based on global speech absence probability for adaptive feedback cancellation," *J. Central South University*, vol. 21, no. 2, pp. 646–650, 2014. (Cited on pages 27, 63, and 82)

[96] G. Panda, N. Puhan, *et al.*, "A vss sparseness controlled algorithm for feedback suppression in hearing aids," in *Proc. IEEE Int. Symp. Signal Process. and Inf. Technol. (ISSPIT)*, pp. 151–156, IEEE, 2015. (Cited on pages 27 and 82)

[97] H. Schepker, L. T. T. Tran, S. Nordholm, and S. Doclo, "Improving adaptive feedback cancellation in hearing aids using an affine combination of filters," in *Proc. IEEE Int. Conf. Acoust., Speech, Signal Process. (ICASSP)*, 2016. (Cited on pages 27 and 63)

[98] J. Arenas-García, A. R. Figueiras-Vidal, and A. H. Sayed, "Mean-square performance of a convex combination of two adaptive filters," *IEEE Trans. Signal Process.*, vol. 54, no. 3, pp. 1078–1090, 2006. (Cited on pages 27 and 63)

[99] N. J. Bershad, J. C. M. Bermudez, and J. Y. Tourneret, "An affine combination of two LMS adaptive filters: transient mean-square analysis," *IEEE Trans. Signal Process.*, vol. 56, no. 5, pp. 1853–1864, 2008. (Cited on pages 27 and 63)

[100] R. Candido, M. T. Silva, and V. H. Nascimento, "Transient and steady-state analysis of the affine combination of two adaptive filters," *IEEE Trans. Signal Process.*, vol. 58, no. 8, pp. 4064–4078, 2010. (Cited on pages 27 and 63)

[101] M. Guo, T. B. Elmedyb, S. H. Jensen, and J. Jensen, "Analysis of acoustic feedback/echo cancellation in multiple-microphone and single-loudspeaker systems using a power transfer function method," *IEEE Trans. Signal Process.*,, vol. 59, no. 12, pp. 5774–5788, 2011. (Cited on pages 28, 29, and 33)

[102] A. Spriet, *Adaptive filtering techniques for noise reduction and acoustic feedback cancellation in hearing aids*. PhD thesis, 2004. (Cited on page 28)

[103] M. Guo, S. H. Jensen, and J. Jensen, "Evaluation of state-of-the-art acoustic feedback cancellation system for hearing aids," *J. Audio Eng. Soc.*, vol. 61, no. 3, pp. 125–137, 2013. (Cited on page 28)

[104] C. R. C. Nakagawa, S. Nordholm, and W.-Y. Yan, "Dual microphone solution for acoustic feedback cancellation for assistive listening," in *Proc. IEEE Int. Conf. Acoust., Speech and Signal Process. (ICASSP)*, pp. 149–152, 2012. (Cited on pages 28 and 29)

[105] A. Spriet, G. Rombouts, M. Moonen, and J. Wouters, "Combined feedback and noise suppression in hearing aids," *IEEE Trans. Audio, Speech, Lang. Process.*, vol. 15, no. 6, pp. 1777–1790, 2007. (Cited on page 28)

[106] G. Rombouts, A. Spriet, and M. Moonen, "Generalized sidelobe canceller based combined acoustic feedback-and noise cancellation," *Signal Process.*, vol. 88, no. 3, pp. 571–581, 2008. (Cited on page 28)

[107] M. Guo, T. B. Elmedyb, S. H. Jensen, and J. Jensen, "Comparison of multiple-microphone and single-loudspeaker adaptive feedback/echo cancellation systems," in *Proc. 19th Eur. Signal Process. Conf.*, pp. 1279–1283, IEEE, 2011. (Cited on pages 28, 29, and 33)

[108] M. Brandstein and D. Ward, *Microphone arrays: signal processing techniques and applications*. Springer Science & Business Media, 2013. (Cited on page 28)

[109] H. Schepker, L. T. T. Tran, S. Nordholm, and S. Doclo, "Acoustic feedback cancellation for a multi-microphone earpiece based on a null-steering beamformer," in *Proc. IEEE Int. Workshop Acoust. Signal Enhan. (IWAENC)*, 2016. (Cited on page 28)

[110] F. Denk, M. Hiipakka, B. Kollmeier, and S. M. Ernst, "An individualised acoustically transparent earpiece for hearing devices," *Int. J. Audiology*, pp. 1–9, 2017. (Cited on page 28)

[111] A. Lombard, K. Reindl, and W. Kellermann, "Combination of adaptive feedback cancellation and binaural adaptive filtering in hearing aids," *EURASIP J. Advan. Signal Process.*, vol. 2009, no. 1, p. 968345, 2009. (Cited on page 29)

[112] S. S. Pradham and V. Reddy, "A new approach to subband adaptive filtering," *IEEE Trans. Signal Process.*, vol. 47, no. 3, pp. 655–664, 1999. (Cited on page 32)

[113] T. Gansler, S. L. Gay, M. M. Sondhi, and J. Benesty, "Double-talk robust fast converging algorithms for network echo cancellation," *IEEE Trans. Speech, Audio Process.*, vol. 8, no. 6, pp. 656–663, 2000. (Cited on page 34)

[114] Gänsler, Tomas and Benesty, Jacob, "The fast normalized cross-correlation double-talk detector," *Signal Process.*, vol. 86, no. 6, pp. 1124–1139, 2006. (Cited on page 34)

[115] S. Y. Low, S. Venkatesh, and S. Nordholm, "A spectral slit approach to doubletalk detection," *IEEE Trans. Audio, Speech, Lang. Process.*, vol. 20, no. 3, pp. 1074–1080, 2012. (Cited on page 34)

[116] T. van Waterschoot, G. Rombouts, P. Verhoeve, and M. Moonen, "Double-talk-robust prediction error identification algorithms for acoustic echo cancellation," *IEEE Trans. Signal Process.*, vol. 55, no. 3, pp. 846–858, 2007. (Cited on page 34)

[117] T. Gansler and J. Benesty, "An adaptive nonlinearity solution to the uniqueness problem of stereophonic echo cancellation," in *Proc. IEEE Int. Conf. Acoust., Speech, and Signal Process. (ICASSP)*, vol. 2, pp. II–1885, IEEE, 2002. (Cited on page 34)

[118] J. M. Kates, "Room reverberation effects in hearing aid feedback cancellation," *J. Acoust. Soc. Am.*, vol. 109, no. 1, pp. 367–378, 2001. (Cited on pages 34, 35, and 46)

[119] ITU, "Perceptual evaluation of speech quality (PESQ), and objective method for end-to-end speech quality assessment of narrowband telephone networks and speech codecs," *ITU-T Rec. P. 862*, 2000. (Cited on page 35)

[120] P. C. Loizou, *Speech enhancement: theory and practice*. CRC press, 2013. (Cited on pages 35, 49, 95, and 103)

[121] I. Rec, "BS. 1387: Method for objective measurements of perceived audio quality," *Int. Telecommun. Union, Geneva, Switzerland*, 1998. (Cited on pages 35, 58, and 103)

[122] P. Kabal, "An examination and interpretation of ITU-R BS. 1387: Perceptual evaluation of audio quality," *TSP Lab Technical Report, Dept. Electrical & Comput. Engineering, McGill University*, pp. 1–89, 2002. (Cited on page 35)

[123] C. R. C. Nakagawa, S. Nordholm, and W.-Y. Yan, "New insights into optimal acoustic feedback cancellation," *IEEE Signal Process. Lett.*, vol. 20, no. 9, pp. 869–872, 2013. (Cited on pages 37, 70, and 75)

[124] K. Kashima, A. Kawamura, M. Sunohara, K. Nishiyama, N. Hiruma, and Y. Iiguni, "Adaptive feedback canceller with howling detection for hearing aids," *Proc. Asia-Pacific Signal and Inf. Process. Assoc. Annual Summit and Conf. (APSIPA)*, pp. 704–710, 2015. (Cited on page 37)

[125] J. Chen, H. Bes, J. Vandewalle, and P. Janssens, "A new structure for sub-band acoustic echo canceler," in *Proc. Int. Conf. Acoust., Speech, Signal Process. (ICASSP)*, pp. 2574–2577, IEEE, 1988. (Cited on page 37)

[126] L. T. T. Tran, S. Nordholm, H. Schepker, H. H. Dam, and S. Doclo, "Two-microphone hearing aids using prediction error method for adaptive feedback control," *submitted to IEEE/ACM Trans. Audio, Speech, Lang. Process.* (Cited on page 39)

[127] J. S. Garofolo, "Getting started with the DARPA TIMIT CD-ROM: An acoustic phonetic continuous speech database," *Nat. Inst. Standards and Technol. (NIST), Gaithersburgh, MD*, vol. 107, 1988. (Cited on page 47)

[128] J. R. Deller Jr, J. G. Proakis, and J. H. Hansen, *Discrete time Process. of speech signals*. Prentice Hall PTR, 1993. (Cited on pages 49, 65, and 85)

[129] T. van Waterschoot and M. Moonen, "Adaptive feedback cancellation for audio applications," *Signal Process.*, vol. 89, no. 11, pp. 2185–2201, 2009. (Cited on page 57)

[130] L. T. T. Tran, H. Schepker, S. Doclo, H. H. Dam, and S. Nordholm, "Proportionate NLMS for adaptive feedback control in hearing aids," in *Proc. IEEE Int. Conf. Acoust., Speech, Signal Process. (ICASSP)*, 2017. (Cited on page 62)

[131] T. Aboulnasr and K. Mayyas, "A robust variable step-size LMS-type algorithm: analysis and simulations," *IEEE Trans. signal process.*, vol. 45, no. 3, pp. 631–639, 1997. (Cited on page 63)

[132] D. I. Pazaitis and A. G. Constantinides, "A novel kurtosis driven variable step-size adaptive algorithm," *IEEE Trans. Signal Process.*, vol. 47, no. 3, pp. 864–872, 1999. (Cited on page 63)

[133] L. A. Azpicueta-Ruiz, A. R. Figueiras-Vidal, and J. Arenas-Garcia, "A normalized adaptation scheme for the convex combination of two adaptive filters," in *IEEE Int. Conf. Acoust., Speech and Signal Process. (ICASSP)*, pp. 3301–3304, IEEE, 2008. (Cited on page 63)

[134] J. Arenas-Garcia, V. Gomez-Verdejo, and A. R. Figueiras-Vidal, "New algorithms for improved adaptive convex combination of lms transversal filters," *IEEE Trans. Instrum. Meas.*, vol. 54, no. 6, pp. 2239–2249, 2005. (Cited on page 63)

[135] J. Arenas-García and A. R. Figueiras-Vidal, "Adaptive combination of proportionate filters for sparse echo cancellation," *IEEE Trans. Audio, Speech, Lang. Process.*, vol. 17, no. 6, pp. 1087–1098, 2009. (Cited on page 63)

[136] F. Albu, C. Paleologu, and S. Ciochina, "New variable step size affine projection algorithms," in *Proc. 9th IEEE Int. Conf. Commun. (COMM)*, pp. 63–66, 2012. (Cited on page 63)

[137] F. Albu and C. Kotropoulos, "Modified gauss-seidel affine projection algorithm for acoustic echo cancellation.," in *IEEE Int. Conf. Acoust., Speech and Signal Process. (ICASSP)*, pp. 121–124, 2005. (Cited on page 63)

[138] D. L. Duttweiler, "Proportionate normalized least-mean-squares adaptation in echo cancelers," *IEEE Trans. Speech and Audio Process.*, vol. 8, no. 5, pp. 508–518, 2000. (Cited on pages 63 and 67)

[139] J. Benesty and S. L. Gay, "An improved PNLMS algorithm," in *Proc. Int. Conf. Acoust., Speech, and Signal Process. (ICASSP)*, vol. 2, pp. II–1881, IEEE, 2002. (Cited on pages 63 and 68)

[140] T. van Waterschoot, G. Rombouts, and M. Moonen, "Optimally regularized adaptive filtering algorithms for room acoustic signal enhancement," *Signal Process.*, vol. 88, no. 3, pp. 594–611, 2008. (Cited on pages 63 and 64)

[141] C. Paleologu, J. Benesty, and S. Ciochină, "An improved proportionate NLMS algorithm based on the l 0 norm," in *Int. Conf. on Acoust. Speech and Signal Process. (ICASSP)*, pp. 309–312, IEEE, 2010. (Cited on pages 63 and 68)

[142] F. Albu, "Simplified proportionate affine projection algorithms," in *Proc. 19th Int. Conf. Syst., Signals and Image Process. (IWSSIP)*, pp. 368–371, IEEE, 2012. (Cited on page 63)

[143] F. Albu, R. Nakagawa, and S. Nordholm, "Proportionate algorithms for two-microphone active feedback cancellation," in *Proc. 23rd Eur. Signal Process. Conf. (EUSIPCO)*, pp. 290–294, IEEE, 2015. (Cited on pages 63 and 64)

[144] S. Lee, I. Kim, and Y. Park, "An efficient feedback canceler for hearing aids based on approximated affine projection," in *Comput. Intell. and Bioinf.*, pp. 711–720, Springer, 2006. (Cited on page 63)

[145] Y. Gu, J. Jin, and S. Mei, "lo norm constraint LMS algorithm for sparse system identification," *Signal Process. Lett., IEEE*, vol. 16, no. 9, pp. 774–777, 2009. (Cited on page 69)

[146] M. Hiipakka, M. Tikander, and M. Karjalainen, "Modeling the external ear acoustics for insert headphone usage," *Journal of the Audio Engineering Soc.*, vol. 58, no. 4, pp. 269–281, 2010. (Cited on page 69)

[147] T. Sankowsky-Rothe, M. Blau, H. Schepker, and S. Doclo, "Reciprocal measurement of acoustic feedback paths in hearing aids," *J. Acoust. Soc. Am.*, vol. 138, no. 4, pp. EL399–EL404, 2015. (Cited on pages 69 and 75)

[148] L. T. T. Tran, H. Schepker, S. Doclo, H. H. Dam, and S. E. Nordholm, "Adaptive feedback control using improved variable step-size affine projection algorithm for hearing aids," in *Proc. Asia-Pacific Signal and Inf. Process. Assoc. Annual Summit and Conf. (APSIPA-ASC)*, 2017. (Cited on page 83)
